INFORMATION TO USERS

This manuscript has been reproduced from the microfilm master. UMI films the text directly from the original or copy submitted. Thus, some thesis and dissertation copies are in typewriter face, while others may be from any type of computer printer.

The quality of this reproduction is dependent upon the quality of the copy submitted. Broken or indistinct print, colored or poor quality illustrations and photographs, print bleedthrough, substandard margins, and improper alignment can adversely affect reproduction.

In the unlikely event that the author did not send UMI a complete manuscript and there are missing pages, these will be noted. Also, if unauthorized copyright material had to be removed, a note will indicate the deletion.

Oversize materials (e.g., maps, drawings, charts) are reproduced by sectioning the original, beginning at the upper left-hand corner and continuing from left to right in equal sections with small overlaps. Each original is also photographed in one exposure and is included in reduced form at the back of the book.

Photographs included in the original manuscript have been reproduced xerographically in this copy. Higher quality 6" x 9" black and white photographic prints are available for any photographs or illustrations appearing in this copy for an additional charge. Contact UMI directly to order.

UMI

A Bell & Howell Information Company
300 North Zeeb Road, Ann Arbor MI 48106-1346 USA
313/761-4700 800/521-0600

De-Inking Toner-Printed Paper by Selective Agglomeration

by

Bret Alan Snyder

A dissertation submitted in partial fulfillment

of the requirements for the degree of

Doctor of Philosophy

University of Washington

1996

Approved by  Chairperson of Supervisory Committee

Program Authorized to Offer Degree Department of Chemical Engineering

Date 10/28/96

In presenting this dissertation in partial fulfillment of the requirements for the Doctoral degree at the University of Washington, I agree that the Library shall make its copies freely available for inspection. I further agree that extensive copying of this dissertation is allowable only for scholarly purposes, consistent with "fair use" as prescribed in the U.S. Copyright Law. Requrests for copying or reproduction of this dissertation may be referred to University Microfilms, 1490 Eisenhower Place, P.O. Box 975, Ann Arbor, MI 48106, to whom the author has granted "the right to reproduce and sell (a) copies of the manuscript in microform and/or (b) printed copies of the manuscript made from microform."

Signature Bret A. Snyder

Date October 29, 1996

Univserity of Washington

Abstract

De-Inking Toner-Printed Paper by Selective Agglomeration

by Bret Alan Snyder

Chairperson of the Supervisory Committee: Professor John C. Berg

Department of Chemical Engineering

Laser printers and copy machines produce an increasing quantity of difficult-to-recycle paper. In the last several years, the need for an effective process to de-ink the toner has prompted a number of facilities to try toner agglomeration. The method requires the use of small amounts of an appropriate oil which serves to collect the toner into agglomerates that can be removed from paper fibers by screens or centrifugal cleaners. The technique shows promise by being simple, economical, and often very effective; however, it currently requires high-temperature and performs inconsistently, preventing significant use. A fundamental study of agglomeration is needed to determine how it operates, the key variables and their interactions. Therefore, the present study provides a fundamental understanding of agglomeration, laying the groundwork for process enhancement.

We identify the key factors in agglomeration: concentration of cationic starch released from sheets in the repulper, oil composition, agitation rate, time and temperature. Furthermore, we examine how and why each factor influences agglomeration, and a population balance model is developed to help determine the quantitative relationships between the key variables. Cationic starch adsorbs to toner and oil interfaces, rendering them electrosterically stable to coalescence, thus preventing oil drops from reaching toner particle surfaces. However, when the oil contains an oil-soluble surfactant, the cationic starch adlayer is engulfed and some agglomeration resumes. Direct and novel use of the

atomic force microscope provides insight into the cationic starch-induced reduction in oil-toner collision efficiency. Agitation rate and temperature influence the particle breakup rate, the latter by increasing aggregate strength by fusing toners above 35 °C. The model effectively predicts the experimental results, and shows how the competition between aggregate growth and breakup determines both the rate and degree of agglomeration. The results yield the agglomeration mechanism, quantitative expressions relating key variables and performance, and practical suggestions.

TABLE OF CONTENTS

LIST OF FIGURES

LIST OF TABLES

ACKNOWLEDGMENTS

The author wishes to express gratitude to his advisor for guidance, generosity and support given during his time as a graduate student. Professor Berg takes an active interest in his students, and provided numerous opportunities to publish, attend conferences, and improve oral communication, in addition to being a superb teacher both in and out of the classroom. The author would be most remiss if he did not gratefully acknowledge the companionship, assistance and enjoyment he derived every day from his peers in the Interfacial Phenomena Group, including Dr. Pauline Jacob, Dr. Jill Seebergh, Dale Schmidt, Jorge Sunkel, Phil Harding, Susie Stenkamp and D. Eric Aston. Close, lifelong friendships have developed with most of these companions, not to mention the research advice, the listening to talks, the help with techniques and the general guidance shared. Also, the author has benefitted from the project's chief liason at the Weyerhaeuser Company, Dr. Tom Friberg. He provided support, feedback, enthusiasm and remains in the author's mind the best possible sponsor for research. The author likewise acknowledges the other members of the Weyehaeuser Company with whom he has come into contact, and, in particular, the financial support of the Weyerhaeuser Foundation (Fisken Fellowship). The author also acknowledges the Forest Product Laboratory (Madison, Wisconsin) for financial support of some of the early research.

The friends, faculty and staff at Benson have provided a most enjoyable environment in which to work. The author's family has been a consistent aid behind the scenes. Although not directly involved in the research effort, the author's wife, Anna Lee Quisel, is such a joy that she truly "doubles every victory, and halves every defeat" of the author.

DEDICATION

To Anna Lee Quisel, the dearest person I know.

CHAPTER ONE

INTRODUCTION

1.1 Background

Because landfill typically contains 50% discarded paper products (Basta, 1991) and political pressure to reduce natural resource consumption remains high, overwhelming incentives exist to increase paper recycling. Most of the easily collected and processed paper products, such as newsprint are already at nearly maximum recycle capacity. Pulp and paper manufacturers are therefore increasingly driven to expand their range of recycled materials to include more difficult-to-handle paper. Because of its high-quality fiber content and ease of collection on one hand, and its notorious resistance to de-inking on the other, both manufacturers and researchers have begun to focus on finding better methods for de-inking toner-printed office wastepaper. Toners are the printing inks used in the dry, electrostatic printing method of xerographic and laser-printer devices. As these machines become more plentiful and sophisticated, the need to find effective de-inking methods for them becomes increasingly urgent.

Unlike other wastepaper, toner-printed papers contain fused thermoplastic particles on the paper surface which form large flakes during recycling. These flakes produce visible specks on the final sheet if not removed (Quick and Hodgson, 1986). Neither the conventional de-inking processes of washing, flotation, centrifugation and screening remove them reliably, nor is bleaching effective. Although those involved do not feel they completely understand the reasons for the difficulty in removing toner, most agree their size and shape, taken together, is a primary factor. During repulping, the first stage in a recycle mill when shear disintegrates the paper in a water slurry, the toners release from the fibers

as flakes only 10-30 μm thick, so they pass through the screens and centrifugal cleaners, but 50-500 μm wide, so they pass through flotation cells and washers (Vidotti, *et al.*, 1993; Rhodes and Ferguson, 1993). The thermoplastic resin in the toner shields the carbon black pigment from oxidative bleaching.

Efforts have focused on three major methods for improving toner de-inking: better flotation, agglomeration and dispersion (Rhodes and Ferguson, 1993). Dispersion requires the addition of another unit operation and breaks the toner flakes into sub-visible particles that are better removed by conventional processes, or at any rate, will not produce visible specks in the finished sheet (Aspler, *et al.*, 1989, ch. 2, p. 29). The method accomplishes size reduction by applying heat and intense shear to a concentrated fiber-toner slurry, using fiber-fiber rubbing to crumble the toner flakes. It requires a large capital investment and high energy input, making it a second choice to *effective* flotation or *agglomeration*. Research both elsewhere and in our laboratory has focused on improving the flotation process for toner flakes (Schmidt and Berg, 1995; Vidotti, *et al.*, 1993, Vidotti, *et al.*, 1994). This investigation, therefore, limits itself to the study of the agglomeration process for de-inking toner-printed papers.

1.2 Agglomeration Techniques

Currently, several mills use agglomeration primarily on a trial basis, whereas others have discontinued after ambiguous results.

The process is designed to occur during repulping, the first unit operation in a paper recycling mill. In a typical plant, several tons of baled wastepaper are loaded into an agitation vessel with hot caustic water and intensely agitated to disintegrate the paper into fibers and release the toner particles. The system thus becomes an *aqueous codispersion of hydrophilic fibers and hydrophobic toners*. Other paper components are also present:

- filler particles (e.g. TiO_2 and $CaCO_3$)
- oil-based ink drops (from non-toner-printed paper)
- cationic polymers, such as cationic starch (in solution)

The total solids in the repulper is commonly between 5 and 20 wt% (Ferguson, 1992b).

To accomplish the solid-solid separation of toners and fibers, their *wettability differences* are used. The addition of a small amount of an immiscible oil to the repulping unit will lead to its dispersion into fine drops which selectively attach to the hydrophobic toners. The oil-wet particles then collide and adhere through the formation of liquid bridges. The strength of the bridge derives from its curved interface which leads to a capillary-induced pressure reduction inside the liquid, in accord with the Young-Laplace equation:

$$\Delta P = \kappa\sigma \tag{1.1}$$

Equation 1.1 states the pressure reduction equals the local surface curvature, κ, times the interfacial tension, σ. We have confirmed that, with selection of an appropriate oil in conjunction with raising the temperature, the oil can sometimes dissolve the thermoplastic resin of the toner and lead to toner-particle fusing, increasing the agglomerate strength beyond that provided by liquid bridges (see Chapters 5 and 7).

Figure 1.1 shows a schematic of the agglomeration process. Conventional unit operations of screening and centrifugal cleaning of the pulp slurry can then easily remove large toner agglomerates, leaving only the clean cellulose fibers in the product.

The initial attempts at agglomeration de-inking of toner-printed papers have, despite their promise, proven problematic:

• The processes require high temperature, typically 50-70 °C, adding the expense of heating large volumes of water and endangering personnel.

• Most mills have problems with sticky agglomerates depositing on process equipment, requiring periodic plant shutdown for solvent cleaning. The high temperatures currently required would contribute by softening the toner resins.

• Most importantly, current treatments are unreliable, sometimes leaving the mill with a failed batch of pulp full of toner particles. This forces the operators to pull the contaminated pulp off line and dilute it with clean fibers, reducing product quality and slowing production.

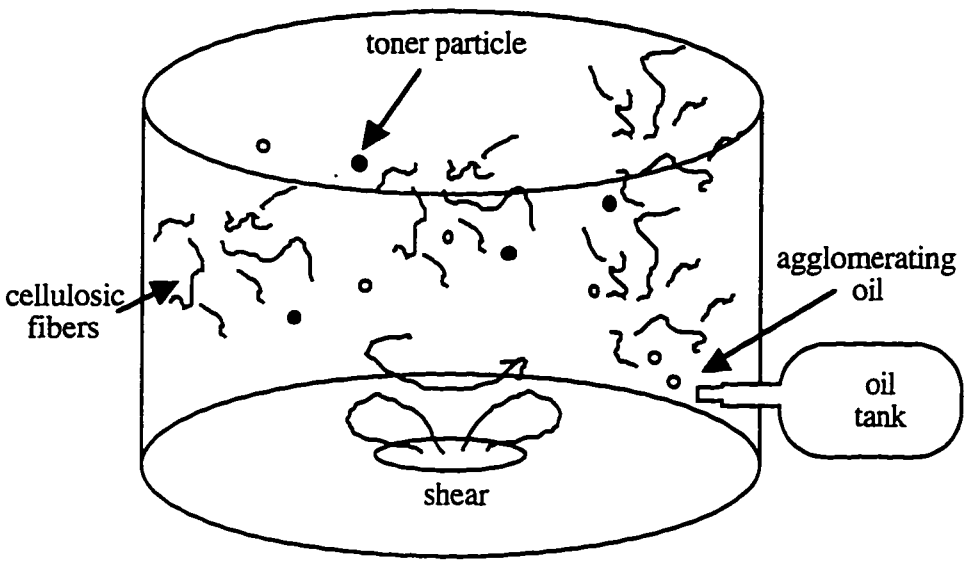

.c8.**Figure 1.1** Schematic of the repulper during agglomeration treatment.

However, the process has potential:

• Possibly very low (<5% of production costs) expense if the agglomerating oil can be formulated with commodity chemicals

• No additional unit operations for existing recycle mills, and thus insignificant capital investment

• High reliability and effectiveness in some trials

Clearly, while manufacturers hurry to exploit the potential of agglomeration de-inking, large problems remain. Only a better *fundamental knowledge* of the factors involved and their interaction is likely to lead to a more rationally designed and effective process.

The proposed study aims to complete the first step of developing this knowledge base.

1.3 Outline of Document

The organization of the dissertation follows:

Chapter 2 reviews the existing scientific literature on toner de-inking, agglomeration de-inking, oil-assisted agglomeration and agglomeration process modeling.

Chapter 3 describes our early work (Snyder *et al.*, 1993; Snyder and Berg, 1994a) where we characterize the surface chemistry and physical properties of toners from different sources and their susceptibility to flotation removal. We show the importance of the source of the toner for its de-inking properties.

Chapter 4 presents the first-ever reported investigation of liquid bridge agglomeration applied to the collection of toner particles (Snyder and Berg, 1994b). The results show the technique's effectiveness and attractiveness for operation at low temperature. Furthermore, we describe the critical effect of the cationic starch released in

the repulper on the surface chemistry of all the species present, resulting in the disruption of agglomeration.

Chapter 5 describes a comparison study between a simple oil and an oil/surfactant blend to determine how each responds to cationic starch. We discover that cationic starch adsorbs to the interfaces and blocks agglomeration by forming a polymer adlayer that sterically prevents the oil drops from coalescing onto the toner particle surface and inducing agglomeration (Snyder and Berg, 1996a). Most importantly, we show the oil/surfactant blend avoids such a barrier to coalescence because its more polar composition allows the engulfment of the cationic starch adlayer.

Chapter 6 presents the results of novel use of an atomic force microscope to directly measure the coalesceability of toner particles interacting with oil drops (Snyder *et al.*, 1996). The results show cationic starch engenders long film drainage times between oil drops and toner particles and directly indicate a resulting reduction in collision efficiency.

Chapter 7 provides an overall perspective on agglomeration de-inking by combining a population balance model with experimental measurement of agglomerate size distributions (Snyder and Berg, 1996c). We show how the key variables identified in previous chapters as cationic starch additives, agitation rate, time, temperature and oil composition control the dynamic and steady-state evolution of the particle size distribution. Simple, quantitative relationships between process variables and agglomeration performance emerge by effective use of numerical solutions to the population balance model. We observe how all factors in agglomeration affect either the aggregation or the breakup rates, and the consequences of this for process improvement.

Chapter 8 presents the major conclusions of the work and practical recommendations the conclusions indicate.

CHAPTER TWO

LITERATURE REVIEW

2.1 Toner De-Inking

The toners used by laser-printer and photocopiers consist of a thermoplastic resin blended with pigment and printing-control additives. Compositions of several toners are given in Table 3.1. The solid blend is added to the printing device as a powder of approximately 10 μm particles. During the printing process, the photo-conducting surface of a cylindrical drum is charged in the desired pattern by reflected light (photocopier) or a laser (computer printer). This charge is transferred to the blank sheet of paper which then receives a cascade of toner particles bearing an opposite charge. Static electricity holds the toner in place until the sheet passes through hot rollers where heat (100 to 200 °C) and pressure (75-200 psi) fuse the toner into place. The individual particles soften, fuse together and flow around the fibers, held in place by physical entanglement and adhesion (Seldin, 1985).

Shortly after the invention of the photocopy process, problems in recycling were realized. Three basic approaches have been explored for toner de-inking: improvement of the flotation process, dispersion of the toner particles into small sizes and agglomeration of the toner particles into large sizes. The remainder of this section reviews chronologically the work in all three areas.

The first attempts to handle toner-printed paper occurred during the period of high environmental concern in the early 70s. Green (1972) and Mestetsky and Webster (1974) both proposed solvent-based methods, where a solvent is mixed with the fiber-toner slurry, collects or dissolves the toner particles, and then rises to the surface in an organic layer

containing toner that can be skimmed away. Such a technique, with its heavy solvent consumption, is not currently practical, considering the onerous disposal problem it produces.

In 1979, focusing on flotation, Pfalzer proposed that toner-printed papers could be effectively de-inked by low-temperature, high-soap repulping for long times followed by flotation. No one since, however, has found it to work as well as he reports, possibly from changes in toner composition or printing device design since then.

The first agglomeration attempts followed. In 1981, Quick proposed adding a slightly polar oil such as a long chain alcohol and beads of another polymer, all at high temperature, to soften the toner and collect it on the beads. His work began a series of patents on variations of the process, which continue currently, and are discussed further below in section 2.2, agglomeration de-inking. Wood and Wood (1985) proposed a variation where no beads are added, but a slightly polar oil is mixed with a nonionic surfactant and high temperature is maintained to collect the toner into agglomerates.

The first real *study* of the de-inking of toner-printed papers was done by Quick and Hodgson (1986). Among their many findings, they showed that washing and flotation are marginally effective, but two stage float/wash and float/float systems can achieve acceptable ink removal. The greatest drawback, however, was unacceptably large fiber losses (25 and 18%, respectively). This accords with their observation that much of the toner remained attached to the fiber after repulping (Vidotti *et al.*, 1993, 1994). They found that the patented toner collection process of Quick (1981) was effective, but only if the batch consisted of nearly 100% toner-printed paper. They also found large differences in de-inking performance with machine and toner type. Separately, pulping consistency and mechanical dispersion were shown to have large influences on the toner particle size distribution produced (McCool and Silveri, 1987).

The field becomes increasingly active only as recently as the late 80s, as the supply of toner-printed paper continues to grow rapidly. Lapointe, Marchildon and Bonnelly (1988), continuing Pfalzer's work on flotation, examined the effectiveness of flotation surfactants on one type of toner-printed paper, and found increasing unsaturation of the surfactant beneficial, although no clear mechanism is presented.

At about the same time, another agglomeration technique was proposed by Darlington (1989) and is described more fully in his patent (1992). The process consists of adding a polymeric material, such as beads, with a softening point from 20 to 70 °C and an agglomerating agent of the composition:

$$(C_6 \text{ to } C_{20} \text{ alkyl})\text{-}(\text{ethoxy})_{1\text{-}20}\text{-}(\text{phenoxy, chloro, or } C_1\text{-}C_4 \text{ alkoxy})$$

The chemical is thought to lower the T_g of the toner and soften it for fusion with the added polymer beads. The process requires elevated operating temperatures of 45 to 75 °C. This is basically a variation on the process described by Quick (1981).

Carr's review (1991) clearly portrays the approaches of dispersion and agglomeration for toner-printed paper de-inking, as well as summarizes many observations on how the toner particle size (40 to 400 μm) and plate shape prevent their full removal in conventional processes such as screening, washing, and reverse cleaning.

Work on dispersion, to reduce the toner particle size and increase the sphericity, was endorsed as effective by de-inking research of Okada and Urushibata (1991). The focus was to make the particles amenable to flotation removal. Jones (1992) also claimed that this is an effective method for toner de-inking.

Quite recently, agglomeration work is continued with great intensity, shown particularly in the announcements of Olson *et al.* (1993a, 1993b) and patents of Richmann and Letscher (1992, 1993a, 1993b, 1994). They propose an agglomeration process,

where, unlike previous proposals (Quick, 1981; Wood, 1985; Darlington, 1992) that required the addition of polymer beads, only an oil/surfactant blend is added to enhance the toner-toner agglomeration. The problems and potential of current agglomeration efforts, however, were catalogued aptly by Rhodes and Ferguson (1993). They report on agglomerate deposits, incomplete agglomeration, and high temperatures used. Also, they indicate that the flow pattern in the repulper affects performance, which is related to the statistical chances of collision between two toner particles—an aspect that indeed we find important from our population balance model, as reported in Chapters 7 and 8.

Toner-printed paper de-inking has only recently received the attention of fundamental researchers again since the work of Quick and Hodgson (1986), certainly because process difficulties still remain. Much of this work focuses on flotation. At the University of Maine, Vidotti *et al.* (1992, 1993, 1994), Pan *et al.* (1992, 1993, 1994a,1994b, 1994c), Paulsen *et al.* (1993, 1996) and Johnson and Thompson (1995) have undertaken to examine the flotation process for toner removal primarily, with some secondary studies of repulping. Their work has focused on modeling current flotation and relating the size of the toners to efficiency of removal, looking particularly at the particles that contain attached fibers. Results suggest fibers remaining attached to large toner particles reduce their removal efficiency by flotation. Schmidt and Berg (1995) have examined specifically the role of particle shape on flotation with high-speed motion picture films of actual toner particle-bubble collisions. Epple and Berg (1994) and Epple *et al.* (1994) have examined the surface chemistry of toners in the presence of surfactants and its effect on flotation removal, finding an optimum dosage of frother surfactant. Similarly, Snyder *et al.* (1993) and Snyder and Berg (1994a) provided a comparison study of 8 toners and found that laser-printer toners, being denser and thicker on the sheet, repulp to form larger particles and are more difficult to remove by flotation.

For fundamental research on agglomeration, Snyder and Berg (1994b) performed the first (and still only) systematic study of agglomeration de-inking for toners. This work showed the effectiveness of a simple oil in agglomerating the toners at room temperature, and then the potent effect of dissolved cationic starch released by repulped paper on blocking the ability of the oil to coalesce on the toner at an appreciable rate.

Two novel de-inking methods have also been recently investigated, both currently with unclear prospects as they await further research and testing. First, Norman *et al.* (1994) has proposed the use of ultrasound to break down toner particles to sizes removed by washing or flotation, expanding the ideas put forth by Turai and Teng (1978) and Naimpally (1981) to toner-printed paper. Second, Jeffries *et al.* (1994) have also reported some success using an enzymatic treatment of the pulp slurry before moving it through the conventional de-inking steps. Although definite conclusions of the mechanism involved in both of these novel approaches have not been identified, the authors speculate that these methods may improve release of toner from the paper fibers. Furthermore, ultrasound, though energy intensive, may help break down the toner flakes into a size and shape more amenable to washing or flotation.

At least one radically different approach for toner-printed paper recycling has been pursued to the commercial level. Described by Geake (1994), a "reverse copy machine," produced by Ricoh, Inc. accepts a toner-printed page, strips the toner off with heat and solvent to aid in release of the toner and returns a clean sheet. The device can only clean one sheet at a time, at a rate of three per minute. It practically reverses the xerographic process.

To summarize, toner-printed papers have been difficult to de-ink and recycle since they first appeared, and very little fundamental research on de-inking them has been published, almost all of which has focused on improving flotation. The techniques of

agglomeration and dispersion have few systematic studies, but a handful of commercial process patents.

From contact with mill personnel and trade literature, it appears the "brute force" method of adding chemicals and high consistency mechanical dispersion to make the toner into small, spherical particles, although it requires lots of energy and additional unit operations, remains available for effective, albeit expensive, de-inking. Flotation has been attempted and found marginally effective, the reasons for which are only presently becoming clear with systematic studies of the fundamentals. Agglomeration has been considered since Quick's patent in 1981. Here in particular, we see that the work has been approached completely from the product development side with little or no study of the underlying fundamentals (except Snyder and Berg, 1994b). The mixed results for agglomeration in practice could undoubtedly be improved by the continuation of such work.

2.2 Agglomeration De-Inking

A brief synopsis of major developments will be given here. First, no scientific study of the agglomeration process has been reported excepting Snyder and Berg (1994a). So the "literature" consists only of patents and trade articles that report the experience of particular mills.

Patents. All patented processes use high temperature fusion of the toner into agglomerates or onto added beads for separation. These can be subdivided into two groups: 2-component and 1 component systems. Two-component methods require the addition of polymer beads onto which the toner particles collect, while 1-component methods rely on the toner self-agglomeration. All use an added oil or surfactant to induce agglomeration, and this agent is always added at approximately 1% by weight on dry fiber

in the slurry (approximately equal to the weight of the toner particles themselves). Table 2.1 contains the various agents:

Table 2.1 Components of patented agglomeration formulations.

Components	Patent	Chemical Nature
1	Richmann and Letscher (1992, 1993a,b, 1994)	low HLB, nonionic surfactants, particularly nonionic alkylphenol ethoxylates and propoxy/ethoxy block copolymers, mixed with aliphatics ($C_{(9\ to\ 12)}$)
1	Wood (1985)	$C_{(9\ to\ 15)}$-OH mixed with $C_{(9\ to\ 15)}$-(ethoxy)$_{(1\ to\ 5)}$
1	Borchardt (1993)	$C_{(9\ to\ 11)}$-OH
2	Quick (1981)	$C_{(5\ to\ 20)}$-OH
2	Darlington (1992)	($C_{(6\ to\ 20)}$ alkyl)-(ethoxy)$_{(1\ to\ 20)}$-(phenoxy, chloro, or $C_{(1\ to\ 4)}$ alkoxy)

As is apparent from Table 2.1, the formulations of the commercial agglomerating agents are all similar: long chain alcohols and/or ethoxylated surfactants are present in every formulation. Our investigations reported in Chapter 5 indicate that the polarity of these mixtures serves the important function of imbibing cationic starch adlayers.

Trade articles. Rhodes and Ferguson (1993) report the problems with incomplete toner removal, inconsistent results and agglomerate deposition on process equipment. They did have enough success with it, however, to continue with it for over a year. Successful agglomeration at another mill was achieved, according to Ferguson (1992a), but

this mill was operated in part by the agglomerating chemical supplier as a product showcase, so it may have used most favorable feedstocks and conditions, etc. In general, private communications with paper company personnel have indicated that many mills experience poor performance from agglomeration trials.

2.3 Oil-Assisted Agglomeration

Since all commercial systems use water-insoluble agents, the drops of the oil-like agent must attach to the toner particles to be effective. A similar process is the attachment of a simple (and inexpensive) pure oil to agglomerate the toner particles. Such a process would be a liquid bridge agglomeration process.

Using oils to selectively agglomerate hydrophobic particles (or the converse: using water in a non-aqueous medium to selectively agglomerate hydrophilic particles) has received attention since the early 1960s. Farnand *et al.* (1961), Sutherland (1962) and Puddington and Sparks (1975) describe the process, calling it 'spherical agglomeration,' after the shape of the agglomerates formed. Other names are 'oil agglomeration,' 'oil-assisted agglomeration,' 'selective agglomeration' and 'liquid bridge agglomeration' (our term, after the mechanism). The separation involves the addition of an immiscible liquid which preferentially wets the solids and forms liquid bridges between colliding particles. *Selective* agglomeration occurs when the added liquid preferentially wets only one type of the dispersed solid particles. As such, it is selective on the basis of *wettability.*

The first observations of assisted agglomeration were Kruyt and van Selms (1943) and Stock (1952). Smith and Puddington realized that both Kruyt and van Selms and Stock had observed the same phenomenon. Later, Puddington and Sparks (1975) reviewed the process, and described the sensitivity of the size of the agglomerates obtained to the ratio of bridging liquid volume to particle volume, observations originally made for

granulation by Newitt and Conway-Jones (1958). This universally observed behavior of liquid bridge agglomerate type with immiscible liquid addition level is depicted in Figure 2.1.

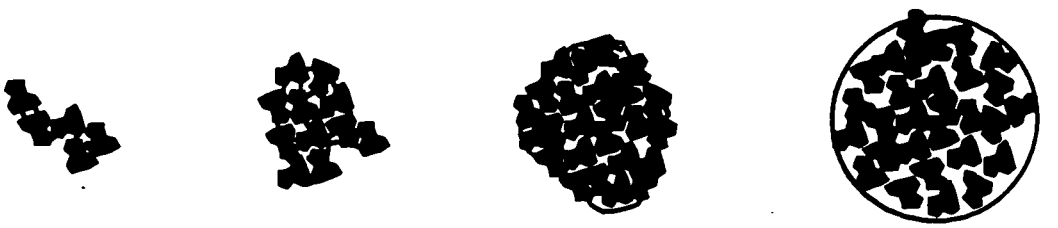

Figure 2.1 Agglomerate states produced during assisted agglomeration. Immiscible liquid addition increases from left to right. Pendular aggregates contain little liquid, normally less than 25% of amount needed to fill the pore volume between the individual particles. They are small and weak. Funicular aggregates are larger and more spherical, and typically form at liquid dosages of 25 to 90% of pore volume. The largest, strongest and most spherical aggregates are found in the capillary state, and appear at liquid dosages of 90-110% of pore volume. Higher dosages of immiscible liquid produce *drops* containing particles. This is effectively liquid-liquid particle transfer. Although these can be large, they are weak and easily fragmented. (From Newitt and Conway-Jones, 1958; Puddington and Sparks, 1975)

Numerous liquid bridge agglomeration studies have been reported since, focused primarily on coal beneficiation (reviewed by Mehrota and Sastry, 1985; Capes and Darcovich, 1984) or selective mineral recovery (reviewed by House and Veal, 1992). The process resembles flotation: it separates on the basis of wettability by attaching hydrophobic particles to immiscible fluid particles. Flotation has been a long-standing mineral beneficiation technique (in fact, it remains the primary separation process for ores, processing over 10^9 tons of ore annually according to Schulze (1984, p. 15)) that the paper industry adapted to de-inking. Possibly, oil agglomeration may find similar use.

2.4 Population Balance Modeling

The basic concept of population balance modeling was first used, in general terms, by Hulburt and Katz (1964). Since then, aerosol science, granulation of solids, comminution, floc breakup, crystallization, precipitation, fluidized beds, particulate reactors, mass-transfer and reaction rates in liquid-liquid systems have all been extensively studied with the aid of population balance equations. Ramkrishna (1985) provides an extensive listing and review of the field. For our purposes, we view the population balance equations as simply a formulation of conservation of mass applied to a dispersion of particles that undergo changes in size distribution from physical processes. Thus, the population balance is purely a method of *accounting* for gains and losses of particle counts at different sizes. The key physics of the processes must be added in the form of rate expressions that mathematically describe how particle counts at each size change in time; as a function of the number of particles present at each size and physical parameters of the system, such as, for instance, the agitation intensity.

In our system, we have only two basic processes: aggregation and breakup. We exclude therefore more complicated models that include, for example, phase changes such as crystallization, heat and mass-transfer and chemical reactions. To obtain a general expression for the rate of aggregation, we ask: how often do two particles of volume v_i and v_j collide in a tank of given agitation rate? For particles less than 0.5 μm, this occurs largely by Brownian motion; for larger particles such as dispersed toners (minimum size 10 μm) collisions occur almost exclusively by macroscopic fluid motion. Numerous investigators have answered this question, deriving expressions that vary only slightly with the assumptions used in deriving them (this and the discussion that follows is based largely on the chapters by Ayazi Shamlou and Titchener-Hooker, 1993, and Bagster, 1993). The

original expression of Smoluchowski (1917) is used by us, with G, the laminar shear rate, replaced by $(\varepsilon/\nu)^{1/2}$, a measure of the typical shear rate in a turbulent stirred tank,*viz.*

$$J_{ij} = A_1(\varepsilon/\nu)^{1/2}\left(R_{ij}\right)^3 n_i n_j, \tag{2.1}$$

where J_{ij} is the number of collisions per unit time per unit volume of dispersion, A_1 is a constant, ε is the energy dissipation per unit time per unit mass of fluid from agitation, ν is the fluid's kinematic viscosity, R_{ij} is the collision radius, usually taken to be equal to the sum of the two particle radii, and n_i and n_j and the number of particles of i and j present per unit volume in the fluid. Equation 2.1 is strictly valid only for binary particle collisions and only when the particle size is less than the scale of the smallest turbulent eddies, the Kolmogorov microscale $1/\lambda$, which is

$$1/\lambda = (\varepsilon/\nu)^{1/4} \tag{2.2}$$

In our studies, $1/\lambda$ is between 30 and 48 μm. Thus our smaller toner particles are in the correct range, but not the larger agglomerates formed. For larger particles, the expression should be

$$J_{ij} = A_2 \varepsilon^{1/3}\left(R_{ij}\right)^{7/3} n_i n_j. \tag{2.3}$$

In practice, however, since the primary particle size falls well within the region where Eq. 2.1 is valid, most researchers have preferred to use this. In our preliminary population balance model described in Chapter 7, we followed their lead and obtained very satisfactory results. In any case, slightly reducing the exponents in Eq. 2.1 to obtain Eq. 2.3 is not expected to significantly alter the model results. Furthermore, our large agglomerates,

ranging from 500 to 1500 μm diameter, probably fall outside the range of validity of Eq. 2.3 (Schwartzburg and Treybal, 1968), since the inertial effects of particle size and shape become increasingly important and the turbulence no longer isotropic on such a scale, and simple theories are not available for particle interactions in such cases. We therefore leave elaboration of the model expression of the aggregation rate to future research should it appear beneficial to increase the model's rigor and complexity.

Eqs. 2.1 and 2.3 yield the expected rate of particle collisions, not the rate of aggregate formation. To obtain the latter, a collision efficiency is introduced as a coefficient on the right-hand side of the equations (Higashitani *et al.*, 1982, 1983). The collision efficiency, α, is the ratio of those that aggregate to those that collide. In other words, α is the probability of aggregate formation on collision. In our system, this is an important measure of the coalesceability of oil drops with toner particles, and appears to be about 0.04 for good agglomeration, and an order of magnitude less than this, at least, for poor agglomeration caused by the presence of cationic starch (see Chapter 7).

For particle breakup, we followed the lead of numerous investigators who have written the aggregate breakup rate as

$$rate_i = -B\left(d_i/d_0\right)^{\nu} n_i, \tag{2.4}$$

where the loss in number of particles of size i per unit volume per time is given in terms of the breakup rate constant, B, the diameter of the particle, d_i over the diameter of a primary particle, d_0, raised to a power, ν, times the number of particles of size i per unit volume, n_i. This expression, while apparently lacking strong theoretical support, is nearly universally used for describing the rate of particle breakup (Chen, 1992; Lu and Spielman, 1985; Valentas *et al.*, 1966; Ramkrishna, 1974; Pandya and Spielman, 1982; Huang and Hellums, 1993; Tomi and Bagster, 1974).

Only four attempts have been made by previous researchers to specifically address modeling of an oil-assisted agglomeration process. The earliest work was by Kawashima and Capes (1974, 1976) focused on developing an empirical model of the increase in the population density of agglomerates, which they found to follow an exponential increase, indicating first order growth kinetics. The significant efforts of Bemer (1979) considered a number of models to correspond with their experimental results. Investigating primarily cases where a sub-optimum ratio of binding liquid to particles is used, they observe, instead of smoothly increasing average particle size, a growth behavior characterized by a rapid growth to a moderate size, followed by a large plateau region, followed by a second period of rapid increase, ending with a stable size thereafter. Bemer and Zuiderweg (1980) find the rate-controlling step is the squeezing of liquid from the pores onto the pellet surface, and relate the time spend in the plateau region to the inverse of the capillary liquid velocity in the pores.

Dunstan *et al.* (1986) describe a simple kinetic model for oil agglomeration that posits the collisions between the solid particles and binding liquid droplets as the rate-controlling step. Only aggregation is considered, as a model for the rate of growth of aggregates is sought, not a prediction of the steady-state size distribution. Their first-order, linear ordinary differential equation set is solved analytically, and they find qualitative agreement with the dependence of the rate of aggregation on solids and oil concentration. The only really sophisticated model to consider oil-assisted agglomeration is that of Spoelstra (1989). He posits a two-step model: first, oil drops coalesce on coal particles, and then these wet particles collide and adhere to one another. Four parameters appear in the equations: the rate constant of oil-wetting the dry coal particles, the amount of oil needed to wet and activate a coal particle, the amount of oil needed to wet an agglomerate to activate it for further agglomeration (as opposed to the amount needed to wet and activate a single dry particle), and the rate constant of doublet formation. Like Dunstan *et al.* (1986),

Spoelstra (1989) is only attempting to predict the rate of agglomerate growth, which his equations seem capable of doing. Particle breakup is not considered, and therefore no predictions for a steady-state particle size distribution can be made.

In conclusion, we see that while population balance modeling is widespread and well-developed, no researcher has addressed the oil agglomeration process with a complete set of equations describing particle aggregation and breakup. Thus, by using the population balance framework, including well-accepted expressions for aggregation and breakup rates, useful results can be hoped for in understanding oil-assisted agglomeration for toner de-inking, and indeed this is discussed in Chapter 7.

CHAPTER THREE

TONER CHARACTERIZATION AND FLOTATION STUDIES

3.1 Introduction

This chapter presents early work done to clarify the surface chemistry of toners and investigate how this affects their flotation response. Although flotation is not the focus of this dissertation, the results presented here have important implications for any program of de-inking, as the variation in surface chemistry and toner particle size formed during repulping are examined among different toners and particular machines.

3.2 Background

The flotation process has been used for over 100 years in mineral separations, and has been successfully employed in de-inking for several decades (Ortner, 1981). It depends on separating finely divided solids by wettability and requires only air, water, low power, and (usually) small amounts of chemicals to modify the surface chemistry. For hydrophilic solids the most important chemical is the collector, which adsorbs on one of the solids to render it hydrophobic. Adjustments of pH, frothers, activators, depressors, and other special compounds are also present in many cases, and hydrodynamic factors that influence particle-bubble collision also play a large role (Schulze, 1984, ch. 2-3).

Pfalzer reported in 1979 that toners could be easily floated away from fibers at nearly 100% removal if the repulping temperature is kept low, pulping is continued for 60 minutes, and 0.2% dispersing agent, 1.5% soap, and 2% NaOH (all by weight on dry fiber) are added. However, Quick and Hodgson published a study in 1986 showing that flotation was not particularly effective for many toners, the effectiveness varying with the

type of machine used to print the paper (Quick and Hodgson, 1986b). They found that flotation removed typically about 75% of the toner, and that some of the toner remained attached to the fibers after repulping. Other investigators have confirmed the influence of machine type on the effectiveness of de-inking, and, in addition, most authors have indicated that effective flotation depends on the toner particle size (Amand and Perrin, 1991, Larsson, 1987, Marchildon, *et al.*, 1989, Vidotti, *et al.*, 1993, Woodward, 1992). This study attempts to quantify the aspects of the toner surface chemistry likely to be important in flotation, which will be the same factors important for any surface-chemistry-based de-inking process, such as oil-assisted agglomeration.

3.3 Materials and Methods

Zeta potentials were measured by microelectrophoresis in the Rank Brothers Mark II device. The toners were used as powders received from the manufacturer before printing. They were dispersed in a solution of Triton™ X-100 (2.5 g/l) in deionized water. The pH was adjusted by adding NaOH or HCl. The pH and conductivity were measured with a Radiometer PHM 84 and CDM 83 before determination of zeta potential. In all cases, the toners had been dispersed for 3 to 7 days before zeta potential measurements.

To determine the contact angles of solutions on toners, the powdered toners were heated in a sand bath to the point of softening and drawn out with a glass stirring rod into thin fibers approximately 1 mm in perimeter. The fibers were cut into 1 cm lengths and suspended from a Cahn electrobalance, in an apparatus described by Berg (Berg, 1986). The pH of the probe solutions was adjusted with NaOH, HCl, and buffers, if necessary. The surfactant solutions were identical to those used in flotation and were either hexadecyl trimethyl-ammonium bromide (HTAB) 5 mg/l, Triton™ X-100 5 mg/l, and NaOH to give pH=11.7, or the same with sodium dodecyl sulfate (SDS) 5 mg/l in place of HTAB. The

same fiber was used for all measurements of each toner type, and between measurements the fibers were copiously rinsed with distilled water to assure complete removal of surfactant. Completeness of removal was verified by close repeatability of measured values. After all measurements were made, hexamethyldisiloxane was used as a known wet-out (0° contact angle) liquid to determine the perimeter of the fiber. This allowed calculation of the advancing and receding contact angles.

Flotation runs were performed by adding approximately 13 g of paper printed with a known toner to 2 liters of deionized water with 0.00325 M NaOH (2% by weight on fiber), yielding a 0.65% consistency and a pH of 12. The 2% by weight on fiber of NaOH and the low (24 °C) temperature was chosen to follow the work of Pfalzer (1979). A low consistency was selected so that the entire slurry could be made into one handsheet, helping to eliminate concerns about obtaining a representative sample of the slurry. The slurry was repulped in a Messmer Instruments Disintegrator Mark.IIIC for 75,000 cycles (25 minutes), and then transferred to a 2.5 liter Wemco flotation cell. One-half to 1 liter of additional deionized water was added during flotation to maintain the liquid level. Flotation was continued for 2 minutes, after which a single handsheet 16 cm in diameter was made from the slurry. The temperature for all the runs was 24 °C.

Before repulping, one of three surfactant combinations was added: Hexadecyltrimethyl ammonium bromide (HTAB) with Triton™ X-100 (each at 5 mg/l), sodium dodecyl sulfate (SDS) with Triton™ X-100 (each at 5 mg/l), or Triton™ X-100 only (5 mg/l). Triton™ X-100 is an octylphenol polyethoxylate (n=10) nonionic surfactant. The purpose of the three surfactant combinations was to probe the effect of surfactant charge on the flotation efficiency by using a representative cationic, nonionic, and anionic surfactant. The concentrations were chosen to optimize between too little froth at lower surfactant concentrations, and too much froth and fiber loss at higher concentrations. The concentrations used gave an 85% fiber yield.

The handsheet was dried and analyzed on both sizes with image analysis. Lens power was set to give a view field 3 cm across horizontally, and all settings were kept constant to ensure comparability of results. Eight areas were randomly chosen on each handsheet (four on each side) for image analysis. Since each area analyzed was about 7:75 cm^2, the total area examined on the sheet was 62 cm^2. The total dirt was measured and reported as parts per million (ppm) area of the paper surface covered by toner particles. To determine the percentage toner removal, the ppm surface coverage was compared with that for a control. A control was prepared by following the procedure outlined using the nonionic surfactant solution but omitting flotation.

Since the image analysis software lists the area of each dirt speck on the handsheet, spreadsheet software was used to determine the size distribution of toner particles. The toner particle sizes are calculated as equivalent circular diameters, so the size of the toner particles refers to the diameter of a circle having an area equal to that measured by image analysis. The resulting data contained a listing of all the particle areas. From this a size distribution is easily constructed and the fraction dirt area attributed to given particle sizes determined. Comparison of handsheets from flotation runs with the control handsheet for each type of printing machine allowed calculation of percentage toner removal (flotation efficiency) for each run, both overall and as a function of toner particle size.

Hallimond tube experiments were made with a 70 mL tube constructed identically to those described by Larsson and Fuerstenau (Fuerstenau, *et al.*, 1991, Larsson, *et al.*, 1984a). The toner was dispersed in the surfactant solution of either SDS and Triton™ X-100 (each at 100 mg/l), HTAB and Triton™ X-100 (each at 100 mg/l), or Triton™ X-100 alone (at 100 mg/l), and stirred for 20 minutes. Flotation was performed for 10 minutes under constant stirring with a single stream of bubbles, and the absorbance of the accepts and rejects was measured at 580 nm on a Bausch & Lomb Spectronic 20. With a calibration

curve relating the toner concentration to absorbance (which was linear over the range of interest), the toner recovery was determined.

3.4 Results and Discussion

3.4.1 Toner Investigation

Table 3.1 describes the toners used in the experiments. The composition data were obtained from Material Safety Data Sheets provided by the manufacturers, and the densities were measured by a Micromeritics AccuPyc 1330 V2.01 pycnometer. The toners selected for study were chosen to represent the variety of toners in use and likely to be found in a wastepaper stream. Six manufacturers, two laser printers, and both low- and high-capacity machines are present.

Four of the 8 toners are magnetic. Whether a toner is magnetic or not depends on the type of machine in which it is used: slower-printing machines typically use magnetic toners, while faster-printing machines use a magnetic developer (also called a carrier), which is not printed on the paper, and nonmagnetic toner. As would be expected, the magnetic toners containing Fe_3O_4 are significantly denser than the nonmagnetic toners. The density of pure Fe_3O_4 is 5.2 g cm^{-3}, of polystyrene is 1.04-1.07 g cm^{-3}, poly(methyl-methacrylate) 1.11-1.28 g cm^{-3}, and carbon black 1.8-2.1 g cm^{-3} (Perry, *et al.*, 1984, p. 3-95, 23-54). For all the toners whose resin composition is known, the resins are copolymers of polystyrene, and either poly(butadiene) or poly(acrylate), although some toners are based on polyesters (Okada and Urushibata, 1991). These materials have low surface energies and give toners their hydrophobic character.

To further investigate the toners both before and after printing, scanning electron micrographs of the unprinted toner powders and of the printed toners on a page were taken.

Table 3.1 Sources of toners and toner properties.

Letter	Source	Resin	Additives	Magnetic?	Density ($g\ cm^{-3}$)
A	Canon NP-115 Copier	Unknown	Unknown	yes	1.55
B	Pitney Bowes 750A	Unknown	Dye	no	1.17
C	Heathtek Laser Writer	Unknown	Unknown	yes	1.49
D	Xerox 5042	Styrene/acryl copolymer	Amorphous silica, zinc stearate	no	1.17
E	Xerox 5065	Styrene/butadiene copolymer	Rosin acid, qauternary ammonium salt	slightly	1.27
F	Xerox 1090	Styrene/acryl copolymer	Quaternary ammonium salt	no	1.14
G	Sharp 8570	Styrene/acryl copolymer	Quaternary ammonium salt	no	1.14
M	Apple Laser Writer	Styrene/acryl copolymer	Salicylic acid chromium chelate	yes	1.52

The results are shown in Figures 3.1-3.4. Figures 3.1 and 3.2 are typical views of toner particles (at different scales). The nearly spherical shape and fairly narrow size distribution

of the toners around 10-15 μm can be seen from the pictures. In their unprinted form all toners appeared the same, with one exception: small particles are seen on the surface of the toner in Fig. 3.1, and analysis by ESCA (electron spectroscopy for chemical analysis) indicates these are silica particles. Contact with toner manufacturers revealed that silica and titania particles of approx. 1 μm diameter are frequent additives, used to improve the powder flow properties in the machine. Our electron micrographs showed that the silica/titania particles were present in all the magnetic toners, but none of the nonmagnetic ones. This is probably because the magnetic particles have a greater tendency to stick to one another. In Figs.s 3.3 and 3.4, the effects of the heat and pressure used in the printing process are apparent. Nearly complete fusion of the independent toner particles into a thin, almost flat coating of the paper surface occurs.

Figure 3.1 Scanning electron micrograph of Apple Laser Writer™ toner. Picture is 27 x 18 μm.

Figure 3.2 Scanning electron micrograph of typical toner particles. (From a Pitney Bowes 750A.) Picture is 80 x 54 μm.

Figure 3.3 Scanning electron micrograph of a printed letter on a page. Picture is 710 x 470 μm

Figure 3.4 Scanning electron micrograph of the edge of a printed letter. Note the fusion of the toner particles. Picture is 183 x 122 μm.

3.4.2 Zeta Potential and Contact Angle Measurements

The zeta potential data are presented in Figure 3.5. Three things are noteworthy about the data: first, the toner zeta potentials are negative across the majority of the pH range, and even those that become positive at low pH become only very slightly positive; second, all the toners' zeta potentials follow a nearly identical pattern of change with respect to pH, each toner changing its zeta potential about the same amount for the same change in pH; and third, the zeta potentials form nearly a continuum in values over a 40 mV range at all pH values. The results suggest that the surface chemistry determining the zeta potential is similar in cause, and varies in degree.

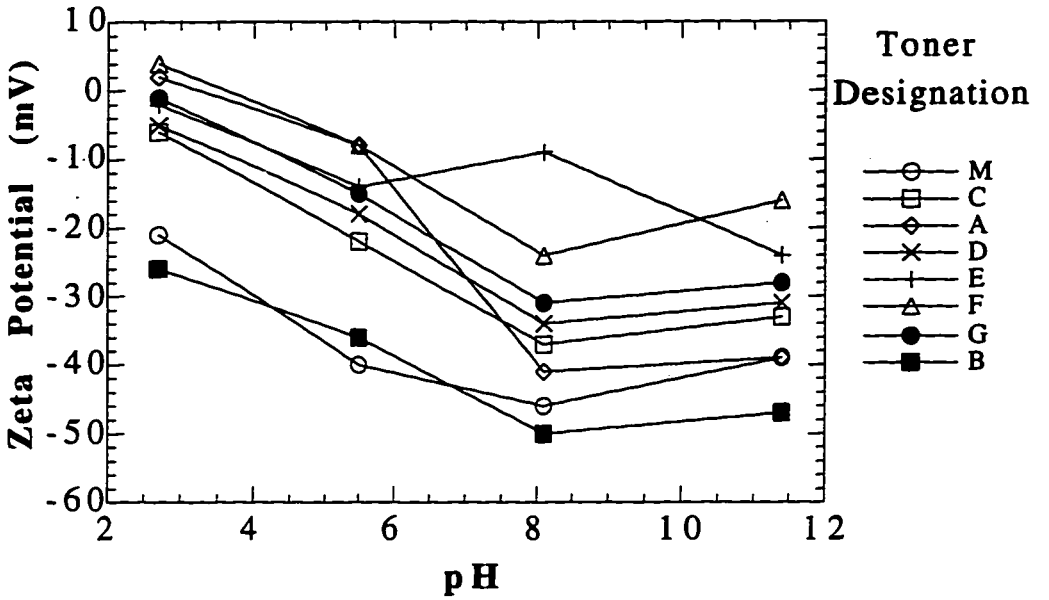

Figure 3.5 Zeta potential of toners vs. pH. Temperature = 24 °C.

The advancing and receding contact angles of solutions of pH from 4 to 12 are presented in Figs. 3.6 and 3.7. The contact angles were large for both advancing and receding modes, indicating the high degree of hydophobicity of the toners. The contact angles are also seen to be only weakly dependent on pH, with the exception of toner M, the Apple Laser Writer toner, where the receding angle is 0° at pH>10. It should be noted that the pH can affect the oxidation state of the Fe_3O_4 (if any resides on the surface) and thus the wettability, and this may be a factor in the contact angle vs. pH data for the magnetic toners, such as toner M (Wang and Audebert, 1988). The contact angle hysteresis (the difference between the advancing and receding angles) averaged 34° for all the toners over the pH range tested. The hysteresis represents the physical and chemical heterogeneity of

the surface (Johnson and Dettre, 1969) and a 34° average hysteresis is not unusual for a multicomponent material prepared without steps to minimize surface roughness.

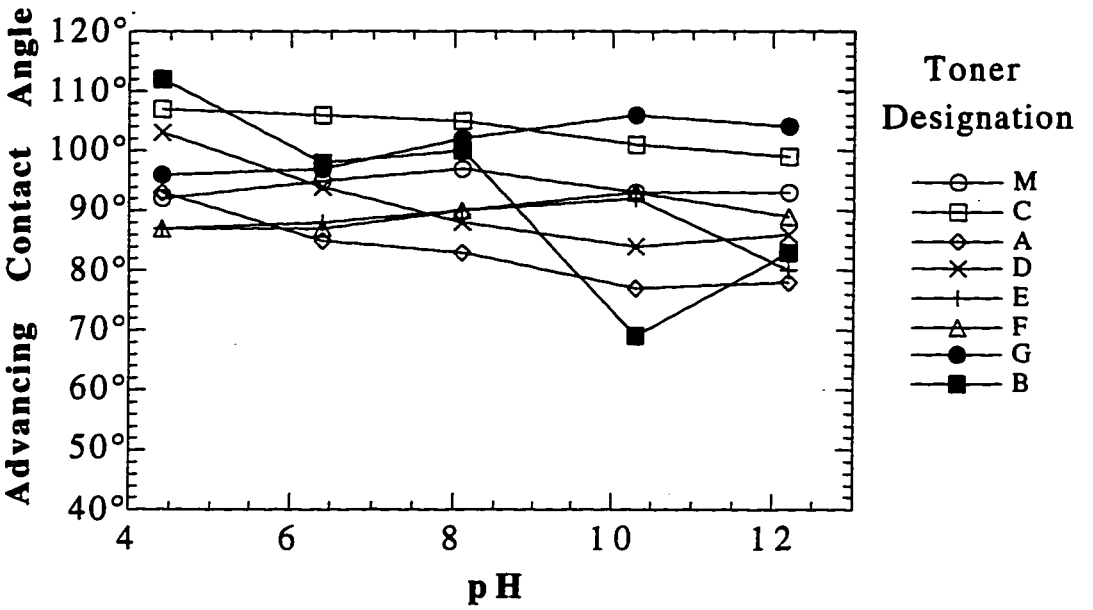

Figure 3.6 Advancing contact angle of toners vs. pH. Temperature = 23 °C.

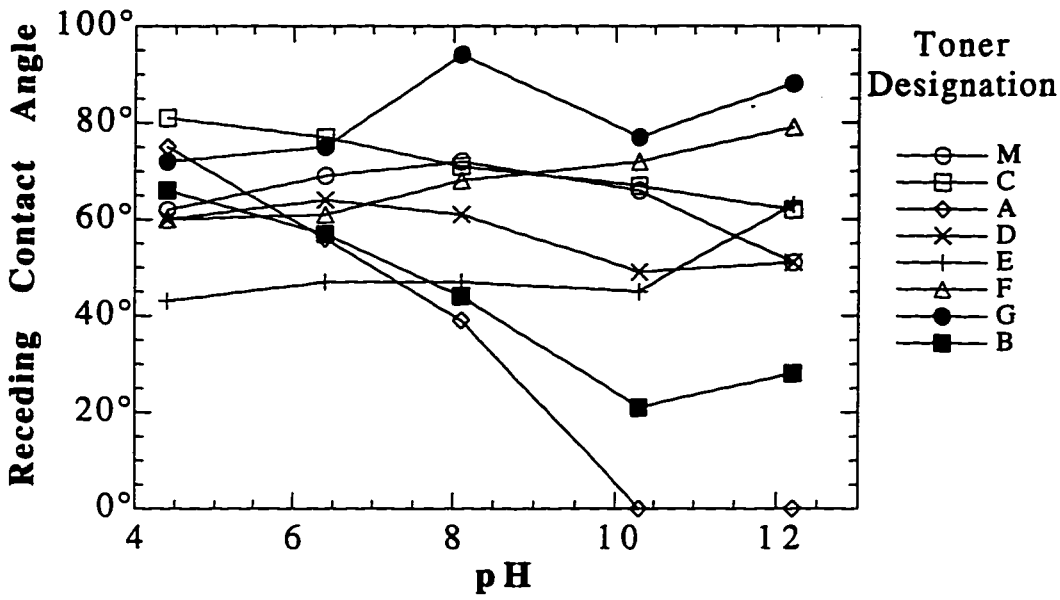

Figure 3.7 Receding contact angle of toners vs. pH. Temperature = 23 °C.

A comparison of the measured contact angles and the zeta potentials for all the toners at pH 12 is presented in Figure 3.8. In general, the lower the zeta potential, the lower the receding contact angle, while the advancing contact angle remains nearly constant. Since the receding contact angle most represents the hydrophilic regions on the toner surface (Johnson and Dettre, 1969), it can be concluded that the surface chemistry that gives the toner a low zeta potential is more hydrophilic than other parts of the surface. This is expected because the surface charge responsible for the zeta potential is probably caused by ionized functional groups on the toner surface or the specific adsorption of ions in polar regions of the surface. In addition, the advancing contact angle, which is representative of the most hydrophobic regions of the toner surface, such as polystyrene chains, is essentially independent of the zeta potential.

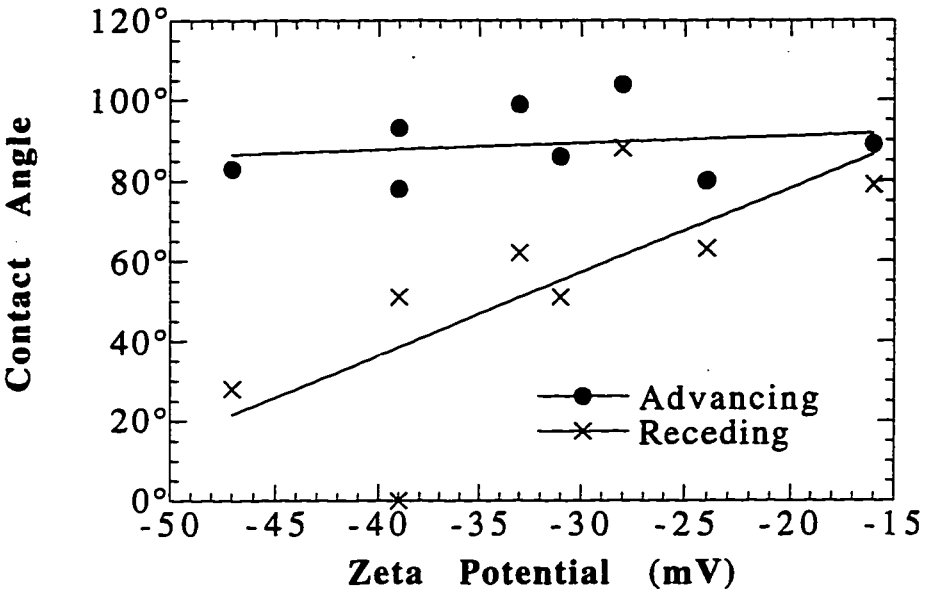

Figure 3.8 Contact angle of toners vs. zeta potential. Temperature = 24 °C, pH = 12.

The measurement of the wettability of the toner as represented by the contact angle and the surface charge as represented by the zeta potential provide important characterization of the toner surface. In the present study, insight into the flotation de-inking of the toners is sought, and flotation separates finely divided solids based on wettability differences. Very often, however, the wettability differences need to be controlled by addition of the proper surface active compounds. Primary among these is a collector chemical that functions to adsorb to one particle's surface to render it hydrophobic. Finding such a chemical can make possible or greatly enhance a flotation separation. By characterizing the surface, therefore, some guidance in the type of collector that might be most useful is sought.

Our measurements of toner contact angles indicate the toners are naturally hydrophobic, while previous work on pulp fibers has shown that they are more

hydrophilic, with average advancing contact angle at pH 12 of approximately 29°, and receding angle of 0° (Jacob and Berg, 1993). Compared with the toners (average contact angle at pH 12 is 89° advancing and 53° receding), it appears that the flotation of toner particles away from the pulp fibers should occur spontaneously, with the addition of only a frothing agent. This is analogous to the case in mineral flotation of separating graphite or talc or another naturally hydrophobic mineral from its gangue. Nonetheless, flotation experiments carried out with the addition of the nonionic surfactant Triton™ X-100 at 5 mg/l with NaOH did not give better than an average 76% toner removal. An attempt to float the toners without any added surfactant was made, but the lack of frothing prevents any separation from occurring. The results for adding a small amount of Triton™ X-100 nonionic surfactant are included in Figure 3.9, and are not significantly better than using the Triton™ X-100 in combination with an equal amount of HTAB or SDS.

3.4.3 Flotation Performance of Printed Sheets in Wemco Cell

The results of the flotation experiments are presented in Figure 3.9. On average, each of the 3 surfactant combinations was equally effective, removing 76% of the toner. However, if the anomalous results for the Canon NP-115 toner are removed, there is 78% average removal with the SDS and frother, 81% average with the frother only, and 84% average with the HTAB and frother. These results indicate that the cationic collector functions most effectively, the anionic collector least effectively, with the nonionic frother intermediate. Because of the negative zeta potentials of the toners at pH 12 (the conditions of the flotation experiments), it is expected that the cationic collector would best adsorb to the toner surface in a head-down fashion and maintain the toner hydrophobicity and the anionic collector would do the opposite, giving the trends mentioned. The effect, however, appears to be small, and the opposite result was found with the Canon NP-115 toner.

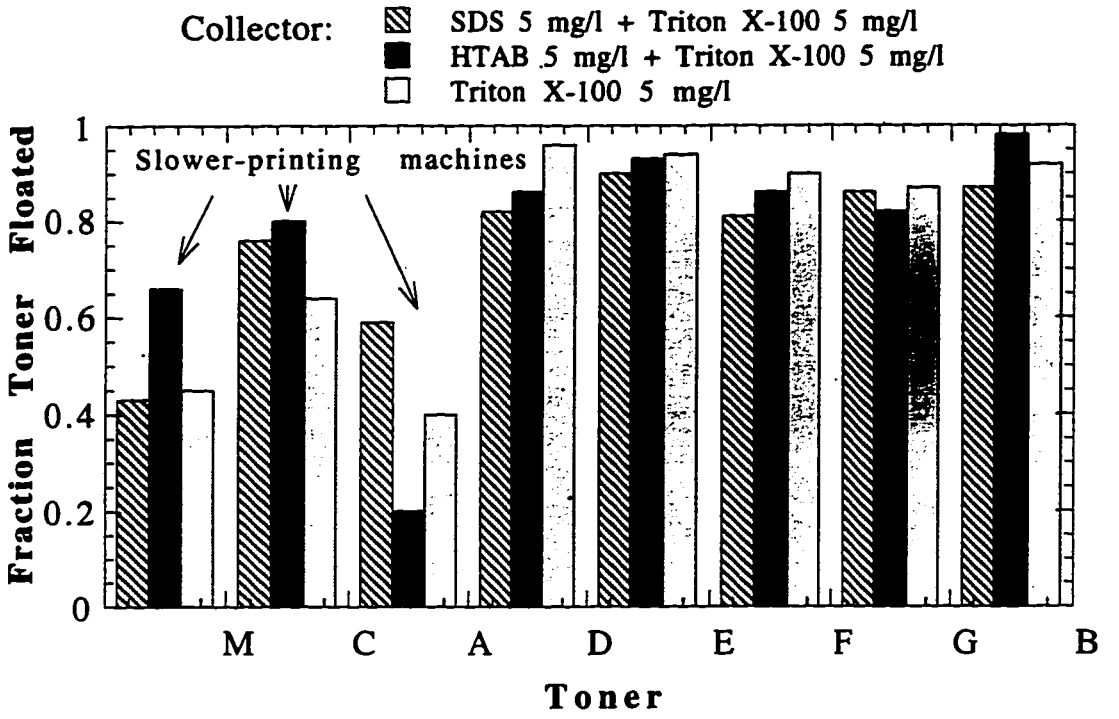

Figure 3.9 Fraction toner floated vs. toner type. SDS: 5 mg/l SDS + 5 mg/l Triton™ X-100. HTAB: 5 mg/l HTAB + 5 mg/l Triton™ X-100. TRITON™: 5 mg/l Triton™ X-100. Temperature = 24 °C. Consistency = 0.65%. pH = 12. Flotation time = 2 minutes.

To gain better insight into the flotation performance, contact angles of the flotation solutions of SDS and HTAB were measured on the toner fibers. The surface tension of the solutions was measured by the Wilhelmy method and found to be 47.3 mN m^{-1} at 23 °C for the SDS solution and 45.3 mN m^{-1} for the HTAB solution. The average contact angles obtained are presented in Table 3.2. These results accord with the view that the HTAB adsorbs more strongly in the head-down position on the toner surface and thus gives a larger receding contact angle. The lower advancing contact angle of the HTAB solution probably results partly from the lower surface tension of the HTAB solution. Among the different toners, the contact angles did not vary greatly and the contact angle and flotation

recovery are unrelated for either the SDS or HTAB solutions for both advancing or receding angles. These graphs are presented in Figures 3.10 and 3.11.

Table 3.2 Average contact angles on all 8 toners for aqueous solutions of SDS and HTAB.

Solution	Advancing	Receding
SDS	68°	13°
HTAB	60°	26°

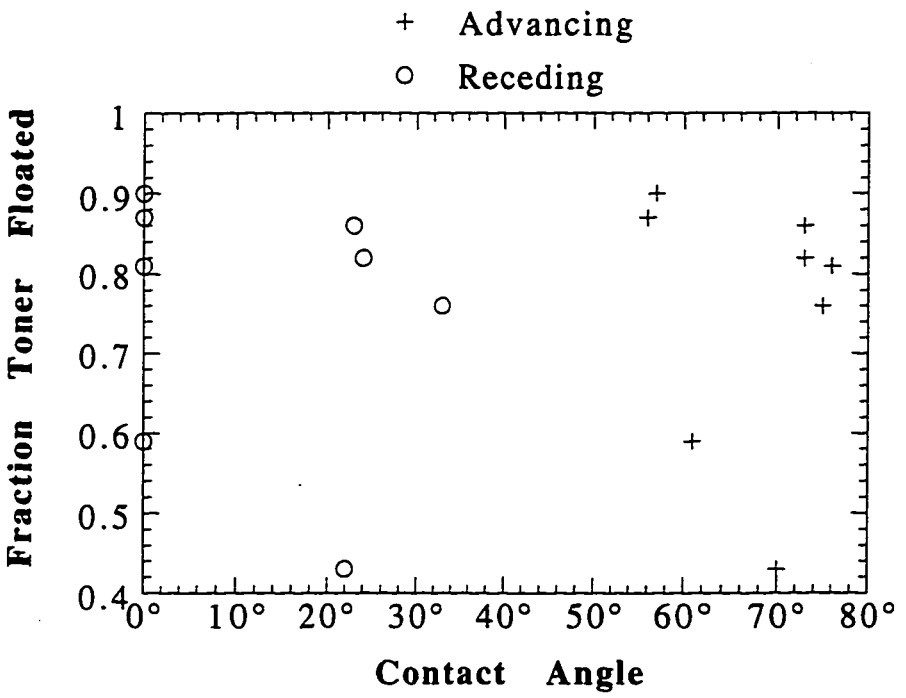

Figure 3.10 Flotation performance vs. contact angle for SDS solutions. 5 mg/l SDS + 5 mg/l Triton™ X-100. Temperature = 24 °C. pH = 12.

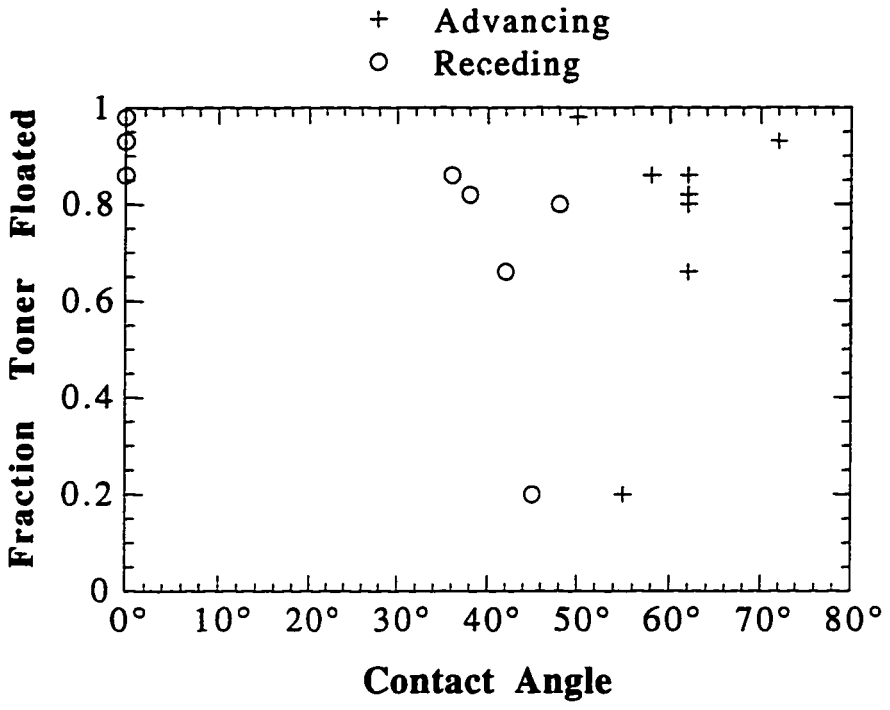

Figure 3.11 Flotation performance vs. contact angle for HTAB solutions. 5 mg/l HTAB + 5 mg/l Triton™ X-100. Temperature = 24 °C. pH = 12.

The most significant difference in flotation performance exists among the three slower-printing machines, the Apple Laser Writer, Heathtek Laser Writer, and Canon NP-115 Copier, and the five faster-printing machines. The slower-printing machines averaged a 55% toner removal, with a range from 20% to 80%, while the five faster-printing machines averaged 89% toner removal with a range of 81% to 98%. The toners from the slower-printing machines are magnetic and much denser, while the toners from the faster-printing machines are nonmagnetic and have a density closer to water, except for the Xerox 5065 toner. This toner is observed to be slightly magnetic, but its low density indicates that Fe_3O_4 is only a small fraction of its composition, unlike the slower-printing toners, where Fe_3O_4 appears to be present at 30-60 wt%.

3.4.4 Flotation Performance of Toner in Hallimond Tube

To better control the flotation process, studies were performed with a Hallimond tube allowing the bubbles to enter one at a time. Furthermore, the Hallimond tube studies were performed with unprinted toner powder, giving a constant toner size distribution, and since no pulp fibers were added, the floatability of the toner apart from any fiber effects was studied. A comparison of the fraction toner removed with that in the Wemco cells is shown in Figure 3.12. The average percentage toner removed for all the toners in the Hallimond tube is 55% versus 75% for the Wemco cells, but more notably, the two showed opposite trends for each of the toners, so that the toner the best removed by one method is likely to be the toner least well removed by the other method. In particular, the toners from the slower-printing machines were best removed by the Hallimond tube. However, the runs are not directly comparable since to disperse the toner in the Hallimond tube, 20 times the concentration of all surfactants was used. This is because the vigorous action of the pulper disperses the toner easily at much lower surfactant concentration in the runs on the Wemco cells than does the magnetic stir bar agitation used for the Hallimond tube.

The difference in flotation recovery between the Wemco cells and the Hallimond tube is probably caused largely by differences in particle size. Both upper and lower limits to particle sizes that are effectively floated are well known in the flotation literature, with the exact numbers depending on the particular system (Amand and Perrin, 1991, Schulze, 1991, Woodward, 1992). In the Hallimond tube, the toner particles are 10-15 μm while the particles in the Wemco cells were 10-1000+ μm, with a *number* average near 100 μm. Flotation performance is reduced as the particle size approaches the lower practical limit, and for flotation de-inking of oil-based inks, reduction in flotation performance is often observed below 20 μm (Larsson, *et al.*, 1984b; Amand and Perrin, 1991, Larsson, *et al.*, 1984b, Woodward, 1992). The difference in the trends observed between the Hallimond

tube and Wemco cell for the toners of the slower-printing machines probably depends on two factors: first, the toners from the slower-printing machines are denser so they more effectively collide with bubbles, particularly at small particle sizes; and second, the magnetic toners from slower-printing machines have a tendency to aggregate very quickly when dispersed in solution. Both effects would increase the ease of floating small particles.

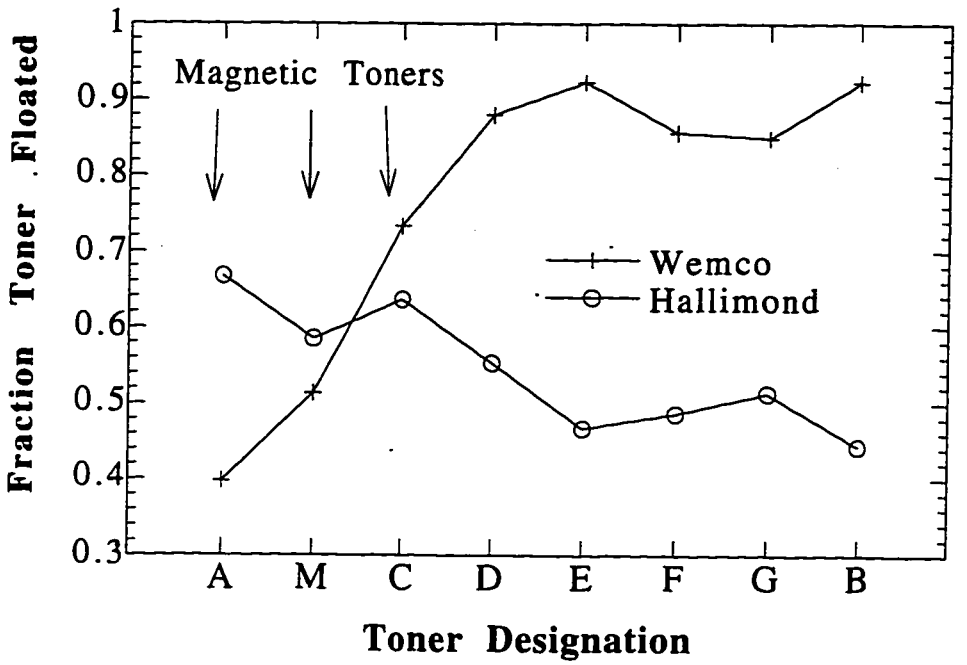

Figure 3.12 Comparison of flotation performance for Wemco cell and Hallimond tube.

3.4.5 Toner Particle Size Analysis

Figure 3.13 shows the cumulative size distribution of one slower-printing machine toner and one faster-printing machine toner. The size distributions are those after repulping

and before flotation, calculated with the control (no flotation) handsheet. The size distributions are *area*-weighted, so F(A) is the fraction of the dirt area attributable to particles smaller than a given size. The slower-printing machine toner is seen to have a much larger size distribution, with a median size of 600 μm compared to 400 μm for the faster-printing machine. These results are found for *all* the toners and lead to the conclusion that the slower-printing machines produce larger toner particles during repulping. This may be true only for the low consistency disintegrator repulping used in this study, because the repulping conditions would affect the toner particle size distribution. In any case, the larger particles may be less effectively removed by flotation.

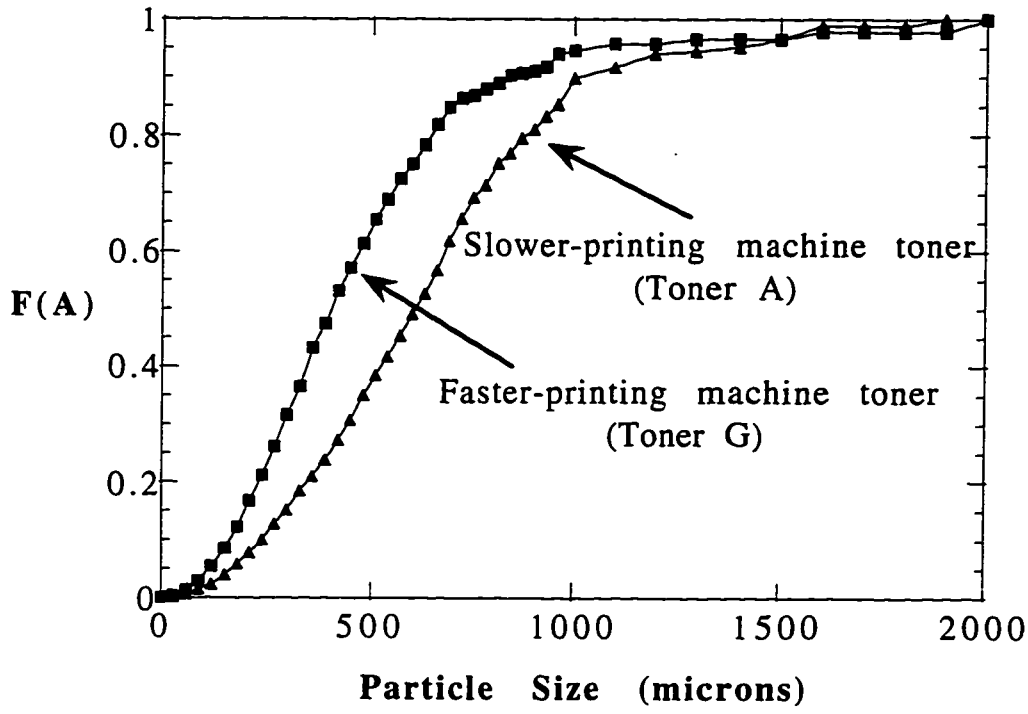

Figure 3.13 Representative toner particle size distributions after repulping.

But more striking, Figure 3.14 indicates that the two types of machines show different behavior when the flotation effectiveness is plotted versus toner particle size. Here, the average of the faster-printing machines shows that these toners are effectively floated at all particle sizes. In fact, the larger particles appear to be removed even more effectively than the smaller particles. However, the removal of the toner particles from the slower-printing machines contrasts with this. These toners are well removed at the smallest particle sizes (less than 100 μm), but removal efficiency decreases steadily with increasing particle size, approaching nearly zero for particles 900 μm in diameter. Therefore, the poorer flotation removal of the toners from the slower-printing machines is primarily attributable to the particles larger than 100 μm.

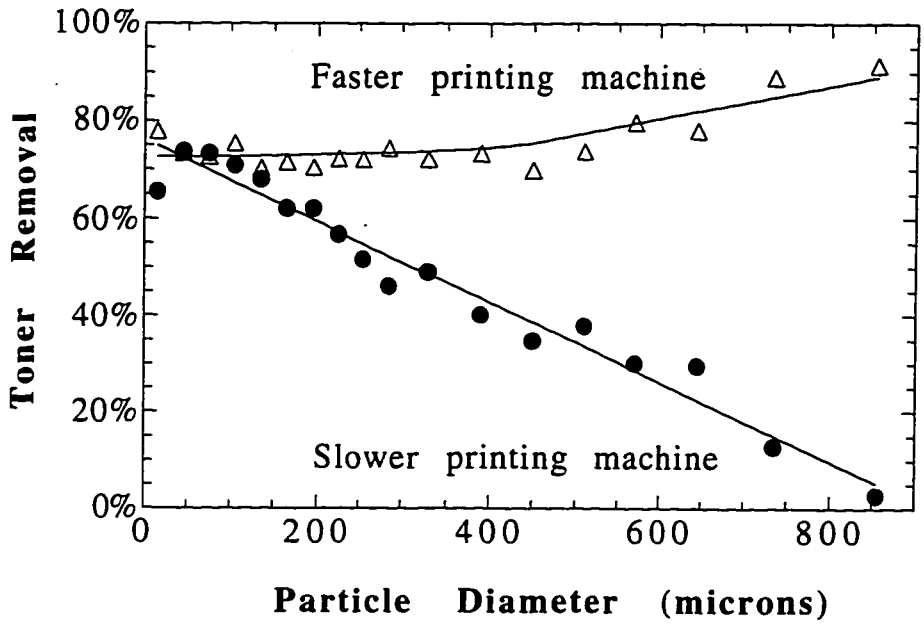

Figure 3.14 Flotation efficiency vs. particle size. Faster-printing machine = Pitney Bowes 750A. Slower-printing machine = Apple Laser Writer.

In considering why the trends of removal efficiency with particle size are so different for the two types of machines, we recall that the slower-printing toners are denser and magnetic. Because of the magnetite (Fe_3O_4) present at 10-30 wt%, the densities of these toners average 1.5 ±0.04 g/mL, while the toners from the faster-printing machines average 1.2 ±0.07 g/mL. The denser particles may not effectively attach to the bubbles during flotation, but more likely the denser particles are less likely to remain attached to the bubbles in the turbulent flotation cell. A maximum size of particles that are effectively floated is a well-known phenomenon in mineral flotation, and models given by those such as Schulze indicate that the maximum particle size depends on density (Schulze, 1984, ch. 2-3).

Another explanation suggests itself when printed sheets from the two types of machines are carefully examined. The slower-printing machines produce printing that appears to be darker and thicker. This may be a natural consequence of the longer time the sheets spend in the printing process. In particular, the slow passage through the hot roller section of the printing device may lead to deeper fusing of the toners to the paper fibers by mechanical entanglement. The result of this is that the larger toner particles produced by the slower-printing machines contain attached fibers after pulping. The larger the particles, the more likely a particle contains fibers and the more fibers it contains. These fibers greatly retard effective flotation for two reasons: first, the fibers are hydrophilic and have no driving force to attach to the bubbles. Second, when the toner-fiber conglomerates are attached to the bubbles, the fibers increase the exposure of the particle to the turbulent forces present in the flotation cell and increase the rates of particle detachment, reducing the chance the particle is carried into the froth layer.

Strong evidence for the second explanation of poor floatability is provided by Pan *et al.* (1993). For their system, examination of toner particles fed into the flotation cell finds that 58% contain attached fibers. The flotation rejects contain only 10%, while the

accepts contain 68%. Furthermore, Pan *et al.* find that virtually all the large (>500 μm) particles fed to the flotation cell contain attached fibers, while 76% of the medium (200-500 μm) and only 30% of the small (<200 μm) contain any attached fibers.

Both explanations of the trends of poor flotation efficiency of the large toner particles from the slower-printing machines indicate that these particles are easily detached from the bubbles in the flotation cell. Both mechanisms may operate together. In any case, the causes for the observed trends of the slower-printing machines are not present to any significant degree for the faster-printing machines.

3.5 Conclusions

Despite the variety of machines from which the 8 toners originate, the toners are more similar than different. In particular, all toners have a moderately negative zeta potential at pH values above 3, and all the toners are hydrophobic, exhibiting high advancing and receding contact angles across the pH spectrum. Furthermore, the more negative the zeta potential, the lower the receding contact angle, indicating the greater density of hydrophilic sites that become negatively charged in solution. It seems likely that the toners have the same kind of surface groups and features, but that the number of the ionizable groups varies by toner. For acrylate copolymers, one possible type of ionizable surface group is carboxylic acids formed by ester hydrolysis.

The differences in the de-inkability of the toners by flotation are not great, except for the slower-printing machines with magnetic toners. These toners are much more dense, produce larger toner particles on breaking up during repulping, and appear to be printed more thickly on the paper. The differences in ease of flotation de-inking are most likely related to one of these factors and not to differences in basic surface chemistry. The large toner particles formed and the thicker printing of the sheets are probably most responsible.

Other authors have observed a dependence of flotation performance on the kind of machine used for printing (Quick and Hodgson, 1986, Cathie and Crow, 1991). The slower-printing machines may fuse the toner more solidly to the fibers, which remains attached to the fibers and in thicker, larger pieces after the same repulping treatment. These pieces may be too large and dense to attach effectively to the bubbles in flotation, and toner particles attached may be more easily detached by the turbulence of the flotation cell. Similarly, fibers remaining attached to the toner particles may retard bubble attachment and enhance detachment because of the increased drag exerted on the particle-fiber pieces. The strong dependence of flotation performance on size is well known, and there is an optimum size range for the particles, which, when exceeded or not reached, gives poor flotation results.

The Hallimond tube results may be so sensitive to the size of the toner particles that the results depend primarily on the agglomerating tendency of the fine, unprinted toners. These small toner particles agglomerate to different degrees when dispersed with surfactants. The magnetic toners, probably because of magnetic attraction forces, are observed under a microscope to agglomerate most easily and these are the toners that give the best recovery with the Hallimond tube. This, and the greater densities of the magnetic toners, are probably most responsible for the better recovery of these toners in the Hallimond tube. In both the Wemco cells and the Hallimond tube, the flotation results appear to be more determined by the particle size and density than wettability phenomena within the examined range of conditions. However, the lower average toner recoveries in the Hallimond tube compared with the Wemco cell are probably related partly to the 20 times greater concentration of surfactant used in the Hallimond tube, which significantly reduces the nonwetting nature of the toners. Unpublished work of the authors has shown that increasing the surfactant concentration decreases the toner removal, because the strong adsorption of the surfactant at the toner/solution interface reduces the hydrophobicity of the toner.

The results on toner particle size suggest three things for de-inking. First, difficulties in flotation de-inking of the electrostatic inks are probably caused by the sheets from slower-printing machines. Second, the larger particle sizes from these machines are the most troublesome. Third, optimizing repulping to produce the smallest toner particles and to achieve the greatest toner-fiber separation is a key step for successful flotation of electrostatic inks.

For truly effective flotation de-inking, the toners need to be removed with efficiencies of 99+%, and the natural hydrophobic character of the toner combined with the more hydrophilic nature of the pulp fibers indicates that this should be achievable. The size and shape of the toner particles formed from repulping printed sheets and residues of toner remaining attached to hydrophilic fibers after repulping are likely causes of sub-optimal performance. The toner and fiber wettability differences should accomplish the separation by flotation if only the minimum necessary amount of frother is added and the hydrodynamic and mechanical aspects of flotation (such as particle and bubble size) are optimized. For those interested in an in-depth study of the effect of toner particle shape and size on their flotation removal, pursued partly in consequence to the observations reported above, see Schmidt and Berg (1994,1996).

CHAPTER FOUR

LIQUID BRIDGE AGGLOMERATION

4.1 Introduction

This chapter extends the work from the previous chapter which describes the surface chemistry of a variety of toners, to the first-ever reported study of agglomeration de-inking. In the present investigation, a simple liquid bridge agglomeration method is used to collect toner particles, and this is examined under a variety of conditions, including in the presence of the numerous components of commercial paper. This provides a model for a low-temperature agglomeration process, which is valuable in itself (see Section 1.2) and also provides a beginning for the systematic understanding of how agglomeration operates.

4.2 Background

Toner-printed furnishes are often difficult to handle with conventional de-inking methods. One solution may be to agglomerate the toners with suitable chemicals (Ferguson, 1992b). In this process, such chemicals are added to the repulper while a certain temperature and good mixing are maintained. Typically, agglomerates form within 15 to 45 minutes. Screening (size differences) or centrifugal cleaning (density differences) separates the toner downstream.

Unlike dispersion, agglomeration is a de-inking process that a mill can add without significant capital investment. In addition, it usually handles toner-printed furnishes

effectively, allowing high-grade fibers to be recovered. These factors combine to make the process attractive.

Current agglomeration processes rely on proprietary chemical formulations and require elevated temperatures (40 °C to 70 °C) (Darlington, 1989, Olson, *et al.*, 1993b). We believe these processes chemically fuse the toners to one another, and therefore produce very strong agglomerates. This chapter presents the results of a study directed at using a different technique to agglomerate the toners. This technique requires only cheap commodity chemicals, like fuel oil, and can be done at any convenient temperature. The agglomerates that result are not chemically bound together, but held together by liquid bridges between the toner particles. These agglomerates are undoubtedly weaker, and the presence of highly sized fibers and cationic starch disrupt the process, but we anticipate further work can minimize these problems. We call this technique "liquid bridge agglomeration."

To separate the toner particles from the fiber slurry, liquid bridge agglomeration uses the difference in the toner and fiber wettability. In this respect, the process is similar to flotation where the toner particles attach to the bubbles because they are hydrophobic while the fibers do not because they are hydrophilic. Likewise, in liquid bridge agglomeration, the added oil droplets stick to the toner particles because they are hydrophobic but not to the fibers because they are hydrophilic. The toner particles then become coated with oil droplets. When two coated toner particles collide, the oil droplets form a liquid bridge between them, holding them together. The process continues until many toner particles are collected into a large, spherical agglomerate (which can be 1 or more cm in diameter) amenable to removal by centrifugal cleaning or screening. The process is depicted in Figure 4.1.

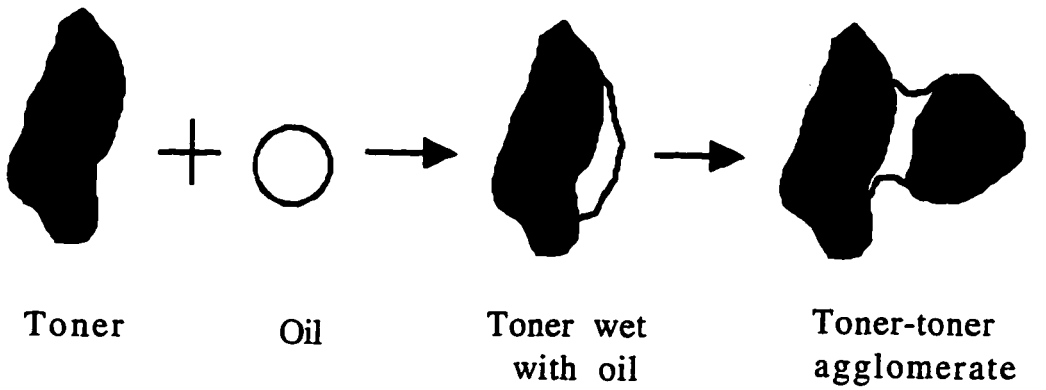

Figure 4.1 Schematic of liquid bridge agglomeration process.

Pietsch (1990, p. 41) outlines liquid bridge agglomeration as a separation technique, and general information is also contained in Snow, *et al.* (1984). "Liquid bridge agglomeration" is our term, and refers to the underlying mechanism; in the literature the technique is often called "spherical agglomeration," "oil agglomeration," "selective agglomeration" or "assisted agglomeration."

Liquid bridges are formed when a small amount of wetting liquid occurs between two solids. The liquid, because it adheres to the solids and develops a curved interface, exerts a force that pulls the solids together. A standard feature of liquid bridges is that the smaller they are, the stronger they are (Farnand, *et al.*, 1961). Thus, very large toner particles are not held together as well as small toner particles in liquid bridge agglomeration. However, it appears that liquid bridges are strong enough to collect and hold together the toner particles produced in the repulper.

The process has aroused the greatest interest in separating coal from ash. The coal particles are hydrophobic like the toner particles, and the ash is hydrophilic like pulp fibers. Just as flotation was adapted to de-inking from the mineral processing field, liquid bridge agglomeration may also find use in de-inking. In fact, one process for de-inking newsprint that uses liquid bridge agglomeration was recently described (Blain, *et al.*, 1993).

4.3 Experimental

The toner composition for the Apple Laser Writer™ toner is presented in Table 4.1 Although it is not mentioned, a few weight percent carbon black is likely present as the pigment. In any case, the predominant component is the styrene-acrylate polymer resin, which is a random copolymer of the two monomers, created so that its glass transition temperature is betwee 50 and 100 °C, making the toner neither too easily fused during shipping, nor too difficult to fuse during its rapid pass through the machine's hot rollers.

Table 4.1 Toner composition for Apple Laser Writer™ toner. Information from the Material Data Safety Sheet provided by the manufacturer (Canon Corporation, Lake Success, NY).

Component	Weight %
Styrene/acrylate copolymer	55-65
Magnetite (Fe_3O_4)	30-40
Salicylic chromium chelate	<2

For the experiments on toner powders without the presence of fiber, the desired amount of the agglomerating oil, n-hexadecane, was volumetrically measured and added to 200 mL deionized water. The mixture was blended at high speed on a VirTis™ "23" homogenizer for 2 minutes to disperse the oil into small droplets. The dispersion was put into a 500 mL beaker and agitated by a magnetic stirbar. While stirring, 0.067 g of a toner from an Apple Laser Writer laser printer was added, initiating agglomeration. After 2 minutes, the run was stopped (it was found that no further agglomeration occurred after

this time for these runs). Samples of toner particles were observed and photographed through a Bausch & Lomb™ light field optical microscope, yielding the pictures shown in Figures 4.4 to 4.7.

For the experiments with both fibers and toner present, a different apparatus was used. It consists of a Cole-Parmer StirPak™ 23 to 2300 RPM 1/10 hp laboratory mixer mounted over a 4 liter cylindrical glass vessel, shown in Figure 4.2.

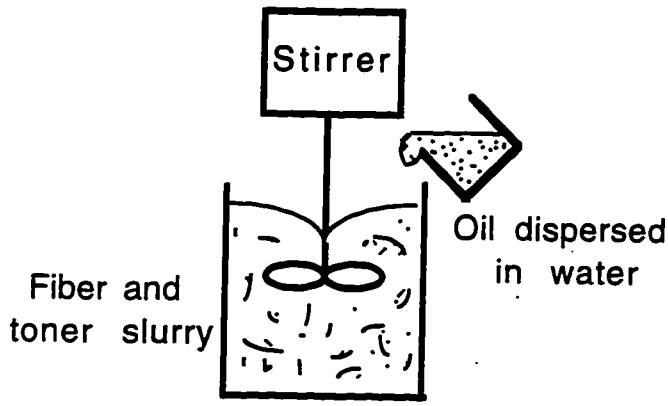

Figure 4.2 Diagram of agglomeration apparatus.

For a typical experiment, the type of paper was selected, weighed out, and torn into pieces. The pieces were added to a 3.8 liter (1 gallon), 3 hp Waring™ blender. The desired amount of an Apple Laser Writer™ toner was then added as an unprinted powder. Lastly, 1.15 liters of deionized water was put in and blended at 15,000 RPM for 2 minutes. The resulting pulp was added to the 4 liter agglomeration vessel and set stirring at approximately 180 RPM. Separately, the desired amount of n-hexadecane was volumetrically measured and added to 200 mL of deionized water and homogenized on the VirTis™ "23" homogenizer at high speed for 2 minutes. The resulting dispersion of hexadecane in water was added to the agglomeration vessel, starting agglomeration. Visual

observations were made during the run, which normally lasted for 30 minutes. Sometimes small samples were taken from the vessel and examined under the Bausch & Lomb™ microscope.

At the beginning of the agglomeration experiments, the pulp was gray and had only very small visible toner specks in it. If the process was successful, the pulp became white, and several 1 to 5 mm toner spheres were formed. Thus, visual observation allowed an effective assessment of agglomeration performance. In unsuccessful runs, the pulp remained gray as no agglomerates were formed. For these runs, examination under a microscope showed many 10 μm toner particles mixed in the fibers.

For the experiment with filler, $CaCO_3$ equal to 20% of the fiber weight was added to the blender and blended with the fiber and toner.

For the experiments with starch, starch equal to 1% of the fiber weight was separately dissolved in 200 mL of deionized water and boiled on a hot plate for 20 minutes. After cooling for 10 minutes, the starch solution was added to the agglomeration vessel before the dispersed oil. To ensure the starch was adsorbing only on the fibers initially, in one experiment the starch was added to the fibers in the blender and repulped with them before the toner was added. The two methods of adding starch gave identical results, however.

Our previous work has shown unequivocally (Chapters 4 and 5) the importance of the cationic polymers that are released from the paper sheet for successful agglomeration (Snyder and Berg, 1994b). Therefore, it is necessary for the acquisition of applicable data that experiments both with and without cationic polymer be performed. The most common cationic polymer in commercial paper is cationically modified starch (van de Steeg, 1992, p. 3). Our work clearly shows cationic starch is released in appreciable quantity during repulping from a sample commercial white paper (Chapter 4). The structure of the molecule is given in Figure 4.3. We will use the commercial brand STA-LOK™ 400,

which consists of a potato-derived starch with qauternary ammonium compounds grafted on the monomer units at a degree of substitution of 0.03. The molecule, like all naturally derived starches, is actually a mixture of two fractions, a mostly linear fraction with molecular weight of the order of 10^5-10^6, called amylose (21% by weight), and a highly branched fraction with molecular weight of the order of 10^7-10^8, called amylopectin (79 wt%) (Swinkels, 1985). The adsorbing properties of this starch have been characterized by us at the surfaces of interest (Chapter 5), and the results of the investigation of the surface forces are expected to increase our understanding of the inhibiting effect of cationic starch for oil drop-toner particle coalescence and thus subsequent agglomeration. The *cationic starch concentration* examined will be either zero, 100 ppm or 1000 ppm.

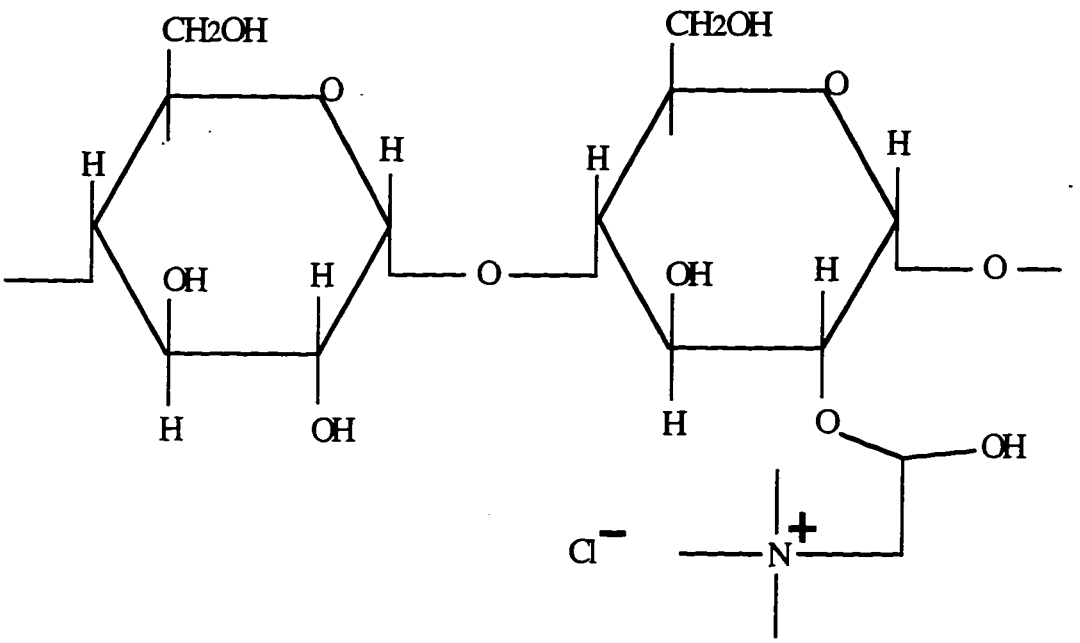

Figure 4.3 Structure of cationic starch. The polymer units are α-glucose, with the cationic groups consisting of trimethyl ammonium chloride. STA-LOK™ 400 has a 0.03 degree of substitution (3 cationic groups per 100 glucose units).

For the experiment on the effect of pH, the deionized water added to the blender for repulping had 0.001 moles of sodium hydroxide added, making its pH=11.

For the 70 °C runs, the standard agglomeration experiment procedure was followed, except hot water was added to the blender for repulping and the agglomeration apparatus was immersed in a constant temperature water bath at 70 °C. All other runs were done at 23 °C.

The agglomeration runs were done at 1% consistency, with 14.3 g weighed fiber (assumed 6% moisture content) added to 1.35 liters of water. Since 14.3 g of paper equals 3 of our standard copy paper (8.5" x 11") sheets, these were printed on an Apple Laser Writer with a standard pattern, and the weight difference before and after printing was determined to calculate the amount of toner on the sheets. The result was 0.114 g per sheet, so 0.342 g of toner was added to the blender to simulate a realistic quantity of toner. Of course, for the runs where printed sheets were used, no additional unprinted toner was added. It was found that whether the toner was added in unprinted form or added as printing on the paper did not matter; either agglomeration occurred in both cases (when filter paper was the paper) or in neither case (when 8.5" x 11" copy paper was the paper). The runs at 5% consistency were identical to those at 1% except for the increase in the amount of toner, fiber, and oil.

N-hexadecane was used as the agglomerating oil because it is nonvolatile (boiling point 287 °C), relatively non toxic, forms a high interfacial tension with water (52 mN m^{-1}) (Israelachvili, 1992, p. 315), and represents a typical fuel oil or diesel fuel, which would be cheap sources of an agglomerating oil. The interfacial tension is important because the strength of the agglomerates depends on it (Pietsch, 1990), and hydrocarbons with significant aromatic contents have lower interfacial tensions with water (about 35 mN m^{-1}) (Israelachvili, 1992. p. 315). If a mill were to use liquid bridge agglomeration, a dosage of

about 20 lbs/ton of fiber would be needed, costing approximately $2 (assuming a wholesale price of $0.50/gallon for diesel fuel and 4 gallons used per ton).

It is important that the oil be added in dispersed form (so that it can reach and contact the toner particles), and this is the purpose of dispersion in the VirTis™ "23" homogenizer. It has two sets of knife-edge blades that rotate at speeds up to 23,000 RPM, producing a dispersion with many 1 to 5 μm size hexadecane droplets (as observed under the microscope). Note that the dispersion is not stabilized by any surfactants, as these would lower the oil-water interfacial tension. Thus, the dispersion coalesces and separates over the course of minutes to hours.

The 8.5" x 11" copy paper was a virgin fiber Hammermill™ paper, while the filter paper was grade 415 VWR™ Qualitative. The starch was STA-LOK™ 400 manufactured by the A. E. Staley Company, Decatur, Illinois, and is a cationic potato-derived starch.

Agglomeration experiments were run for 30 minutes. In general, if agglomeration occurred, it happened within the first few minutes after the dispersed oil was added. Several of the experiments were run longer to observe any further changes (for up to 3 hours), and neither for runs with agglomerates nor for unsuccessful runs was any change after the first 15-30 minutes observed.

4.4 Results and Discussion

4.4.1 Experiments on Toners without Fiber

The agglomeration literature on coal and other hydrophobic minerals suggested that adding a dispersed nonpolar and immiscible liquid ought to agglomerate the hydrophobic particles in a slurry, including toners. To verify that indeed this is the case, we first attempted to agglomerate toner particles in water without fiber or other materials. The concentration of toner in water is based on our calculations of a typical amount of toner in a

repulper (about 0.25 g/liter for a 1% consistency pulp). We vary the oil dosage to observe how this influences the agglomeration.

The oil dosage affects the type of agglomerates formed (Pietsch, 1990, Snow, *et al.*, 1984). Normally, four states are observed (in order of increasing oil dosage): funicular, pendular, capillary, or liquid-liquid particle transfer. In the funicular and pendular states the agglomerates are becoming larger, more spherical, and stronger, until a maximum is reached in the capillary state. This state is reached when the dosage of oil is equal to that which exactly fills the pore volume between the toner particles. For example, if the toners are equally sized spheres the closest packing yields a 0.26 void volume, or an oil/toner volume ratio of 0.35. Further oil addition causes liquid-liquid particle transfer, where the particles disperse in the oil phase. This results in a sharp reduction in strength and soft, spongy agglomerates. The ideal level of oil addition is therefore that which leads to the capillary state.

Figures 4.4 to 4.7 show the results of varied oil dosage on toner particle agglomeration. In Fig. 4.4, the ratio of oil volume to toner volume is 0.08. The individual toner particles show some clumping and appear to be in the funicular or pendular state. In Fig. 4.5, the oil/toner volume ratio is 0.25. In Fig. 4.6 it is 0.6. As is apparent, the size and sphericity of the toner agglomerates increases dramatically with the level of oil addition. By Fig. 4.7, the volume ratio is 0.92. The agglomerate formed is about 1.5 cm in diameter, and the capillary state has been reached. Further oil dosages continue to form centimeter-sized agglomerates, but as expected, the agglomerates became softer and more oily.

These experiments indicate that oil agglomeration works on pure toners and with hexadecane as the agglomerating oil. Also, we know the toners pack more openly than spheres, requiring an oil/toner volume ratio of about 0.92 for the largest and strongest

agglomerates. With this information, we consider agglomeration of toners in the presence of fibers.

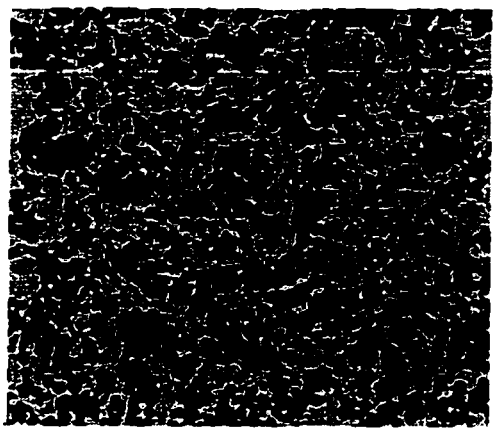

Figure 4.4 Toners agglomerated with 0.08 oil/toner volume ratio. Photomicrograph is 350 μm square.

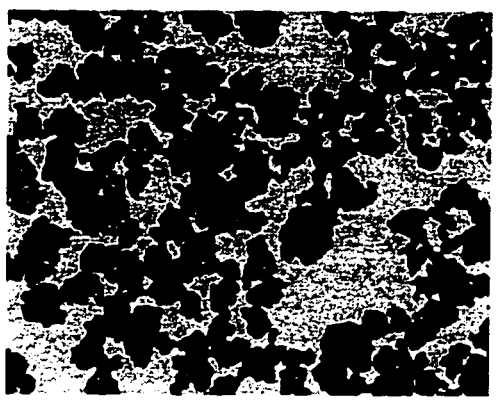

Figure 4.5 Toner agglomerated with 0.25 oil/toner volume ratio. Photomicrograph is 350 μm square.

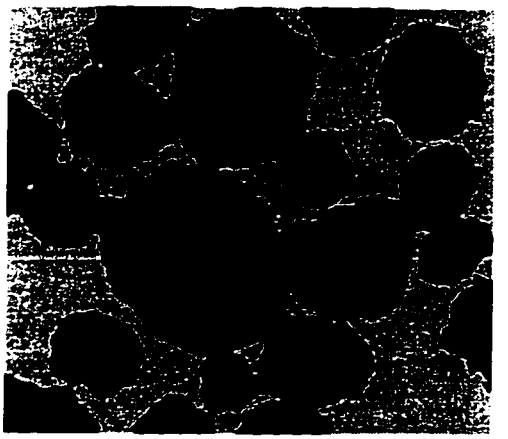

Figure 4.6 Toner agglomerated with 0.60 oil/toner volume ratio. Photomicrograph is 350 μm square.

Figure 4.7 Toner agglomerated with 0.92 oil/toner volume ratio, the ideal. Note this is not a photomicrograph, but a regular photograph. Marks on ruler indicate millimeters.

4.4.2 Experiments on Toners and Repulped Fiber

When unprinted toner particles are added to repulped blank copy papers at 1% consistency, the toner particles no longer agglomerate. If the same amount of toner particles is added to copy paper at only 0.1% consistency, then a modest amount of agglomeration occurs. (A consistency far too low for practical use.) Why does the presence of the copy paper fiber disrupt agglomeration? Further experiments answer this question.

If instead of copy papers, filter paper is repulped, agglomeration is successful, even up to 5% consistency. This indicates that something present in the copy papers but not in the filter papers was responsible. After talking to the manufacturer of the filter papers, we discovered that the filter paper was 70% cotton and 30% wood derived, and had only 0.06% ash content. Also, the filter paper had no filler, starch, or size added.

Working with a dissolving pulp (pure wood cellulose used for making rayon, cellophane, and other materials), we obtain successful agglomeration. This means that the low wood fiber content of the filter paper is not responsible. Adding $CaCO_3$ equal to 20% of the filter paper weight also does not prevent agglomeration in this system, eliminating the filler as responsible.

For investigating the effect of size, 8.5" x 11" sheets with no size and sheets with 5 lbs/ton alkenyl succinic anhydride (ASA) size are tested. The sheets were prepared at the Weyerhaeuser Technical Center in Federal Way, Washington and otherwise were typical paper. On the sheet with no size, a small amount of agglomeration occurs. The slurry becomes significantly less gray, but not white as was the case with the filter paper fibers. Also, the agglomerates are numerous and small. However, when the 5 lbs/ton size papers are used, the agglomeration process was completely disrupted. No agglomerates at all were formed, and the slurry remains dark gray. These experiments thus show that size has a highly deleterious effect on agglomeration, but even without any size, agglomeration is not very effective. The work with cationic starch, discussed next, indicates that it is quite possible that the cationic starch dispersing agent for the ASA size may actually be responsible for the disrupting effect that appears to arise from higher size usage: that is, more cationic starch is present in these sheets as well as size, and it is the cationic starch that interferes with agglomeration.

The effect of the starch is decisive. When added to the filter paper fibers, agglomeration is entirely prevented. Therefore, besides difficulties with highly sized sheets, starch appears to completely block the agglomeration process.

To verify that significant cationic starch is released from our commercial paper, we followed TAPPI test method T 419 om-91 (TAPPI, 1992) for starch in paper using the KI-I_2 analysis. Whitewater from the Hammermill™ white ledger sheets repulped at 1.3% consistency have a starch content of 371 ppm.

The explanation for the disruptive role of the starch is presented in Chapter 5, where the results of an investigation focused on this point is made.

4.4.3 Experiments on the Range of Effective Conditions

Since agglomeration is successful with the repulped filter paper, we can probe its sensitivity to temperature, pH, and consistency. For a temperature of 70 °C, agglomeration is nearly equal to that at 23 °C, indicating that it is not temperature sensitive. Also, the copy paper continues to be unagglomerated at 70 °C, showing that the starch and size maintain their inhibitory effects at this temperature.

Although all experiments reported here are carried out without the presence of caustic (at a pH of 5-7), further experiment established that agglomeration was unaffected by adding sodium hydroxide to raise the pH to 11. Note that the lack of both temperature and pH effects is consistent with the mechanism of liquid bridge agglomeration. The method depends only on the oil droplets sticking to the toner particles, and neither temperature nor pH would affect this strongly.

Experiments at 5% consistency showed that agglomeration works as well as it does at 1% consistency. This is despite the very poor mixing in our apparatus at this consistency. Our equipment does not allow us to attempt any higher consistencies, but as long as the fiber-fiber shearing is not so strong as to breakup the agglomerates that are

forming and that sufficient mixing is available to induce oil-toner and toner-toner collisions at an appreciable rate, higher consistencies will be achievable.

4.5 Conclusions

This chapter reports the investigation of an exceedingly simple method of de-inking toner-printed furnishes. The method requires only 1% by weight on fiber of an inexpensive fuel oil added as a dispersion in water to repulping. Caustic, temperature, and moderate consistencies do not affect the process significantly. In less than 15 minutes, most toner is collected into 1-5 mm agglomerates that ought to be easily removed with conventional downstream processing equipment, such as screens and centrifugal cleaners. The added fuel oil is relatively non toxic: negligible vapor pressure, and easy either to reuse or to dispose of by combustion.

However, cationic starch is found in virtually all stocks and released into the repulper, and this interrupts the agglomeration process. Chapter 5 thoroughly investigates the role of cationic starch in oil agglomeration of toner.

CHAPTER FIVE

ROLE OF CATIONIC STARCH

5.1 Introduction

This chapter describes an investigation focused on understanding why cationic starch effectively blocks agglomeration with a simple oil, but does not affect so markedly the operation of commercial, high-temperature agglomeration formulations. The approach chosen was to compare the behavior of a commercial formulation with the simple oil. Whereas the work presented in Chapters 3 and 4 was needed primarily to *identify* the key issues in successful toner de-inking and agglomeration de-inking in particular, this and subsequent chapters present results of studies that serve to *understand* how the key issues operate in the agglomeration process.

5.2 Background

Betz Paperchem, Inc., PPG Industries, Inc. and Nalco Chemical Company (at a minimum) have developed agents that can be added to the repulper to agglomerate toner particles (Darlington, 1988, Olson, *et al.*, 1993b). The products are often effective (Rhodes and Ferguson, 1993). For both the Betz and PPG products, patents have been obtained which provide detailed composition information. Because Betz sent us a sample, have available patents and one mill found it to be the most effective, we chose the Betz product as the experimental sample.

A description of the use of the Betz product follows (Richmann and Letscher, 1992, Richmann and Letscher, 1993a, Richmann and Letscher, 1993b, Richmann and Letscher, 1994). Paper is repulped that contains at least 10-50% (Betz says 10% is all that is needed, mill says 50%) toner-printed paper. During the repulping the temperature is raised to ideally about 65 °C. The Betz liquid is then metered in at approximately 1% of fiber weight. Continuous agitation in the repulper is maintained, preferably for 60 minutes. During this time the toner particles ought to be collected into large clumps, often a millimeter in diameter. Downstream, about 10% of the toner will come out as the fibers pass through slotted screens (with slot openings 200-300 μm) and the remaining 90% of the toner will be removed by forward cleaners. Forward cleaners are centrifugal separators that remove species that are heavier and have less hydrodynamic drag than the pulp (reverse cleaners remove lighter materials). The composition of the liquid, as described in the most recent patent (Richmann and Letscher, 1994) as the "most preferred embodiment of the invention" is given in Figure 5.1.

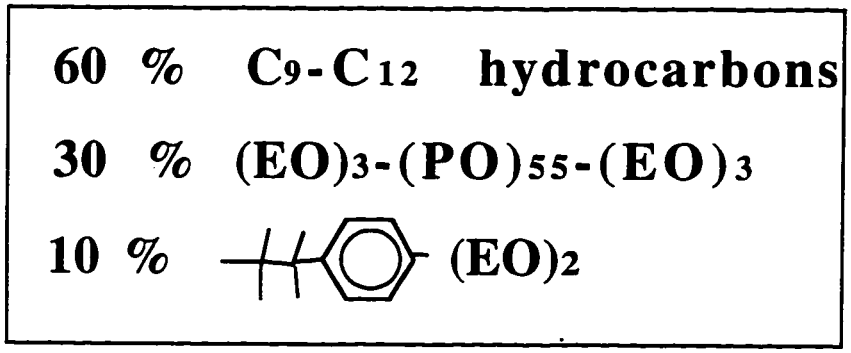

Figure 5.1 Commercial agglomerant composition. Most preferred composition according to Richmann and Letscher, 1994.

Other patents cover all surfactants with an HLB value less than 10 for toner-printed de-inking. The HLB is the hydrophile-lipophile balance and provides a scale for ranking

the relative contributions of a surfactant's hydrophilic and hydrophobic portions (Griffen, 1949). An HLB of 10 indicates a particular surfactant is equally soluble in both water and hydrocarbons (and therefore has approximately equal hydrophilic and hydrophobic portions), while lower numbers indicate increasingly hydrophobic and oil-soluble surfactants, and higher numbers the converse. Normally ionic surfactants, *ipso facto*, are much more soluble in water and so have high HLBs, sometimes up to 40. The use of surfactants of HLB less than 10 (with less than 5 most preferred) indicates species most like oils and with little water solubility. The composition given in Fig. 5.1 includes about 40% of these very low HLB surfactants, with the balancing 60% pure hydrocarbons. This mixture is homogeneous.

An important point about the Betz product is that it requires high temperature for maximum effectiveness, unlike using a simple oil. Also, we notice is that the Betz liquid composition in its most preferred form is a mixture of pure hydrocarbons (like the simple oil) and oil-soluble surfactants. (The surfactants are such low HLB, 1 or 2, that the surfactants are insoluble in water.) So that focuses the investigation into: why does mixing a pure oil with oil-soluble surfactant result in an agglomeration process that operates even with cationic polymers present, while a pure oil alone is ineffective with cationic polymers present?

5.3 Experimental

5.3.1 Agglomeration

The toner powder used is the Apple Laser Writer™ toner used in previous agglomeration experiments. The hydrocarbon oil is n-hexadecane, chosen for its simplicity, nonvolatility, and insolubility in water. The commercial oil blend is the Betz product, as received. Since we have a non-analysis agreement with them, its exact

composition is not known, but the listing in Fig. 5.1 is probably a good guide. Furthermore, when we make up mixtures like that given in Fig. 5.1, they exhibit identical behavior to the sample received from Betz. Thus, its composition is likely very close to that given by their patent. The cationic starch is the same as used in previous agglomeration experiments, STA-LOK™ 400 cationic starch with a degree of substitution of 0.03 (see Fig. 4.3). Sodium chloride is the salt used, with a purity of 99.9%.

Agglomeration experiments are done in the following manner: toner powder was dispersed in water at 0.1 wt% by mixing the toner at 15,000 RPM on a Waring blender for 2 min. Separately, the agglomerating liquid was mixed in water at 1 wt% and blended at 23,000 RPM on a VirTis™ Homogenizer. With a circulating water bath maintaining the desired temperature, 25 mL of the toner dispersion and 2.5 mL of the agglomerating liquid dispersion are mixed into a 30 mL beaker which is inserted into the water bath and stirred moderately from above, yielding the experimental concentrations 0.09 wt% toner particles and 0.09 wt% agglomerating liquid in water. The mixture stirs for 15 minutes to allow agglomeration, immediately after which it is observed for the extent of agglomeration. For runs with cationic starch present, the toner is dispersed in a 0.1 wt% cationic starch solution instead of water and the experimental cationic starch concentration is thus 0.09 wt% (after dilution with oil dispersion).

The experimental run always starts with 23 °C water. At the beginning of the run, the 27.5 mL of dispersion is submersed into a constant temperature water bath. Since the sample size is small, the time constant for temperature equilibrium is small (1.4 min) compared to the run time (15 min). The temperature difference is observed to follow Newton's law of cooling.

The results of the experiments were most reliably indicated by visual observation and ranking on a scale of 0 to 6, where 0 means no detectable difference between in the degree of toner dispersion occurred. A 6 signifies a dispersion that is completely

agglomerated, with no turbidity remaining and all the toner collected into a few >1 mm spheres.

5.3.2 Wettability and Zeta Potential

Wettability of toner surfaces was measured by repeatedly printing the Apple Laser Writer™ toner, using printer of same name, onto a transparency to develop a thick coating. This was then glued to the bottom of a windowed chamber that was filled with either water or a cationic starch solution (0.1 wt%). A mounted syringe filled with the agglomerating liquid is bought near contact with the toner surface, and as fluid is metered out, a drop forms on the toner surface. The advancing contact angle is recorded as the drop advanced on the toner surface, displacing the aqueous phase.

Electrokinetic experiments rely on the dispersing of the toner mechanically (as described above for the agglomeration experiments) with the Waring blender. A Rank Brothers Mark II microelectrophoresis apparatus is used to observe the movement of the 10 μm toner particles in response to the applied electric field (10 V/cm). No dispersing agent for the toner is used since experiments show that this changes the zeta potential. For runs with cationic starch, the toner is dispersed in a 0.1 wt% cationic starch solution.

For the electrokinetic experiments as a function of temperature, it is found that at elevated temperatures (>40 °C) the lower viscosity of water permits excessively rapid settling of the particles. Therefore, all electrokinetic measurements as a function of temperature (figure 5.5) are done in 40 wt% glucose solution. The dielectric constant as a function of temperature is obtained from the literature (Akhadov, 1980). The viscosity as a function of temperature is determined with a Canon-Fenske capillary viscometer, submersed in a thermostatted water bath. During the actual electrophoresis experiments, sample temperature is maintained by a thermostatted water bath surrounding the microelectrophoresis cell. Thermal convection of the observed toner particles is

unavoidable with our set up at higher temperatures. To obtain electrophoretic mobilities, therefore, each toner particle is measured moving in both directions in the cell (that is, with the polarity of the applied potential first one way and then reversed). The results are vectorally averaged, effectively canceling out any underlying particle drift. The results are very reproducible obtained in this manner, both for individual particles and for group averages.

For electrokinetic measurement of liquid drops, the drops are dispersed ultrasonically (see 5.3.3, below) and otherwise treated as any other particle. O'Brien and White theory (1978) is used to convert electrophoretic mobility to zeta potential.

5.3.3 Adsorption Measurements

The adsorption of cationic starch onto toner particles and agglomerating oil drops is measured using the depletion method whereby the cationic starch concentration before and after contact with a known surface area of adsorbent is measured, allowing calculation of Γ, the amount adsorbed per area. To analyze the cationic starch concentration in solution, the technique of Dubois *et al.* (1956) is used. This consists of taking 2 mL of cationic starch solution in a 10 mL test tube (or any other carbohydrate) and adding 100 mg of an 80% phenol solution followed by 5 mL of concentrated sulfuric acid. Immediate good mixing is essential. The H_2SO_4 is then forcefully injected into the tube. After sitting for 20 minutes, the yellow color fully develops, and the absorbance is read at the maximum, 480 nm, on a Bausch & Lomb™ Spectronic 20 spectrophotometer. The calibration curve is found to be linear, with an absorbance of 1 occurring at about 55.7 ppm cationic starch. To analyze solutions with cationic starch concentrations >50 ppm, the solutions are diluted and then assayed, with the concentration determined in the diluted sample multiplied by the dilution factor to obtain the concentration in the original. Variations in measurement results were less than 2% of values.

To determine the surface area of toner particles, the toner is analyzed in a Micromeritics Flow Sorb™ BET analysis device using the single point method for N_2 adsorption at a relative pressure of 0.3. The calculated specific surface for the Apple Laser Writer™ toner area is 1.17 $m^2 g^{-1}$ This is equivalent to spheres of the same density having a diameter of 1.7 μm, instead of the observed size of 10 μm. This additional area is attributed to the roughness of the surface and the presence of 1 μm silica particles mixed with the toner.

For the toner particles, the cationic starch adsorption procedure is as follows. The toner particles are mixed with the desired initial cationic starch concentration and then set shaking with a wrist-action type agitator overnight. After 16 hours, the toner was allowed to settle and the supernatant was analyzed for cationic starch concentration. The time to equilibrium is measured and found to be 8 hours, that is, after which an apparent steady-state Γ is reached up to 24 hours.

For liquid drops, the surface area is determined by centrifugal particle size analysis in a Horiba™ CAPA-5000. This device measures the transmittance of light through the sample as a function of settling time. For our systems the drops are typically 0.5 to 1.5 μm in size and have a density difference of 0.23 and 0.08 g cm^{-3} for the pure oil and Betz oil/surfactant blend, respectively. For effective measurement, this required the application of 1000 or 2000 RPM (equivalent to 110 or 440 relative centrifugal field (RCF)). The resulting size distribution given is area-weighted, so an average size calculated can be directly used to determine the total dispersion interfacial area, using the known dispersed volume.

The liquid drops are sonicated with a Branson Model 250 Sonifier™ which uses high-amplitude ultrasound to create cavitation in the liquid and therefore intense local shear. This provides the basis for the dispersion of the liquids and creation of their substantial interfacial areas.

For the liquids, the adsorption procedure is as follows. The solution of known initial cationic starch concentration is prepared and placed in the sonicator. The power is turned on and during sonication a known volume of liquid is injected directly under the sonicator horn where the agitation is most intense to disperse the liquid as completely as possible. A small amount of liquid always remains on the surface since no surfactant emulsifier is present in the system to completely stabilize the dispersed drops from coalescence. After formation of the dispersion, a portion is immediately set in the particle size analyzer for size determination and the remainder placed in a centrifuge to obtain a clear supernatant layer. Centrifugation is done at 2000 to 8000 RPM for 15-60 minutes, depending on sample (equivalent to 440 to 5,500 RCF). Determining an appropriate centrifugal time and speed takes experimentation and varies for each cationic starch concentration and oil type. The minimum centrifugation needed to provide a non turbid layer of supernatant is used.

The sources of error in determining Γ for cationic starch on liquid drops are (1) incomplete dispersion of the liquid, (2) centrifugation forcing coalescence of some drops, and (3) insufficient separation of some of the smallest drops from the supernatant layer and so the inclusion of some adsorbed cationic starch in the supposedly bulk solution assay. All of these factors tend to make the amount of cationic starch adsorbed, Γ, appear *lower* than it actually is. Therefore, the maximum value for Γ is the most reliable. This is used when measured Γ values are found to vary with centrifugation time and speed. The results show consistent isotherms and are repeatable within the error bars. The error bars (see Figures 5.6 and 5.7) are based on uncertainties in knowing the initial and final cationic starch solution concentrations with the spectrophotometric assay, and represent 95% confidence interval limits.

5.3.4 Light Scattering

For the dynamic light scattering measurements of the liquid drops, dispersions are made by sonication as described above. The dispersions are then passed through a 0.22 μm filter, producing particles of average (z-average) diameter 100 nm for oil drops and 200 nm for Betz liquid drops, both with a narrow size distribution (polydispersities <0.08). These dispersions are very stable when sufficiently dilute, as shown by constant size over time in light scattering. They are mixed with cationic starch solutions of known concentration to determine the adlayer thickness. The equipment consists of a Brookhaven BI-30™ sample cell, goniometer, photomultiplier tube, correlator and software, and a Spectra Physics 35 mW He-Ne laser (λ=634 nm). Viscosity of cationic starch solutions is determined with a Canon-Fenske capillary viscometer.

The latex is a surface-carboxylated polystyrene latex of 303 nm diameter, obtained from Interfacial Dynamics Corporation (Portland, OR). We measure a zeta potential in 10 mM NaCl of -50.9 mV at 25 °C.

Scanning electron microscope pictures are taken with a JEOL JSM 25 on gold sputter-coated samples.

The water used for the wettability, zeta-potential and light-scattering measurements always contained 10 mM NaCl, both in the presence and absence of cationic starch. This was used for two reasons: first, to provide a known electrolyte concentration; second, to keep the results comparable to conditions in the repulper where NaOH and other ions are added in significant quantities. Addition of cationic starch increases the ionic strength of pure water, and comparisons of systems in pure water and in 1000 ppm cationic starch would therefore be at different ionic strengths (equivalent to 0.3 mM NaCl for cationic starch solution versus 0.01 mM NaCl for pure water). Thus by adding ample additional electrolyte, electrolyte effects have a negligible contribution to the differences observed

with and without the presence of cationic starch. Repulper ion concentrations vary, but never approach those of deionized, pure water, such as is available in the laboratory.

5.4 Results and Discussion

5.4.1 Agglomeration Behavior as a Function of Temperature

The first task is to clearly establish the agglomeration behavior of the toner as a function of agglomerating oil, temperature and cationic starch concentration. The results, for no cationic starch, are shown for each agglomerating oil as a function of temperature in Figure 5.2. The pure oil is an effective agglomerant over the entire temperature range. The oil/surfactant blend shows moderate efficacy at low temperatures, and becomes steadily more effective as temperature increases. Interestingly, the toner agglomerates at high temperature somewhat without any additives at all. This likely represents the softening of the toner at its T_g (measured at 65 °C with differential scanning calorimeter, courtesy of TA Instruments, Wilmington, Delaware), causing the particles to stick together upon collision.

In Figure 5.3 the behavior of the same agglomerants in a 0.1 wt% cationic starch solution is presented. Clearly, the behavior is different from that presented in Fig. 5.2. With the pure oil, little, if any, agglomeration is observed at any temperature. This is the well-known disrupting effect of cationic starch reported previously (Chapter 4). With the oil/surfactant blend, cationic starch reduces the degree of agglomeration modestly at low temperatures, but has no effect above approximately 60 °C. This shows the nearly complete insensitivity of the oil/surfactant blend to cationic starch—in complete contrast to agglomeration with the pure oil. This is the basic phenomenon which the remainder of the results in this chapter explain in depth.

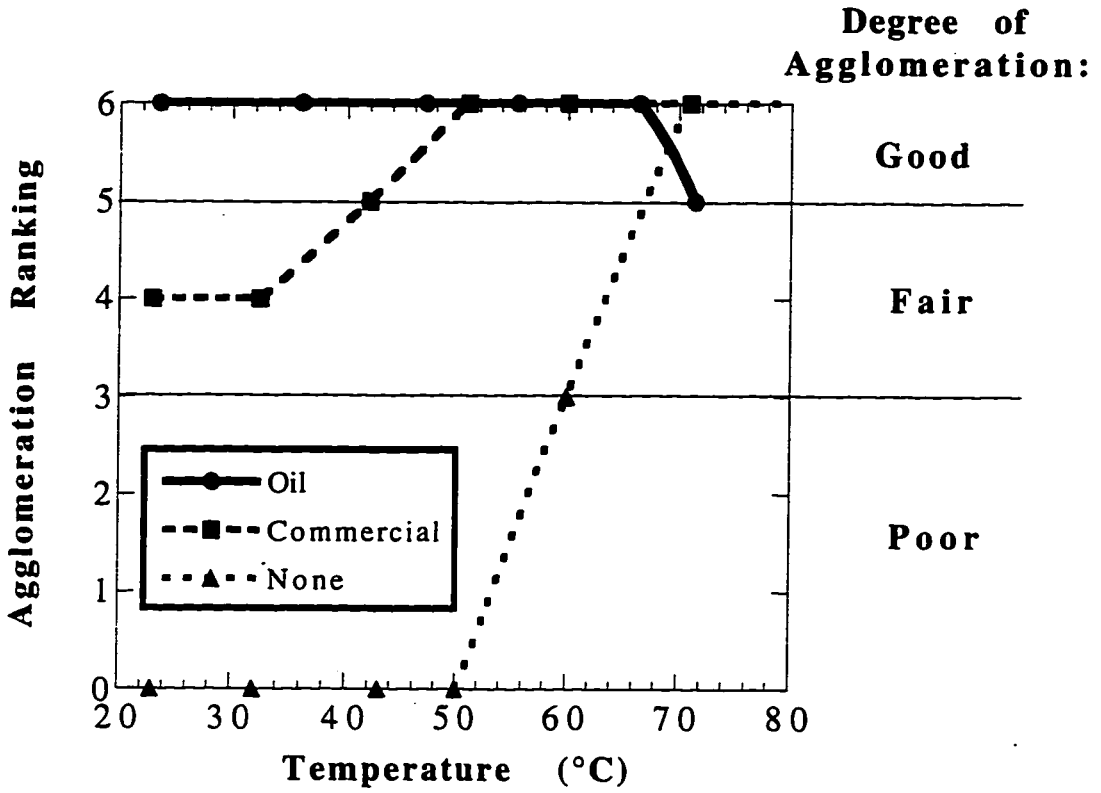

Figure 5.2 Agglomeration behavior of toners vs. temperature with no cationic starch. Oil = 0.09 wt% dispersed n-hexadecane; Commercial = 0.09 wt% Betz liquid (oil/oil-soluble surfactant blend); None = no agglomerating agent added. Note that the oil agglomerates the toners effectively over the entire temperature range. The commercial system causes some agglomeration, but is made most effective by raising the temperature. Also, even without an added agent, high enough temperatures will induce agglomeration.

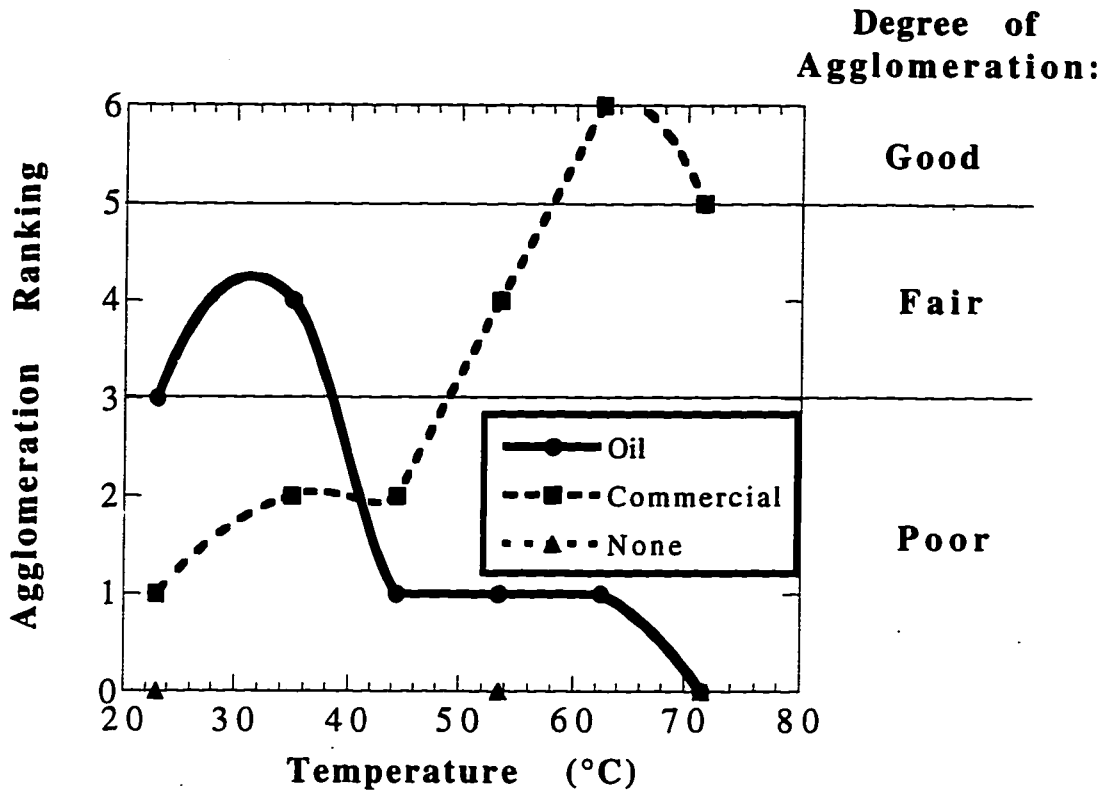

Figure 5.3 Agglomeration performance vs. temperature with 0.09 wt% cationic starch present. Oil = 0.09 wt% dispersed n-hexadecane; commercial = 0.09 wt% Betz liquid (oil/oil-soluble surfactant blend); None = no agglomerating agent added. Note that the commercial agglomerating agent shows behavior just like when no cationic starch is present (Fig. 5.2). In contrast, the simple oil is ineffective at producing good agglomerates at any temperature when cationic starch is present.

5.4.2 Effect of Temperature on Agglomeration

The role of temperature is important for the agglomeration of toners principally with commercial products. This is readily observed and is also reported in the literature (Richmann and Letscher, 1994). Several experiments clarify the reason. First, Figure 5.4 shows the scanning electron micrographs of agglomerates formed at high temperature with the Betz oil/surfactant blend (right) and without any agglomerating agent (left). It is apparent that the commercial blend fuses the toner particles together and indeed, individual

particles are difficult to distinguish in the picture. In contrast, the toner particles agglomerated only with increased temperature (and no added oil of any kind) remain distinct, connected by small solid bridges that look like weld points. Here the natural softening of the toner as it crosses the glass-rubber transition temperature allows for some stickiness of the particles, but they remain solid and incapable of complete fusion. The effect of the commercial agglomerate then is to dissolve and soften the toner particles to a much greater degree, which results in true particle fusion and therefore very strong agglomerates.

In contrast, the liquid bridge mechanism of n-hexadecane oil relies on only liquid bridges to hold the particles together. Although these are weaker than fusion, they still are strong enough to hold 1 mm and larger toner particle agglomerates together in our experiments. No pronounced temperature effect is observed since the liquid bridge strength is nearly independent of temperature. Furthermore, it is observed that the agglomerates formed at high temperature with the pure oil maintain a hard and brittle character like agglomerates formed with no agent at all. Thus, the toners seem to weld together in spots from the temperature, but the simple oil does not dissolve and soften the toners, unlike the commercial surfactant/oil blend.

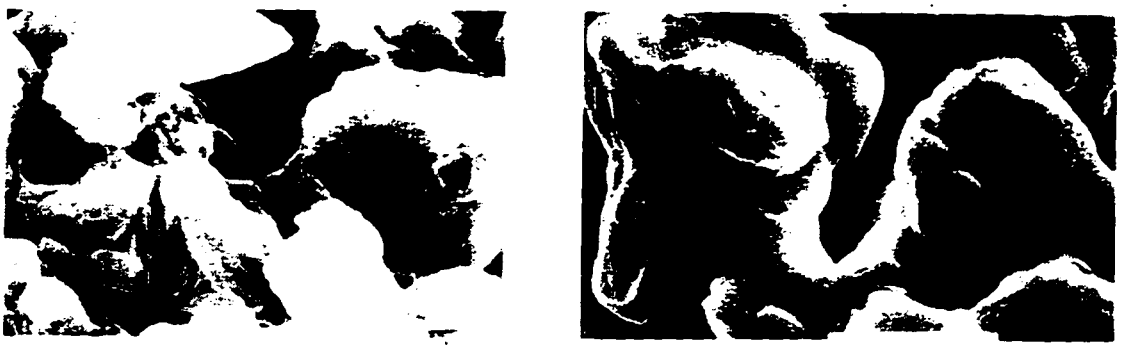

Figure 5.4 Fusion of toners by commercial agglomerant at high temperature. Compare heating only (left) and one obtained by heating with presence of commercial agglomerant (right), where clear fusion of the toner particles occurs, leaving the primary particles indistinct. Images are 30 x 43 μm.

At temperatures near room temperature the commercial blend is only marginally effective because it must rely on liquid bridges, and the strength of these is less than for the pure oil. This is because the liquid bridge strength depends on the interfacial tension, and the surfactant content of the commercial product reduces its interfacial tension with water. The interfacial tension of the pure oil with water is 52 mN m^{-1}, while for the blend it is reduced to 26.5 mN m^{-1} (measured by drop volume method, Adamson, 1990). For two equal spheres held together by a liquid bridge, the force acting to hold them together is given by (Israelachvili, 1992, p.332):

$$F = 4\pi R\sigma\cos\theta \qquad (5.1)$$

Where R is the sphere radius, σ is the interfacial tension, and θ is the contact angle.

To test this effect, agglomerated clusters of toner particles and either pure oil or the commercial oil/surfactant blend are formed. The clusters are pastes formed by mixing with equal volumes of toner particles and liquid, and rolling the paste into 5 mm diameter

spheres. The spheres held together by pure oil are put in one jar and the spheres held together by the blend are put in another, each jar filled with the same amount of water and then set side-by-side on a wrist-action shaker for 10 minutes. The results are striking: for the commercial blend spheres, the agglomerates partly disintegrate into many small toner-liquid fragments throughout the solution. Furthermore, toner particles and many small aggregates are visible under the microscope. However, for the spheres held together by pure oil, the same shaking motion produces no fragments and no particles are visible under the microscope. The results indicate the oil/surfactant blend agglomerates are much more easily broken up shear forces, in accord with their lower interfacial tension.

Thus at low temperatures without cationic starch, the pure oil is more effective since it produces stronger liquid bridge aggregates. For the commercial oil, however, the aggregates produced at low temperature are too weak to grow very large, but as the electron microscopy results in Fig. 5.4 show, at increasing temperature, the toners are dissolved and softened and true fusion of the aggregates occurs, making strong aggregates that can grow large.

That high temperature is needed for effective performance of the commercial agglomerant, therefore, is explained by the increase in aggregate *strength* to sufficient levels to form large aggregates.

5.4.3 Zeta Potential as a Function of Temperature

Since cationic starch is a charged molecule, its adsorption influences the surface potential of the toner, and on this basis a study of the toner zeta potential as a function of temperature is made. To do this, the toners are dispersed in 40 wt% glucose where the viscosity slows the natural sedimentation of the particles to allow time for electrophoresis measurement. The measured electrophoretic mobility is converted to an inferred zeta potential using the Smoluchowski equation (Hunter, 1987).

The results are presented in Figure 5.5. The bottom curve shows the zeta potential decreases slightly as the temperature increases, going from -40 mV at 23 °C to -50 mV at 75 °C. This suggests no large changes in the toner surface chemistry occur at high temperature.

The upper curve shows the behavior of the same toner dispersed in 0.1 wt% cationic starch solution. The dramatic change in zeta potential from negative to positive when cationic starch is added to the solution clearly reflects the cationic starch adsorption on the surface. As a function of temperature in cationic starch solution, the zeta potential increases from +20 mV at 23 °C to +29 mV at 75 °C in a smooth fashion. Again, no large changes in surface chemistry occur as a function of temperature. It must be emphasized that the zeta potential of a particle with a polyelectrolyte at its surface is not a physically well-defined property as it is for a more ideal electrokinetic surface, since bound charge resides both at the surface and in a diffuse adlayer permeable to fluid flow (Koopal, *et al.*, 1988). The zeta potential is only reported to provide an easier-to-recall, more intuitive measure for comparison between systems. It should be remembered, however, that in the Smoluchowski equation the zeta potential is simply a factor times the electrophoretic mobility, which is directly measured.

It is important to ascertain whether surfactants in oil/surfactant blend drops dissolve and diffuse through the aqueous medium to the toner surface. If so, the surfactants could competitively displace the cationic starch on the toner surface. To test this, the toner dispersion in 0.1 wt% cationic starch solution is mixed with dispersed oil/surfactant drops. This mixture equilibrates overnight and the toner particle zeta potential is determined. The results are included in Fig. 5.5, where it is seen that the behavior is identical to that for a solution not in contact with the oil/surfactant blend. We conclude, therefore, (1) no dissolution and adsorption of low-HLB surfactants occur, (2) cationic starch adlayer on toner remains at high temperature and (3) because of points 1 and 2, the commercial

oil/surfactant agglomerant must operate by droplet coalescence on the cationic starch-covered toner for agglomeration.

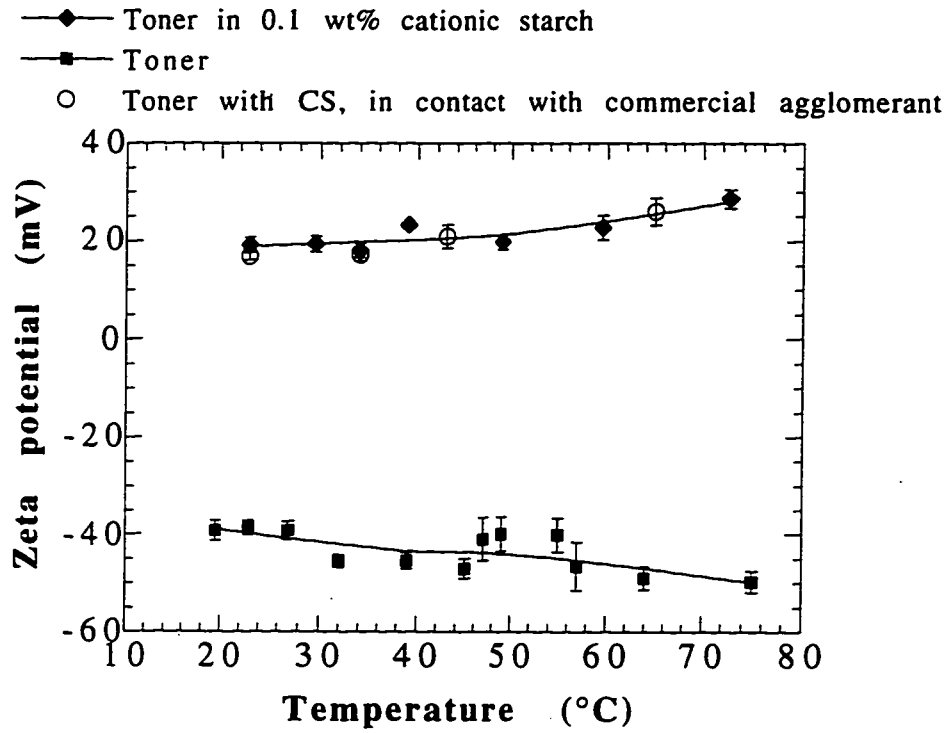

Figure 5.5 Toner zeta potential vs. temperature. While cationic starch causes a large change in zeta potential, the presence of dispersed commercial agglomerant makes no difference, showing no element from the agglomerant is dissolving and removing the cationic starch from the toner surface. Water used is deionized, conductivity=1 microSiemen/cm. Error bars represent 95% confidence limits.

5.4.4 Cationic Starch Effect on Surfaces

Since liquid bridge agglomeration depends on the assisting oil coalescing on the particle surface, and so must wet the surface in preference to the aqueous medium, the influence of the cationic starch on the wettability of the toner by the agglomerating oils is examined. This is done by obtaining liquid-liquid-solid contact angles for the three phase system, with the angle measured through the oil phase for an oil drop advancing across the

toner surface. Table 5.1 presents the results. The toner is preferentially wet (contact angle < 90°) by both the oil and the oil/surfactant blend in 10^{-2} M NaCl, indicating conditions favorable for oil-assisted agglomeration. Note that the difference between the contact angles of 15° and 60° is not reflective of wettability differences necessarily, but rather the interfacial tension between the two liquids. For the hexadecane-water interface, the measured tension is 52 mN m^{-1}, while for the oil/surfactant blend-water interface, it is 26.5 mN m^{-1} due to the surfactant content. In the cationic starch solution, however, the pure oil no longer shows preferential wetting, but instead maintains a contact angle >90° when advancing. This is attributed to the cationic starch remaining at the toner surface and increasing the effective *hydrophilicity* of the toner particle surface. Clearly, this is unfavorable for agglomeration and, indeed, it represents the case where it does not occur. In contrast, for the oil/surfactant blend good wettability is maintained *despite* the presence of cationic starch, indicating that this liquid appears to ignore its presence.

Table 5.1 Wettability of toner surface to agglomerating oils: effect of cationic starch in the aqueous phase. Numbers are contact angle (degrees) of oil/water/toner system, measured through the oil phase.

Aqueous phase: Oil phase	10^{-2} M NaCl	10^{-2} M NaCl + 0.1 wt% CS
n-hexadecane	60°	95°
commercial oil blend	15°	15°

Further characterization of all the surfaces involved was undertaken with electrokinetic data. The results are presented in Table 5.2. Note that the magnitudes of the zeta potentials for the toner are lower than those in Fig. 5.5, due to the presence of added salt in the experiments reported in Table 5.2. The results for both the toner and the oil

show adsorption of large amounts of cationic starch; enough to reverse the electrophoretic mobility. Thus, the pure oil is also an effective starch adsorbent. For the oil/surfactant blend, the zeta potential is made less negative by a measurable and reproducible amount, 3.3 mV. However, the blend appears to adsorb significantly less cationic starch than the pure oil.

Table 5.2 Inferred zeta potentials from electrokinetic measurements of species: effect of cationic starch in the aqueous phase. Units are millivolts.

Aqueous phase: Species	10^{-2} M NaCl	10^{-2} M NaCl + 0.1 wt% CS
toner	-20.1	+5.0
n-hexadecane	-15.7	+6.3
commercial oil blend	-7.7	-4.0

5.4.5 Cationic Starch Adsorption

To quantify the degree of cationic starch adsorption to the surfaces, adsorption isotherms are measured by assaying the depletion of cationic starch in the bulk after exposure to the surfaces. The isotherm for the toner is presented in Figure 5.6. It appears to be of a high-affinity character, as is typical for polymer adsorption (Hesselink, 1983). The plateau adsorption of about 3.5 mg m^{-2} is fairly typical for adsorbing polyelectrolytes (Hesselink, 1983).

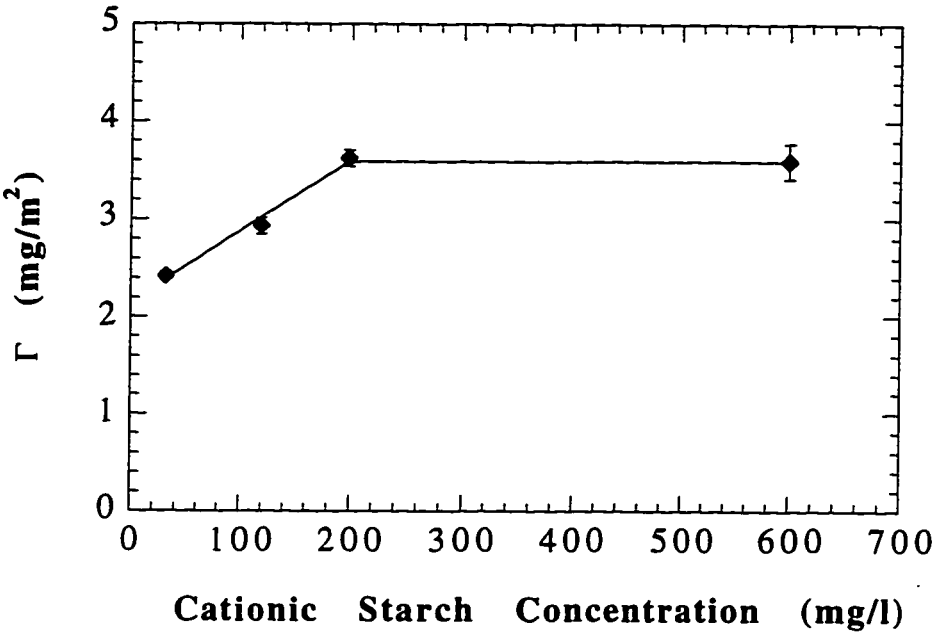

Figure 5.6 Adsorption isotherm for cationic starch on toner particles. (In 10^{-2} M NaCl.)

Similarly, the adsorption isotherms for the liquid drop interfaces are determined, and the results presented in Figure 5.7. We see that the oil drops adsorb a very large amount of cationic starch, nearly 20 mg m^{-2}. In contrast, for the oil/surfactant drops, a measurable amount of adsorption occurs, which appears to be close to 1.5 mg m^{-2} at a bulk concentration of 1000 ppm (0.1 wt%) cationic starch. Thus, all surfaces of interest adsorb cationic starch.

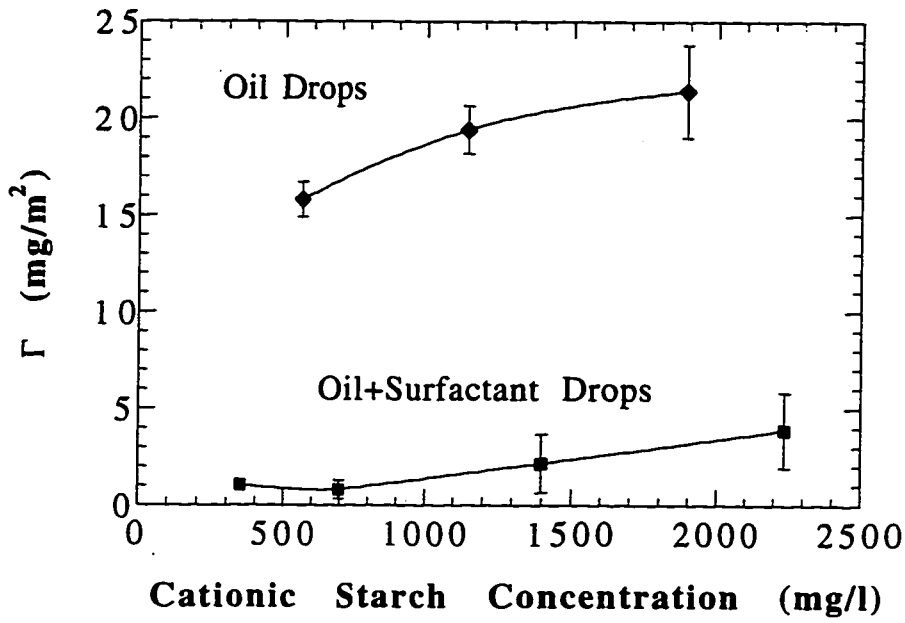

Figure 5.7 Adsorption isotherms for cationic starch onto oil drops and oil/surfactant blend drops. (In 10^{-2} M NaCl.)

5.4.6 Cationic Starch Adlayer Characterization

Knowing the density of the cationic starch adsorption provides important information. To complete the picture, we also want to know the thickness of the adlayer. This was determined by dynamic light scattering. By measuring the change in hydrodynamic diameter for particles on exposure to a cationic starch solution, the adlayer size is directly determined. This can be done for both species of liquid drops since they are available in submicron diameters, but toner particles are too large for measurement. To estimate the adlayer on a toner particle we examine a somewhat similar latex particle. The latex used was 303 nm diameter polystyrene with carboxylate surface groups and a zeta potential of -50.9 mV in 10^{-2} M NaCl. The polymer is similar to the toner (polystyrene versus a styrene/acrylate blend at a ca. 1:1 mole ratio). The results are presented in Table

5.3, along with the measured adsorbed amounts at the same concentration and the inferred segment density distribution in the adlayer, using $\rho_{\text{cationic starch}} = 1.5$ g cm^{-3} (Perry *et al.*, 1984, p. 3-42).

The adlayer measurements show the development of a large (49 nm) adlayer on the latex particles. Also, on the pure oil drops the adlayer is 33 nm. Normally when adlayers are thicker than ca. 10 nm their behavior will dominate the stability with respect to coalescence of the species (Evans and Wennerström, 1994, p. 318), so these adlayers likely act as effective barriers to oil drop-toner particle attachment in cationic starch solution. In the rightmost column of Table 5.3, we see that the inferred average segment densities in the adlayer for the toner particles and oil drops are reasonable, from 0.05 (calculated from Γ for cationic starch on and the δ for cationic starch on the latex) to 0.35 for the oil drops.

However, we observe entirely different behavior for the surfactant/oil blend drops. Within the experimental error of the light scattering measurements (1 nm), no detectable adlayer exists in cationic starch solution. This is surprising since cationic starch is observed to adsorb in measurable amounts to the drops. If the amount adsorbed is combined with an adlayer of 1 nm, the inferred segment density in the adlayer is greater than 1, a physically impossible situation.

Table 5.3 Characterization of the cationic starch (CS) adlayer on species, all at 10^{-2} M NaCl. Properties are all at 0.1 wt% CS (1000 ppm) bulk concentration.

Property: Species	Adlayer thickness δ (nm)	CS adsorbed (at 1000 ppm) Γ (mg/m^2)	Inferred mean segment density, ϕ
toner	49 (latex)	3.5	0.05
n-hexadecane	33	18	0.35
commercial oil blend	<1	1.5	>1.0

5.4.7 Explanation of Cationic Starch Effects

The agglomeration behavior of the two drops and the toner particles is pictured schematically in Figure 5.8. The large adlayers of cationic starch on pure oil drops and toner particles prevent their mutual coalescence through steric stability. Furthermore, as the wettability measurements showed, even when forced together the pure oil does not spread on the toner surface covered with hydrophilic cationic starch molecules. The lack of spreading prevents oil droplet attachment and subsequent liquid bridge formation. For the oil/surfactant blend drops in the commercial agglomerant, no significant adlayer exists on the surface and furthermore the drops are able to penetrate the adlayer on the toner particles and attach and spread on the surface effectively.

The explanation of the behavior is as follows. The oil/surfactant drops appear to imbibe the cationic starch that adsorbs to their surface and, furthermore, engulf the adlayer on the toner particle. This is pictured in Figure 5.9. Large portions of the cationic starch molecule reside inside the drop, probably with the cationic groups remaining at the surface since, as charged groups, they are not normally soluble in a non-aqueous phase. Undoubtedly, the partly polar surfactant character of the drops provides a favorable environment for the underivatized starch segments. The ability of the drop to imbibe the adlayer on the toner likely results from the same cause. Thus a drop that reaches the toner will continue to spread despite the presence of the cationic starch on the toner surface.

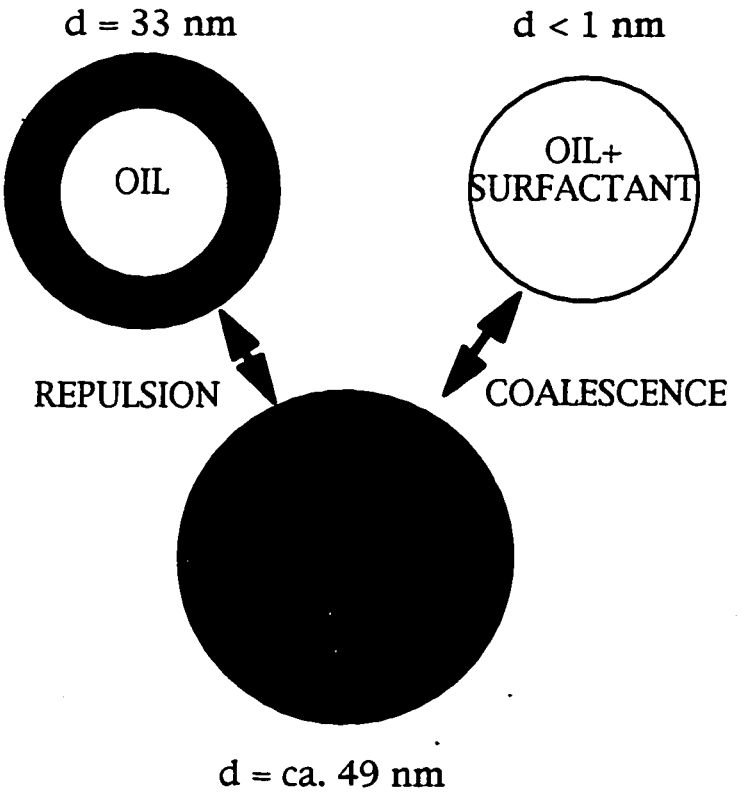

Figure 5.8 Schematic diagram of system in the presence of cationic starch. The oil/surfactant blend is still able to coalesce onto the toner surface, but the hexadecane is completely prevented from reaching the surface by the mutual steric repulsion between the drops and toner surface.

The evidence for this behavior is that the cationic starch adsorbs to the oil/surfactant drops but does not form an adlayer. Furthermore, the oil/surfactant drops wet cationic starch covered toner as well as bare toner (see Table 5.1). Also, the electrokinetic experiments show a change in the oil/surfactant drop zeta potential when cationic starch is present. Since there is no adlayer present, the Smoluchowski equation applies and the calculated zeta potentials should be the potential at the plane of shear. Using O'Brien and White theory (O'Brien and White, 1978; used through the MacMobility™ software written by D. Y. C. Chan), the surface charge can be easily calculated in such cases. The results show a change in surface charge of the drops on exposure to cationic starch (change in

surface charge density equals 0.0077 C m^{-2} for a change in zeta potential from -7.3 to -4.0 mV) that closely approximates the adsorption of cationic starch charged groups per area determined from the adsorption isotherm measurements (change in surface charge suggests 1.1 mg m^{-2} cationic starch adsorbed compared with measured adsorption of 1-1.5 mg m^{-2}).

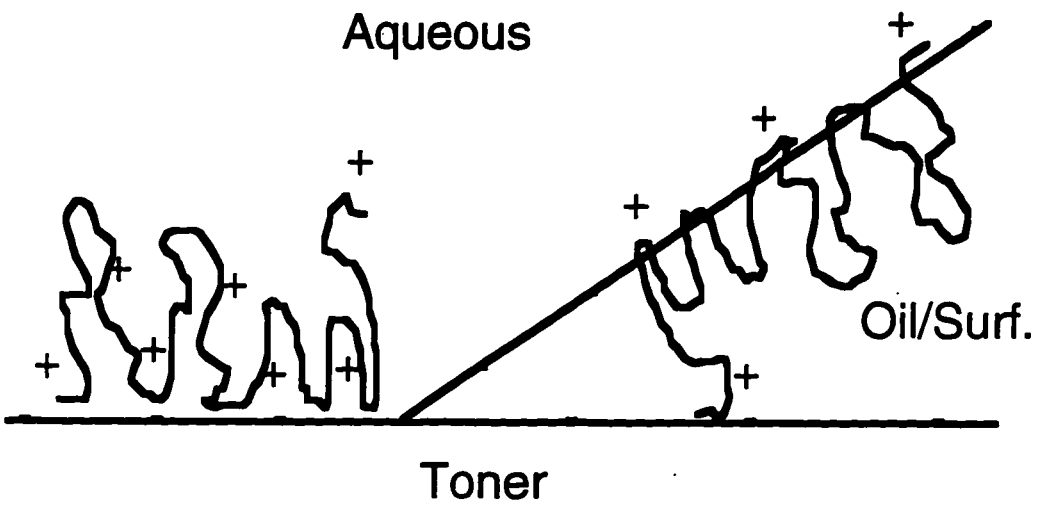

Figure 5.9 Schematic of the behavior of the oil/surfactant drops in the presence of cationic starch. While cationic starch adsorbs to the droplet surface, it is imbibed into the drop and so forms no adlayer on the aqueous side of the drop. Furthermore, the drop is able to engulf the cationic starch adlayer on the toner surface as well, and thereby still wet the surface.

5.5 Conclusions

Surfactant/oil drops continue to agglomerate toner particles in the presence of cationic starch because they engulf the cationic starch. Pure oil drops lack this ability and the resulting build up of adsorbed cationic starch on their surface and that of toners results in the prevention of agglomeration by steric stability against droplet coalescence on the

surface. The pure oil drops are also unable to preferentially wet the cationic starch-covered toner surface.

For these reasons, a simple nonpolar oil is ineffective at agglomeration in a practical setting where cationic starch is present. However, insoluble liquids that contain more polar groups possess the ability to operate with cationic starch present, and therefore can be used as the basis for an effective commercial agglomerant.

The results presented in this chapter provide insight into how and why an important class of additives–cationic polymers–disrupts agglomeration. Chapter 6 shows the consequences, measured directly, of cationic starch adsorption on the coalesceability of oil drops and cationic starch.

CHAPTER SIX

DIRECT MEASUREMENT OF PARTICLE-DROP INTERACTION

6.1 Introduction

This chapter describes using an atomic force microscope (AFM) to gain direct insight into the particle-droplet interaction. Observation of the response of a 10 μm diameter toner particle, glued onto the end of a 180 μm-long cantilever, as an oil drop is rapidly pressed against it, moving at 31 μm s^{-1}, provides the basis of the investigation. The interaction occurs either in pure water or in a 1000 ppm cationic starch solution, and the behavior of these two cases is contrasted.

In using this technique, we follow Ducker *et al.*. who first reported attachment of a 7 μm diameter particle to the cantilever in an AFM and used this particle to probe colloid forces (Ducker *et al.*, 1991). Although many have used attached particles to probe the forces between two solid surfaces, we are aware of only three groups who have investigated the interaction between solid and fluid interfaces, and all of these examined silica particles near air bubbles in water (Ducker *et al.*, 1994; Butt, 1994; Fielden *et al.*, 1996). This work, which examines the interaction of a toner particle consisting mostly of poly(styrene-co-acrylate) with an n-hexadecane oil droplet, in pure water and in 1000 ppm cationic starch solution, is therefore novel technically as well as useful for understanding how cationic starch affects the coalesceability of oil drops and toner particles in oil-assisted agglomeration.

6.2 Experimental

Toner spheres were obtained from the unprinted toner powder for an Apple Laser Writer™. The manufacturer gives the toner composition as 55-65 wt% styrene acryl copolymer (in approximately a 1:1 mole ratio), 30-40 wt% magnetite (Fe_3O_4), and 1-3 wt% salicylic acid chromium chelate. A single sphere of approximately 10 μm diameter was glued with Devcon™ S-208 fast-cure epoxy onto the end of a commercial cantilever. The same sphere was used for all experiments. After these were completed, the sphere was imaged with the AFM and found to be free of large asperities and to have an average radius of curvature of 5.3 μm at the side that faced the oil drop. The cantilever was obtained from Park Scientific Instruments, Sunnyvale, CA, designated as 'ML06A' and considered by the manufacturer to have an approximate spring constant of 0.05 N/m. It is fabricated of Si_3N_4, gold-coated for increased reflectivity, and triangular with a length of 180 μm.

Figure 6.1 shows a schematic of the AFM, while Figure 6.2 shows a schematic of the particular method of holding the drop captive under water. To hold the oil drop under water, a glass cup with a cylindrical shape had a piece of PTFE tubing glued in the center. The tubing had its axis aligned vertically and held the oil drop captive. The glass cup was 19 mm in diameter with 5 mm high walls. The PTFE tube was 3 mm long with a 2.25 mm inside diameter. After oil filled the PTFE tube, water or cationic starch solution was added until it covered the oil drop. The cantilever with attached particle was then lowered into the aqueous phase just above the oil/water interface for the beginning of the experiment. The water used was reverse-osmosis treated and twice-distilled, with a conductivity equivalent to 10^{-5} M sodium chloride and thus an approximate Debye length of 95 nm. For cationic starch solutions, 1000 ppm STA-LOK™ 400 from the A.E. Staley Co., Decatur, Illinois was added to the same quality water and boiled under vigorous agitation for 30 minutes, adding water to keep the volume constant. STA-LOK™ 400 is a potato starch derivatized

with quaternary ammonium groups every 30-35 glucose units. The cationic starch solution had a conductivity equivalent to 3 x 10^{-4} M sodium chloride, and thus an approximate Debye length of 18 nm. Fig. 4.3 shows the cationic starch structure.

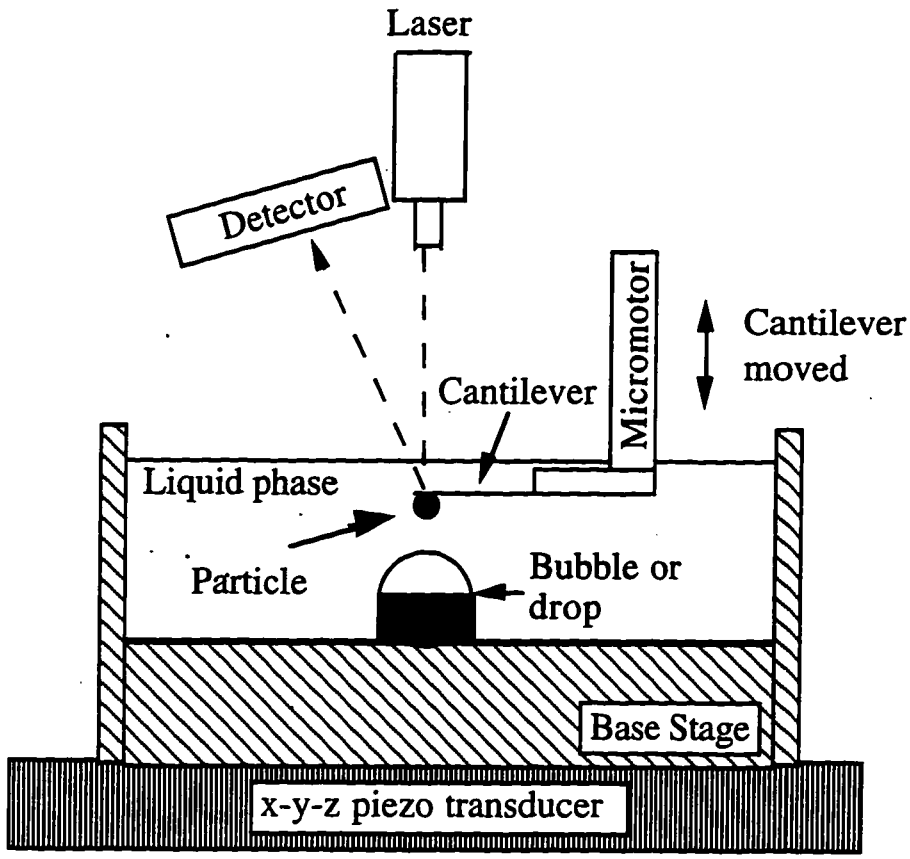

Figure 6.1 Schematic of AFM, showing modified base stage designed to hold an air bubble or immiscible liquid drop. Wettability and capillarity hold the drop fixed. The cantilever deflects as a result of the particle-drop interactions. A laser reflected from the back of the cantilever impinges on a photodiode array, providing a sensitive measure of cantilever deflection.

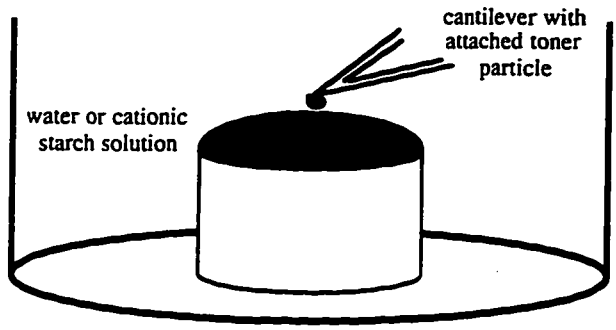

Figure 6.2 Schematic of oil drop trapped under water in the AFM.

The AFM used was a Park Scientific Instruments AutoProbe CP. A laser beam reflected off the back of the cantilever impinges on a position-sensitive photodetector, providing a measure of the cantilever deflection. The force on the cantilever is calculated as the product of the deflection and the spring constant. During an experiment, the oil drop is swept upward to the toner particle and then downward to its initial position in one second. The range of motion is approximately 13 μm, yielding an average speed of 26 μm s^{-1}. Every 2 ms, the time, cantilever deflection and position of the base of the glass dish are recorded. Because of acceleration time, the actual speed of interface movement is measured at 31 μm s^{-1}. This speed was chosen because it is the fastest which allowed us to stop manually the position sweep after one cycle, thus ensuring that we collected the first approach. High speed was selected because this most closely simulates actual collisions that occur between toner particles and oil drops in a vigorously agitated stirred tank, as used in practice. Typical operating conditions are 10 μm diameter toner particles, 5 μm diameter oil drops and an average shear rate of 1000 s^{-1}, calculated as the square root of the ratio of specific energy dissipation in the fluid to the fluid's kinematic viscosity.

6.3 Results and Discussion

Figure 6.3 shows the approach of the toner particle and oil drop interfaces in pure water. We observe the cantilever deflecting at a definite point where the interfaces begin to interact. The cantilever deflects upward as the toner particle is pushed by the oil drop interface. As the oil drop is raised further, the cantilever deflects in proportion, forming a straight line, which indicates constant compliance between the interfaces. Note that positive forces represent upward deflection of the cantilever, away from the drop. This continues until an abrupt downward deflection of the cantilever occurs. Here, the thin film that prevents immediate imbibition of the toner particle into the oil drop has broken and the toner is pulled into the drop. The force on the cantilever before deflection and the time during which the cantilever is moving in constant compliance was surprisingly repeatable. For four repeats, the relative standard errors are about 4.4% for the force and 5.8% for the time.

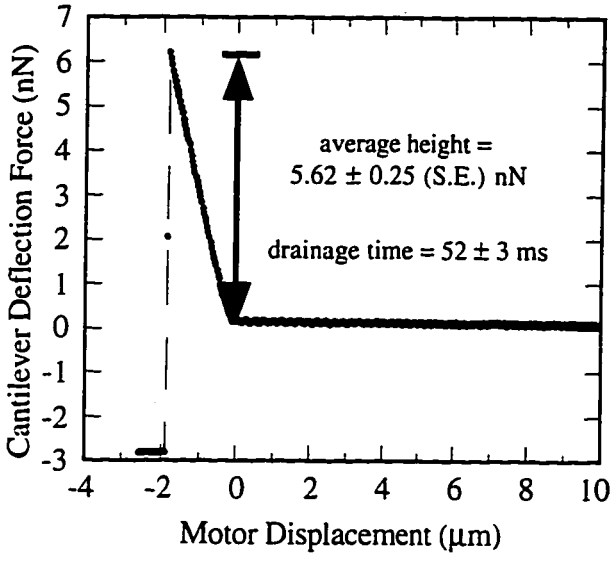

Figure 6.3 Interaction of oil and toner in pure water during rapid approach.

The delay for engulfment of the toner particle into the oil results from the significant time required for the thin film that separates the toner and oil interfaces to thin, become unstable, rupture and form a three-phase contact line. The time needed for the process is called the induction time (Schulze, 1984, p. 121). This averages 52 ± 3 (standard error) ms. The induction time controls the success of particle-bubble attachment in flotation and particle-drop attachment in oil-assisted agglomeration (Meloy, 1962; Ralston, 1983; Schulze, 1984; Luttrell and Yoon, 1988; Fisher *et al.*, 1991; Yoon and Yordan, 1991; Pugh and Manev, 1992; Hewitt *et al.*, 1995; Paulsen *et al.*, 1996). This is the first report of induction time measurement with the AFM in our knowledge. The results, however, while not directly comparable since other investigators have not used toner particles and oil drops, nonetheless are typical of those found for mineral particles interacting with air bubbles (Luttrell and Yoon, 1988; Yoon and Yordan, 1991; Hewitt *et al.*, 1995; Paulsen *et al.*, 1996).

Examining the data just before initial contact of the toner and oil interfaces, we fail to observe any attractive or repulsive force before contact. This indicates DLVO and hydrophobic forces fall outside the resolution limits of the experiment, which is dynamic and not optimized for observing the true force-distance interaction. In particular, data points are spaced in 26 nm steps, so it is likely that no point falls within the last few nanometers of interface separation, the region where colloid forces are strongest. We especially would like to note that this system ought to experience the hydrophobic force (Tsao *et al.*, 1993; Parker *et al.*, 1994; Eriksson and Ljunggren, 1995); this and the van der Waals and electrostatic DLVO forces are undoubtedly present and influence the induction time, but are not themselves directly observed in our experiments.

To summarize Fig. 6.3, we observe that during the 31 $\mu m\ s^{-1}$ of the interfaces, the initial contact of interfaces behaves like a hard wall contact until the induction time is

exceeded, when the toner particle is rapidly pulled into the oil drop. Thus, coalescence in pure water is controlled by film drainage kinetics.

Figure 6.4 shows the results of an identical experiment performed in 1000 ppm cationic starch solution. Whereas in Fig. 6.3 we observe the rupture of the aqueous film separating the oil and toner, we observe no such rupture in Fig. 6.4. Four repeats of the experiment were performed and they all appeared like Fig. 6.4. Since we did not observe film rupture, we cannot measure the induction time when cationic starch is present. However, we determine that it must be at least 191 ms since in our experiments we had toner-oil contact for this long. We were not able to examine longer contact times at the same speed of approach, 31 $\mu m\ s^{-1}$, because the AFM has only a 13 μm range of motion during sweeps.

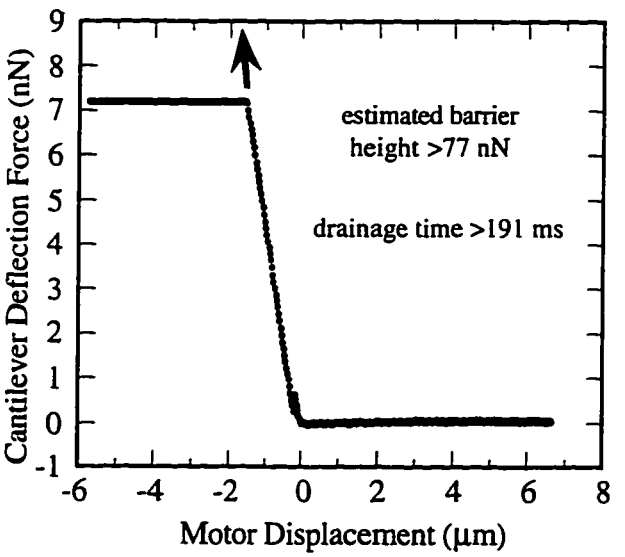

Figure 6.4 Interaction of toner and oil in 1000 ppm cationic starch solution during rapid approach.

In Fig. 6.4, the region of constant compliance between the toner and oil interfaces extends until the signal saturates, causing the data points to flatten out as the two interfaces are pressed further together. We can estimate the maximum force experienced between the interfaces by extending the constant compliance line to the point of maximum pressure which occurs when the surfaces are as closely pressed together as possible, the leftmost point on the abscissa. The force is estimated at 77 nN, much greater than the 5.62 nN at which the toner particle snaps into the oil in pure water, as shown in Fig. 6.4.

Cationic starch adsorbs strongly to both the oil and toner interfaces (Γ=18 and 3 mg/m^2, respectively; see reference Chapter 5 for details), rendering the interfaces electrosterically stable versus coalescence. Thus, a comparison of Figs. 6.3 and 6.4 shows the expected difference in coalescence tendency of the oil drops and toner particles in pure water compared to in cationic starch solution, as observed in the lack of agglomeration on a large scale noted previously (Chapter 4).

Close examination of the initial contact between the oil and toner interfaces in cationic starch solution shows that the interfaces do not move abruptly from no interaction to a region of constant compliance, as they do in pure water. Instead, all four repeats in cationic starch solution exhibited a transition region before constant compliance is established, characterized by an increasing resistance of the interfaces to be brought closer together, sometimes followed by a small snap-in. Figure 6.5 shows an enlargement of the initial contact region of the data presented in Fig. 6.4. Clearly, the interfaces approach and gradually resist approach until they begin to move in constant compliance. A distinct snap-in is observed before constant compliance continues uninterrupted.

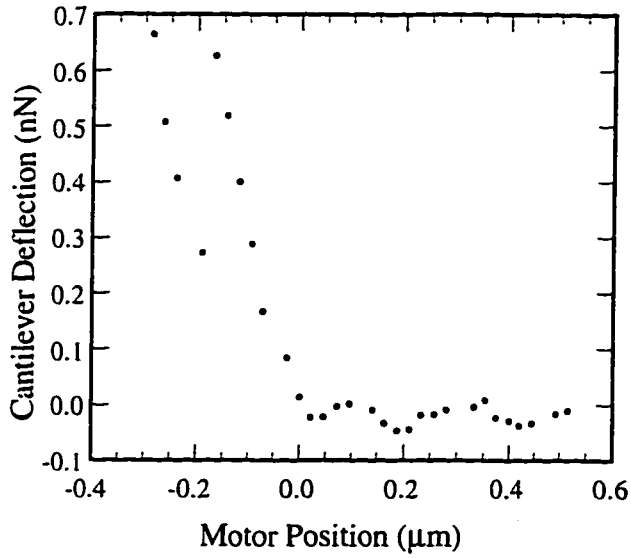

Figure 6.5 Close examination of the first contact of the toner particle with the oil drop in 1000 ppm cationic starch solution. Note the jump occurring at approximately -0.2 μm.

The average time from the beginning of contact to constant compliance is 4.8 ± 0.7 ms. The average distance over which this transitional region occurs is 150 ± 21 nm. In two of the four runs, a distinct jump is observed, one of which is shown in Fig. 6.5. In the other two runs, only the gradual transition from no interaction to constant compliance is observed. We believe these behaviors relate to the presence of the cationic starch adlayers present. We have estimated the adlayer on the toner particle as 49 nm from analogy to a latex particle, and measured with dynamic light scattering the adlayer on the oil as 33 nm (Chapter 5). The adlayers probably exhibit a softness on compression that produces the observed behavior. Furthermore, the jumps are probably caused by the thinning of the aqueous film between the adlayers and then a snap into a weakly flocculated state at a secondary minimum. The presence of the gradual transition from no interaction to constant compliance observed here is nearly identical to that observed by other investigators with

polymer adlayers in good solvents; both with the surface-forces apparatus (Hadziioannou *et al.*, 1986; Klein, 1988) and the AFM (Lea *et al.*, 1993).

6.4 Conclusions

Experiments in our laboratory clearly indicate that oil drops do not readily coalesce on toner particles in the presence of cationic starch, while they do in pure water (Chapter 5); we find direct measurements of dynamic interactions between toner and oil interfaces undertaken with the AFM clearly support this behavior. Most interestingly, the AFM results give measures of the induction time. When more complicated dynamic phenomena are observed, as in the case with cationic starch present in the aqueous phase, we observe these in our interaction traces.

The induction time for a toner particle pushed at 31 $\mu m\ s^{-1}$ into a large oil droplet is 52 ms in pure water. With 1000 ppm cationic starch present, no clear rupture of intervening aqueous film is observed up to the times of 191 ms accessible with the present apparatus. In addition to the importance of these results for understanding the interaction of the components of oil-assisted agglomeration for de-inking toner-printed paper, this work indicates the usefulness of the AFM for obtaining dynamic measurements on the interaction of solid particles with fluid interfaces, fundamental to many applications.

CHAPTER SEVEN

POPULATION BALANCE MODEL AND EXPERIMENTS

7.1 Introduction

In the work described in Chapters 4-6, we identified five key variables in agglomeration: time, temperature, agitation rate, oil composition and cationic starch concentration (also presented in Snyder and Berg, 1994, 1996a). This chapter expands on the work, moving from identifying which factors are important and why to quantifying how the success of the process depends on the key variables and to developing an overall perspective from which to view agglomeration. Both of these objectives are achieved by the development of a population balance model and comparison of the model results with quantitative experiments on the agglomeration response to changes in operating variables. Since an effective process requires the rapid production of an appropriate steady-state toner particle size distribution, the problem naturally lends itself to formulation as a population balance. As the process conditions are modified, a consequent change in the competition between aggregation and breakup shifts, altering both the rate of agglomeration and its ultimate product.

Population balance modeling is a valuable method of accounting for all changes that can occur and the rate at which they do occur in the state of a population of particles (Ramkrishna, 1985). Crystallization behavior, drop-size distributions and aerosol processes are a few applications to which population balance modeling has been applied. The core equation is developed by setting the derivative of particle size with time equal to the sum of all the aggregation and breakup rates affecting particle size.

To effectively model the process, an unambiguous set of experimental data is needed for model comparison and validation. Consequently, the objective of the work described in this chapter is to form a comprehensive picture of agglomeration de-inking by combination of agglomeration experiments and population balance model simulations, incorporating the response of the system to the key process variables of time, temperature, agitation rate, oil composition and cationic starch concentration.

7.2 Materials and Methods

7.2.1 Materials

Toner spheres were obtained from the unprinted toner powder for an Apple Laser Writer™. Information on the toner is presented in Table 4.1 in Section 4.3. The toner has an advancing contact angle in water of approximately 90° and a receding angle of 70° (Snyder and Berg, 1993). Reverse osmosis-treated water was used for all experiments, with a conductivity equivalent to 10^{-5} M NaCl.

Cationic starch was STA-LOK™ 400 (A.E.Staley Manufacturing Co., Decatur, IL), and its structure is described in Section 4.3 and depicted in Fig. 4.3a potato starch derivatized with quaternary ammonium groups with an average of one such group for every 30-35 glucose units (0.30% Nitrogen). These groups maintain a positive charge at all pH and salt conditions. See Fig. 4.3 for structure. Aqueous solutions of 1000 ppm cationic starch were prepared by boiling 1% dry starch in water under vigorous agitation for 30 minutes, and diluting to obtain 1000 ppm.

To investigate the effect of oil composition, the behavior of a pure oil was compared to that of an oil/surfactant blend. The pure oil was analytical grade n-hexadecane (Sigma Chemical Co., St. Louis, MO) used in previous experiments and shown to be effective when cationic starch is not present (Snyder and Berg, 1994). The oil/surfactant blend is based on a commercial formulation discovered by researchers at Betz Paperchem,

Inc. and given in a series of patents (Richmann and Letscher, 1992; 1993a,b; 1994). The formulation is known to overcome the effects of cationic starch, through its solubility of starch molecules (Snyder and Berg, 1996a). Furthermore, the blend is able to fuse the toners together at temperatures above 40 °C, as we have observed from electron micrographs taken of toner agglomerates. The oil/surfactant blend we used is 50 vol% n-hexadecane and 50 vol% Triton X-15 (Union Carbide, Darien, CT), an octylphenol-polyethylene oxide containing an average of 1.5 ethylene oxide units per molecule. The blend was a true solution since Triton™ X-15 is miscible with n-hexadecane. We measured an interfacial tension between the pure oil and water with the drop weight method, as described in Section 5.4.2.

7.2.2 Methods

To perform an agglomeration experiment the following procedure was used: (1) The dispersed toner, dispersed drops, cationic starch (if used), and water were combined, adding the dispersed drops last, until a total volume of 200 mL of dispersion was created with 0.033 vol% toner, 0.035 vol% oil, either 0 or 1000 ppm cationic starch. The temperature was controlled to between 23°C and 55°C by the addition of an appropriate amount of hot water. The dispersion was immediately placed in an insulated, stirred vessel and the experiment begun. (2) For all runs without cationic starch it was found that a steady-state size distribution was formed within 5 minutes, and so agitation was continued for 5 minutes; for runs with cationic starch, time studies were carried out, with runs lasting as long as 60 minutes. (3) At the end of an agglomeration experiment, the entire contents of the vessel were poured onto 3 stacked sheets of 12.5 cm Whatman grade 41 filter paper mounted in a Büchner funnel. A vacuum pump connected to a sidearm flask provided suction. The filter paper with agglomerates was dried for study with image analysis.

(4) Image analysis was performed on the agglomerates to determine the particle size distribution. Detailed descriptions of these steps follow.

Toner was dispersed by adding 1 g of toner powder to 1 liter of water and mixing in a 3.8 liter Waring™ blender at 15,000 rpm for 2 minutes. The oil and oil/surfactant blend dispersions were created by added 70 μL of the liquid to 20 mL of water and sonicating for 20 seconds at 40% power on a 250 Watt Branson probe sonicator (model 250; Branson Ultrasonics Corp., Danbury, CT). Centrifugal size analysis on a Horiba™ CAPA-5000 (Horiba Ltd., Kyoto, Japan) showed the diameter of the drops formed to be predominantly between 0.5 and 1.5 μm. The ratio of the volume of oil to the volume of toner is an important variable for oil-assisted agglomeration, and our previous work showed the most effective ratio for toner powder is 1:1 (Snyder and Berg, 1994). Therefore, this was used in all experiments.

Temperature was maintained by keeping the dispersion well insulated during a run. One and a half centimeter thick foam insulation encased the agglomeration vessel. Temperatures reported are starting temperatures; temperature gradually fell in the vessel in an exponential manner, in accord with Newton's law of cooling, with a characteristic decay time of 107 min.

The vessel used for agglomeration was a VirTis '23' Homogenizer (Virtis Corp., Gardiner, NY) of spherical-type shape, 7 cm high and 9 cm in diameter. It had five baffles built into the walls, evenly spaced and protruding 0.5 cm. The vessel was made of glass which was hydrophobized by Scotchguard™ (3M, St. Paul, MN) fluorocarbon coating to reduce adhesion of oil and toner to its surface. Agitation was provided by a vertical shaft. There were four stainless steel blades, one opposite pair on the end of the shaft and the other oppositely mounted pair 1 cm above the end. Looking axially along the shaft, the blades were set apart 90°. Each blade was 2 cm long and 1 cm wide, rectangular with

rounded corners, and angled 30° from horizontal. Impeller motion directed liquid flow downwards along the shaft.

We found that the useful range of rotational rates was from 900 to 2900 rpm. Below 900 rpm, insufficient churning of the bulk liquid occurred for it to mix well and allow agglomeration. Although speeds up 23,000 rpm were available, our experiments showed no advantage in increasing shear above 2900 rpm, as described in the results and discussion section on the effect of shear rate. To determine the shear rate corresponding to a given rpm, a thermocouple was inserted into liquid and the temperature monitored under agitation. The rise in temperature with time indicated the mechanical energy dissipated in the water; ε, the energy dissipated per unit mass, is then calculated by dividing the energy consumption by the mass of water. The square root of the ratio of ε to the kinematic viscosity of water provides G, a measure of the average rate of shear.

Image analysis was done with a Wild M420 Makroskop (Wild Heerbrugg, Ltd., Heerbrugg, Switzerland) macroscope attached to an MTI 65 video camera (DAGE-MTI, Inc., Michigan City, IN). Output from the camera went into a Data Translation (Data Translation, Inc., Marlboro, MA) frame grabber board. NIH Image freeware, version 1.60b7 (National Institute of Health, Bethesda, MD), was used to analyze the images and obtain particle size counts. To collect the image data, 100x total magnification was used, providing a 0.8 by 1.0 cm image area. The advantage of high magnification is the ability to observe the smallest particles; the disadvantage is the small sample area on the filter paper. At the used magnification, the smallest measurable particle size is 21 μm. We took numerous samples of the filter paper at randomly selected locations. A minimum of 500 particles were counted for a sample; typically 1000 were observed. For samples with a very high degree of agglomeration, we imaged all the particles that were found on the sheet. The data that resulted consisted of a list of particle areas observed by image analysis, and this was fed into KaleidaGraph™ (Synergy Software, Warrington, PA,

version 3.0) and from each particle area an equivalent 'circular' particle diameter was extracted by calculated the diameter of a circle of equivalent area: diameter = (4*area/π).

For determining statistics on the particle size distributions, the characteristic size was calculated as the diameter of a particle of average volume. This is the diameter of the particle of average mass and provides a good measure of where the bulk of the toner resides in the size spectrum. Thus, the average volume, $\bar{v}$, is calculated as:

$$\bar{v} = \frac{\sum_i n_i v_i}{\sum_i n_i} \tag{7.1}$$

And the corresponding average particle diameter, $\bar{d}$, is then given by:

$$\bar{d} = \left(\frac{6}{\pi}\bar{v}\right)^{1/3} \tag{7.2}$$

The standard deviation and skewness were calculated similarly.

Each experimental point was the average of from two to six experiments. Variations between identical runs were rather large; thus the need for averaging. Relative error of the average particle diameter was typically 12%.

7.3 Population Balance Model Description

The population balance model was developed by writing equations to account for the growth and breakup of aggregates. We started from the method described by Hounslow *et al.*. (1988) and then rewrote the equations using volume fraction as the independent variable instead of number density, as Hounslow *et al.*. (1988) used. We first used number density in our simulations but model convergence was too slow and showed

great improvement with volume fraction as the independent variable. No difference in results between the methods was found. The essence of the method is to discretize the spectrum of particle sizes into n bins such that the size bins are spaced geometrically, and then simultaneously solve the n differential equations. The physics of the process, of course, remains in the rate expressions used for aggregation and breakup.

The basic equation can be expressed in words as follows: (change in time of aggregates at size i) = (rate of gain in size i by aggregation of particles smaller than size i) + (rate of gain in size i by breakup fragments produced by the breakup of particles larger than size i) - (rate of loss in size i by aggregation of particles in size i to form aggregates larger than size i) - (rate of loss in size i by breakup of particles in size i to fragments smaller than size i).

The aggregation rate expression is drawn from the literature, following the expression of Camp and Stein (Camp and Stein, 1943), which is cast in number density. Adding the aggregation efficiency, α, which represents the number of collisions that result in aggregation over the number of theoretically occurring collisions (Ayazi Shamlou and Titchener-Hooker, 1993), and converting to volume fraction as the independent variable, we obtain the following expression for the increase in volume fraction in the $i+j$ bin from aggregation events between particles in the i and j bins:

$$\frac{\mathrm{d}x_{i+j}}{\mathrm{d}t} = \frac{4}{3}\alpha V\left(\frac{\varepsilon}{\nu}\right)^{1/2}\left(\frac{1}{v_i}+\frac{1}{v_j}\right)\left(v_i^{1/3}+v_j^{1/3}\right)^3 x_i x_j \qquad (7.3)$$

The breakup rate expression has to account for the inherently complex breakup process. Unlike aggregation, several mechanisms of breakup can occur in the same system (Ayazi Shamlou and Titchener-Hooker, 1993). We followed other investigators, e.g. Grabenbauer and Glatz (1981) and Chen (1992), and used a single power-law relation to

express the increasing tendency of the particles to break up as they get larger. We experimented with other forms for the breakup rate dependence on particle size, particularly with an exponential dependence, but the results did not fit the experimental data. The expression we used is:

$$\frac{\mathrm{d}x_i}{\mathrm{d}t} = -B\left(\frac{d_i}{d_1} - 1\right)^{\nu} x_i \qquad (7.4)$$

This shows the rate of loss of particles in bin i by breakup. B is the (dimensional) breakup rate constant, while $\left(\frac{d_i}{d_1} - 1\right)^{\nu}$ accounts for the dependence of the breakup rate on the size of the breaking particle. The expression is written so that the breakup rate is by definition zero for particles in the smallest size bin. The exponent, ν, is left as a parameter in the model.

To specify the breakup rate completely, we must also describe the size of the breakup fragments formed. It is well known in the literature that particle breakup can occur by splitting and erosion, which represent the extremes of a continuum (Parker *et al.*, 1972; Pandya and Spielman, 1982; Ayazi Shamlou and Titchener-Hooker, 1993). In splitting, particles form a few large fragments; in erosion, ablation removes small particles from a large particle's surface. We decided to use the simplest possible expression that allows either of these mechanisms to occur. We allowed a particle to break up only into two daughter particles. Then we accommodated both splitting and erosion by including a parameter, p, that is the ratio of the mass of the smaller breakup particle to the particle mass. Therefore, if $p = 0.5$, particles only split into equal halves; if $p = 0.01$, particles split into one with 99% of the mass and the other with 1% of the mass. We obtained close fits to experimental data with this expression.

These equations are non-dimensionalized by using the variables τ, β and ρ, which are the non-dimensional time, breakup rate and ratio of breakup rate to aggregation rate, respectively. These are given by:

$$\tau = \alpha V G t, \tag{7.5}$$

$$\beta = \frac{B}{G}, \tag{7.6}$$

$$\rho = \frac{\beta}{\alpha V}, \tag{7.7}$$

yielding for the aggregation and breakup expressions:

$$\frac{\mathrm{d}x_{i+j}}{\mathrm{d}\tau} = \frac{4}{3}\left(\frac{1}{v_i} + \frac{1}{v_j}\right)\left(v_i^{1/3} + v_j^{1/3}\right)^3 x_i x_j \tag{7.8}$$

$$\frac{\mathrm{d}x_i}{\mathrm{d}\tau} = -\rho\left(\frac{d_i}{d_1} - 1\right)^{\nu} x_i. \tag{7.9}$$

The model simulation used 30 bins, each bin twice the size of the previous. We thereby covered a 10^3 range in particle diameter, from 10 μm to 10,000 μm. The resulting system of non-linear differential equations is of the form

$$\frac{\mathrm{d}x_i}{\mathrm{d}\tau} = \sum_{j=1}^{n}\sum_{k=1}^{n} A_{ijk} x_j x_k + \sum_{j=1}^{n} B_{ij} x_j \tag{7.10a}$$

with initial condition

$$x_i(0) = x_{0,i} \tag{7.10b}$$

for dynamic simulations. This simplifies for the steady-state case to

$$0 = \sum_{j=1}^{n} \sum_{k=1}^{n} A_{ijk} x_j x_k + \sum_{j=1}^{n} B_{ij} x_j . \tag{7.11}$$

The key information comes in the coefficients A_{ijk}, a third-order tensor that contains the aggregation information, and B_{ij}, a second-order tensor that contains the breakup information. Both of these are formed at the beginning of the simulation as they depend only on model parameters and then remain fixed during the course of the problem solution.

In early population balance modeling, complex accounting of the oil drops was used, including terms expressing the average oil drop size, the amount of toner particles sufficiently wet with oil to agglomerate further and the amount of oil needed to wet a toner particle. However, in all cases where sufficient oil was present for complete aggregation, the oil had no effect. This is because a single term, the collision efficiency α, accounts both for oil drops coalescing on dry toner particles and two toner particles (at least one of which must be wet with oil) coalescing to form a liquid bridge. Both cases depend fundamentally on the drop-toner particle coalescence. Therefore, the extra complexities of accounting for the distribution of oil in the system produced no appreciable change in observed results, and were rejected in favor of a simpler model. The good correspondence with the experimental data obtained supports this approach, and indeed, in all our experiments an excess of oil is present.

The population balance model was solved by a program written for Matlab 4.2.1 (The Mathworks, Natick, MA). Numerical solution was obtained using a 4th-to-5th order

Runge-Kutta method or a nonlinear equation solver. Simulation times for steady-state problems were usually about 30 s on a PowerMac 7100/66; the dynamic solutions took longer, especially as steady-state was approached, running as long as 30 min. The input consisted of values for the parameters α, β and V, which are used to calculate ρ; v and p. The latter three are the only independent parameters in the model. Using these as input, the evolution of the particle size distribution in time (Eqs. 7.10a,b) or just the steady-state particle size distribution (Eq. 7.11) is produced, depending on the mode in which the model is operated, to produce a smooth size distribution. Statistics were calculated from the simulation results in the same manner as they were from the experimental data.

7.4 Results and Discussion

7.4.1 Experiments

The experiments clearly showed a strong effect of agitation rate on the particle size obtained. Figure 7.1 shows a plot of average particle diameter versus shear rate, comparing the behavior of the pure oil and the oil/surfactant blend. Agglomerate size in both cases falls with increasing shear rate in an approximately linear fashion over the range of shear rates examined. Increasing shear rate increases both the frequency of collision and the likelihood of particle breakup. However, as Fig. 7.1 shows, the tendency to break up predominates. Equally important, we see that at all shear rates, the pure oil produces larger agglomerates than the oil/surfactant blend. Since these data are collected at low temperature where no fusion of the toner particles occurs (Snyder and Berg, 1996a), liquid bridges alone hold the aggregates together. The strength of these is directly proportional to the interfacial tension (Newitt and Conway-Jones, 1958; Pietsch, 1990). Therefore, we expect the agglomerating liquid with the higher interfacial tension to produce stronger agglomerates, and indeed this is what we observe. In fact, we find a direct proportionality between the interfacial tension and size of the agglomerates; the pure oil has both twice the

interfacial tension and twice the average particle diameter. This is expected from previous work (Newitt and Conway-Jones, 1958; Pietsch, 1990). The results indicate the importance of agglomerate strength for successful agglomeration.

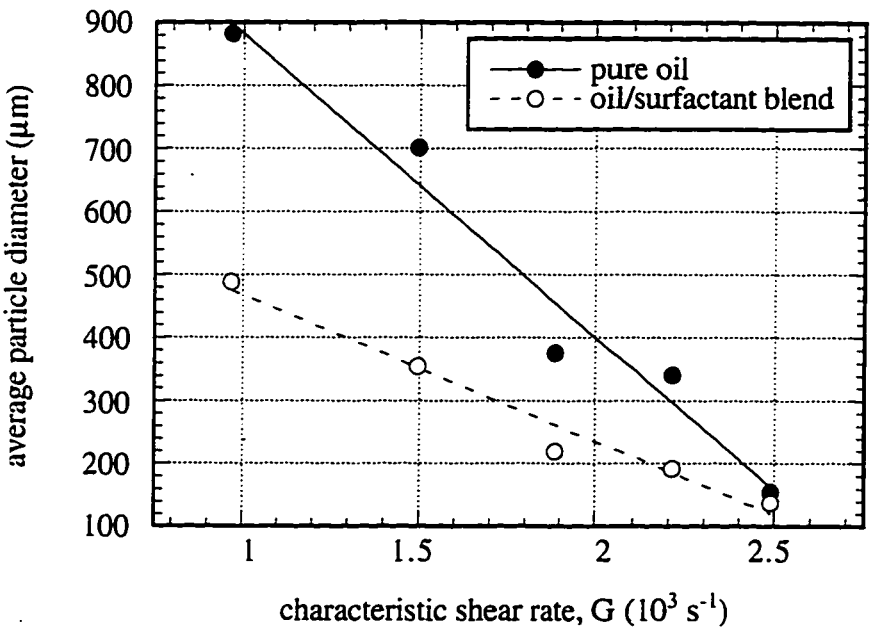

Figure 7.1 Average particle diameter versus shear rate in the aggregation vessel. G = 1000 s^{-1} corresponds to 900 rpm; G = 2500 s^{-1} corresponds to 2900 rpm.

It should be noted that the results presented in Fig. 7.1 represent the trends only over the shear range accessible with our equipment; lower shear rates did not provide adequate mixing, while higher rates were not tested as these were considered unrealistic for typical agglomeration and, in addition, it is clear that little additional size reduction could be expected in any case since the aggregates are already made quite small at the highest shear rate used. Certainly, if the graph were extended into very low shear, we would see a reduction in aggregate size as we enter a region where mixing was insufficient to bring the

particles together. This behavior would concur with other investigators' results for the effect of shear on particle size (Andreu-Villegas and Letterman, 1976).

Figure 7.2 shows the effect of temperature on pure oil and the oil/surfactant blend compared. Dramatically different behavior is observed. While the pure oil produces agglomerates of a fixed size at all temperatures, we see a large increase in particle size produced with the oil/surfactant blend as the temperature is raised. We previously examined the agglomerates formed at high temperature for both types of oil with electron microscopy and found the oil/surfactant blend to fuse the primary toner particles into a much larger, cohesive toner sphere, thereby significantly augmenting the aggregate strength. This increase in aggregate strength fosters the formation of larger particles, emphasizing its importance.

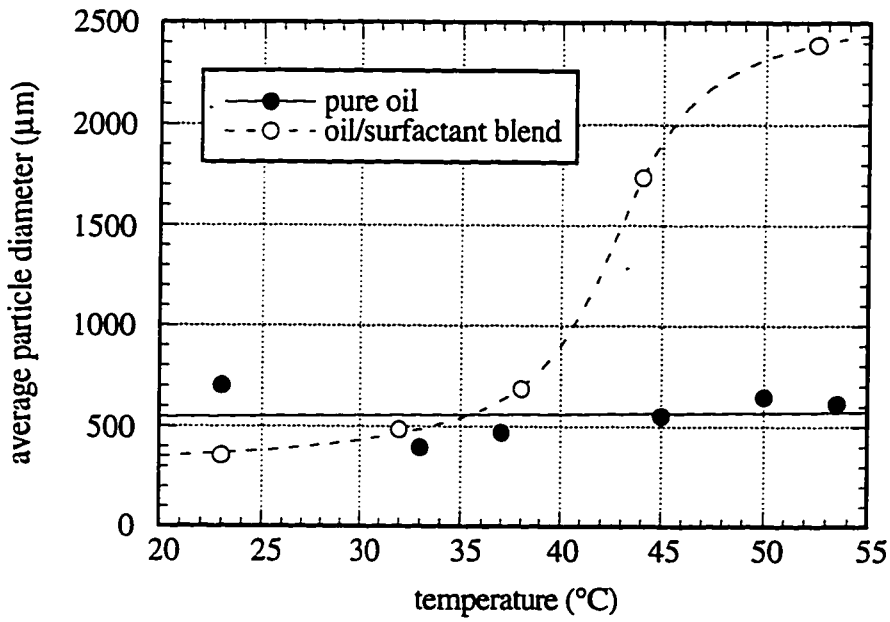

Figure 7.2 Average particle diameter versus temperature. While temperature has no effect on the size of agglomerates produced from pure oil, high temperature drastically increases the size of oil/surfactant agglomerates by fusing them together into aggregates of high strength.

Figure 7.3 depicts the results when cationic starch is present. We have done extensive work on the effect of cationic starch on agglomeration, first identifying it as a key agent for controlling the course of agglomeration (Snyder and Berg, 1994b) and then examining how it affects agglomeration (Snyder and Berg, 1996a). Cationic starch, or other cationic polyelectrolyte, is generally present in paper furnishes as a retention aid to bind filler particles into the paper web or to size the paper, and a significant amount redissolves in the repulper (Marton and Marton, 1976). The conclusion of the latter investigation clearly indicated that cationic starch adsorbs to toner, pure oil, and oil/surfactant interfaces, providing a barrier to coalescence of the interfaces. However, the oil/surfactant interface possesses the important property of engulfing the cationic starch adlayer, and thereby removing its steric barrier to coalescence and providing the possibility of engulfing the adlayer on the toner as well. This has been proven by a combination of adsorption, electrokinetic, wettability and adlayer thickness measurements, as described in Chapters 5 and 6 and reported by Snyder and Berg, 1994b, 1996a. Since the pure oil has no ability for adlayer engulfment, agglomeration is effectively prevented by high concentrations of cationic starch, such as the 1000 ppm used here.

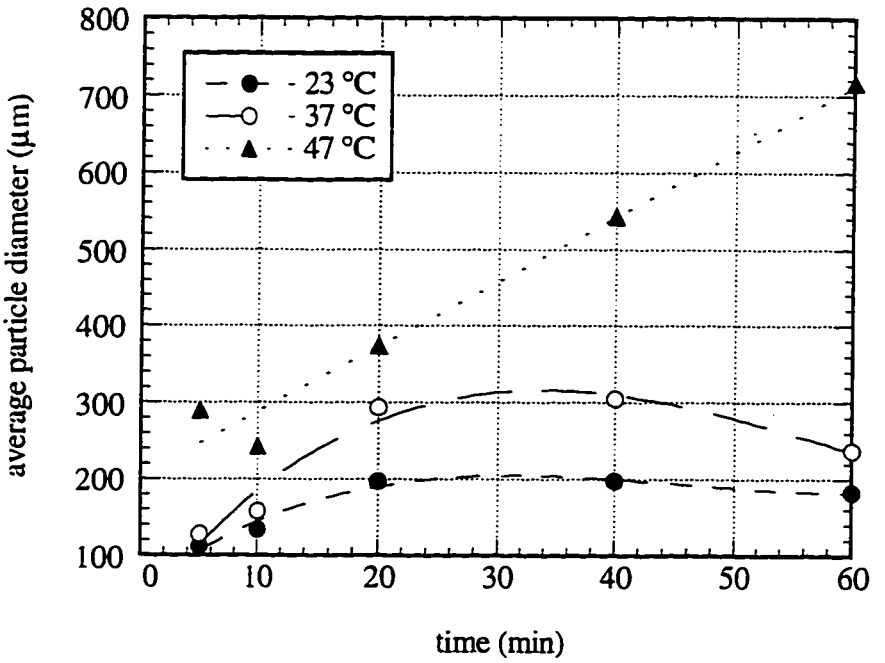

Figure 7.3 Average particle diameter versus time; oil/surfactant blend with 1000 ppm cationic starch at 23, 37 and 47 °C. Increasing temperature increases particle size by strengthening the agglomerates, but the entire aggregation process still requires 30 minutes or more to reach full size, steady-state agglomeration.

Figure 7.3 shows agglomeration in the presence of cationic starch when the oil/surfactant blend is used. First, we notice that the time needed to reach the maximum particle size is at least 30 minutes, much longer than the 3 minutes observed when cationic starch is not present. The explanation is that cationic starch reduces the agglomeration rate by reducing the rate at which droplets and toner particles coalescence. The number of collisions per time is the same, but the efficiency of collisions, α, is reduced, because of the stabilizing effect of the cationic starch adsorption (Snyder and Berg, 1996). This reduction not only slows agglomerate growth, it also reduces the steady-state particle size

distribution because this exists where the aggregation and breakup rates balance, and therefore lowering the aggregation rate shrinks the steady-state size distribution.

The effect of temperature in Fig. 7.3 is similar to that in Fig. 7.2: increasing temperature with the oil/surfactant blend produces stronger agglomerates and thereby increases the ultimate particle size distribution. Clearly, in Fig. 7.3, the sizes obtained are much smaller than in Fig. 7.2 at the same temperature, showing the potent effect of cationic starch, even though the oil/surfactant blend possesses some ability to operate in its presence. In a practical sense, Fig. 7.3 indicates the importance of using long run times when agglomerating with high levels of cationic starch.

To facilitate meaningful comparison of the model and the experimental results, the full experimental size distributions were examined. The distributions making up the individual data points in Figs. 7.1-7.3 had significant variation and were not well-suited to a least-squares fitting of each size distribution by the model. Instead, three statistics of the experimental data were used: the average particle diameter, $\bar{d}$, the relative deviation of particle sizes, $\sigma/\bar{d}$, and the skewness, κ. The variations of $\bar{d}$ with experimental conditions were of course significant; however, $\sigma/\bar{d}$ and κ generally exhibited no trends with experimental conditions. Therefore, the average values of $\sigma/\bar{d}$ and κ, and knowledge of $\bar{d}$, were found to contain the information needed for predicting a particular size distribution. The only exception to this is the significant difference in both $\sigma/\bar{d}$ and κ between runs with and without cationic starch. Table 7.1 presents the characteristic relative deviation and skewness for both the cationic starch and non-cationic starch experiments. The present of cationic starch increases the relative deviation by 16% and the skewness by 88%. Thus, it causes the formation of broader distributions, with a tendency for several large particles to be present amidst a great number of small particles. We believe this results from cationic starch acting unevenly on toner particles, completely preventing some from coalescence and less drastically retarding the coalescence of others. Such behavior

could result from uneven adsorption of cationic starch; for instance, some toners may have different surface chemistry depending on the material exposed predominantly on its surface, with some materials more favorable to cationic starch adsorption and hence more conducive to the development of electrosteric stabilization.

Table 7.1 The average relative deviation and skewness for experimental distributions. A significant increase in both is occurs when cationic starch is present. The variations reported are the standard errors.

	relative deviation, $\sigma/\bar{d}$	skewness, κ
0 ppm cationic starch	1.72 ± 0.08	9.36 ± 1.39
1000 ppm cationic starch	2.00 ± 0.09	17.62 ± 1.64
all experimental runs	1.83 ± 0.06	12.80 ± 1.06

7.4.2 Population Balance Model

In dimensionless form, the model has three independent parameters: the relative rate constant of breakup to aggregation, ρ, the breakup rate exponent of particle volume, ν, and the volume fraction of a breakup daughter particle to the parent, p. The effect of the first is to control the average particle size produced, the second determines the spread in the particle size distribution, and the third most influences the shape, and hence, the skewness of the distribution. Figure 7.4 presents a fit of one experimental size distribution by the model. The experimental size distribution is relatively smooth and thus we expect a close fit by the model, and indeed this is what is found. The fits obtained by matching $\bar{d}$, $\sigma/\bar{d}$ and κ as closely as possible produced very satisfactory results, such as those shown in Fig. 7.4.

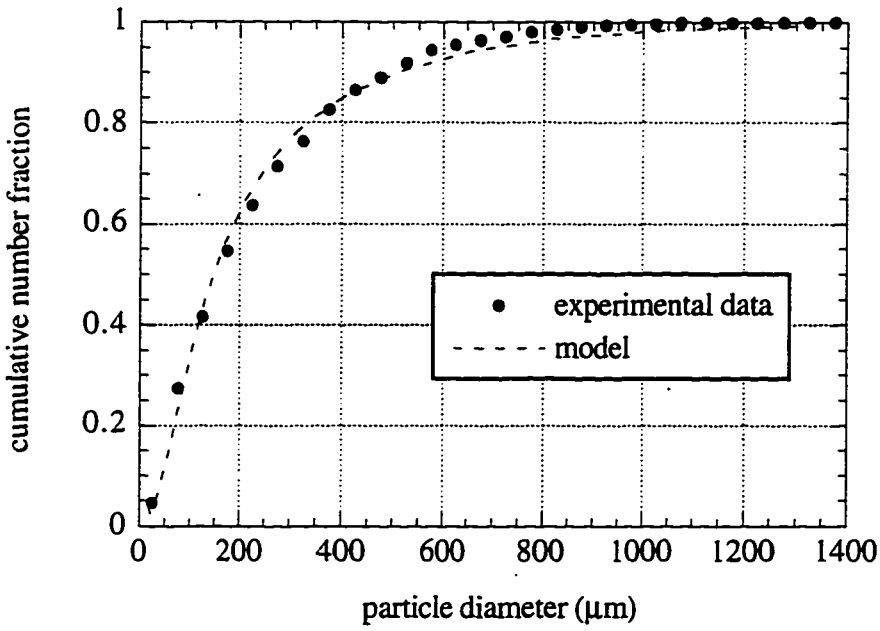

Figure 7.4 A comparison of the experimental data to the best fit of the population balance model.

Figure 7.5 shows the time-evolution of size distributions predicted by the model for sample conditions. Clearly, a smooth increase in particle size occurs until steady-state is reached. A plot of average particle size versus time shows the growth exhibits a slightly sigmoidal behavior.

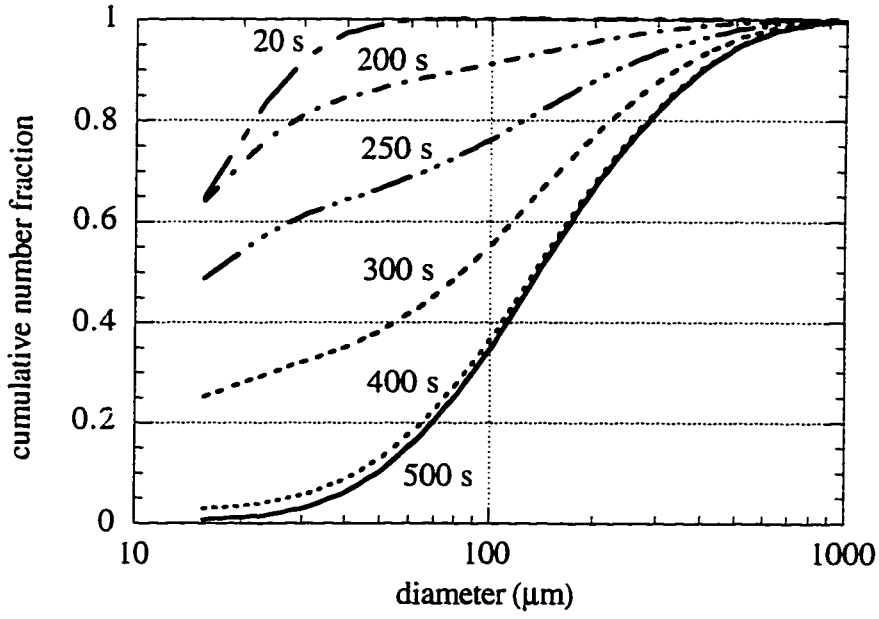

Figure 7.5 Evolution of particle size distributions in time predicted by the population balance model for typical conditions.

In order for the population balance model to correctly fit the experimental data, the three parameters, ρ, ν, and p, must be properly chosen. The best fits are obtained when p = 0.5, indicating particle breakup occurs by a splitting mechanism predominantly, and therefore not by erosion. Furthermore, ν is found to be either 0.735 when 1000 ppm cationic starch is present or 0.884 when it is not present, indicating the particle breakup rate is proportional to particle diameter to a power somewhat less than 1; 0.735 for 1000 ppm cationic starch, 0.884 for 0 ppm cationic starch. All changes in particle size are accounted for by changes in ρ, the ratio of aggregation rate to breakup rate constants. Thus, as experimental conditions vary, it is ρ which varies, changing the particle size, while ν and p remain essentially constant.

When only ρ varies, it is readily related to the average particle diameter:

$$\bar{d} = k\,\rho^{-1/\nu}, \tag{7.12}$$

where k is a constant with units of length. For ν = 0.884 (no cationic starch present), k = 1.86 x 10^{-4} m. When $\nu = 1$, the simple inverse relationship obtains; in our systems, however, ν is slightly less than 1, so the average diameter falls more steeply with ρ. Figure 7.6 shows the effect of varying ρ on $\bar{d}$.

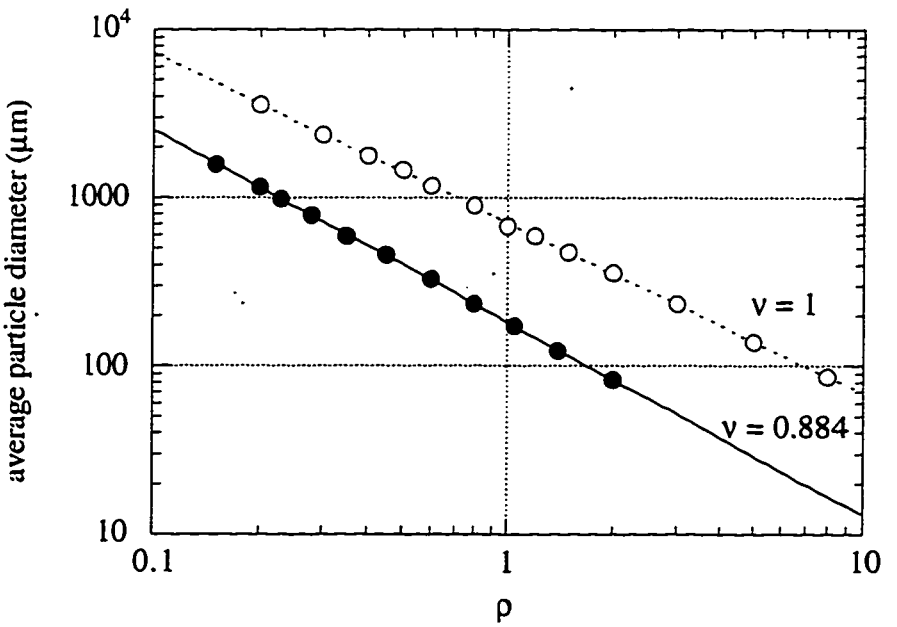

Figure 7.6 Population balance model: average particle diameter versus relative rate constants of aggregation and breakup, ρ, holding ν and p constant. Two values of ν are compared, $\nu = 0.884$ and $\nu = 1$. The fit lines are $\bar{d} = k\,\rho^{-1/\nu}$ where k is a constant.

Table 7.2 presents the relationships between the model parameters and the size distribution statistics. It is observed that ρ controls the particle size, ν controls the spread

of particle sizes at steady-state and p controls the skewness of the distribution, but not in a simple manner. Intuitive physical reasoning supports all these relationships: the balance of aggregation and breakup rates determines the ultimate particle size, the sensitivity of the breakup rate on particle size determines the compactness of the distribution about its average and reducing the size of the daughter particle formed on breakup increases the number of smaller particles while leaving a few large ones.

Table 7.2 Principal relationships between model parameters and size distribution statistics. The relationship obtains when the other two model parameters are held constant.

model parameter	size distribution statistic	relationship
ρ	$\bar{d}$	$\bar{d} = k\rho^{-1/\nu}$
ν	$\sigma/\bar{d}$	$\sigma/\bar{d} = k\nu^{-2/3}$
p	κ	complex; as $p\downarrow$, $\kappa\uparrow$

While ρ, the ratio of the breakup and aggregation rates determines the steady-state particle size, the absolute value of αVG determines the time needed to reach steady-state. Since V and G are fixed in an experiment, it is α that effectively fixes the time for full agglomeration. This is shown in Figure 7.7. When experimental determination of the time needed to reach steady-state is available, α can be numerically evaluated when V and G are known. Analyzing our experimental data, we find for the case when cationic starch is not present, $\alpha \approx 0.04$, since steady-state is found to be achieved in about 3 minutes. In 1000 ppm cationic starch, $\alpha \approx 0.004$ or less, corresponding to 30 minutes or more needed to reach the steady-state, as shown in Fig. 7.3. Thus, 1000 ppm cationic starch reduces the

collision efficiency of aggregation by at least an order of magnitude, even in the presence of the oil/surfactant blend.

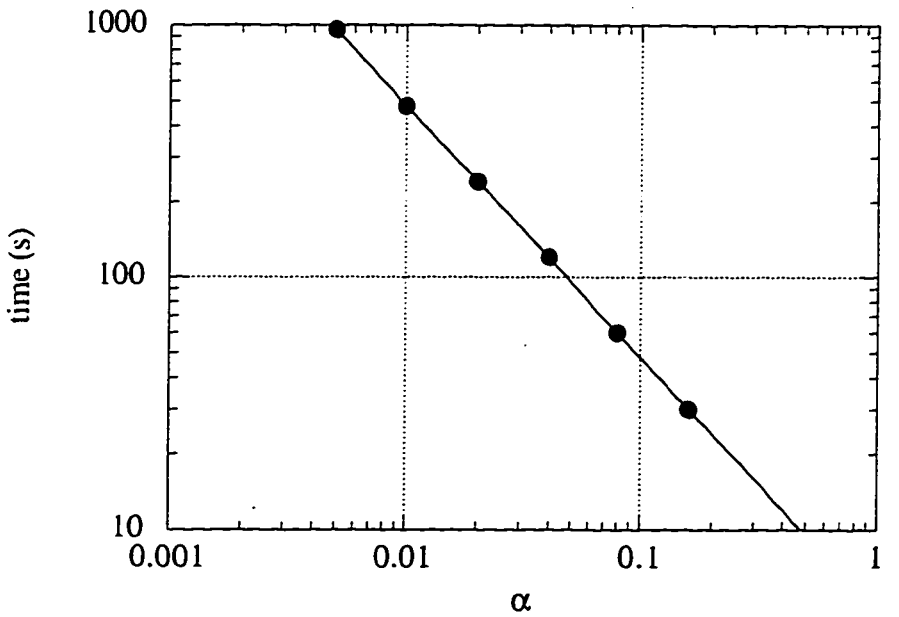

Figure 7.7 Time to reach steady-state average particle diameter versus aggregation collision efficiency, α. The fit line is time = $4.8/\alpha$. Thus, the time to reach full aggregation is inversely proportional to the aggregation efficiency. Typical conditions for other parameters were used: $\nu = 0.884$; $p = 0.5$; $G = 1500\ s^{-1}$; $\rho = 0.4$.

By combining the model results with the experimental trends observed, quantitative relations can be found between agglomeration response and operating variables. For instance, using the linear trends of particle size with shear in Fig. 7.1, the general equation is:

$$\bar{d} = k_1 \sigma (k_2 - G) \tag{7.13}$$

The best fit values give $k_1 = 9.13 \times 10^{-6}$ m^2 s^3 kg^{-1} and $k_2 = 2910$ s^{-1}. Equation 7.13 shows the average particle diameter is directly proportional to the oil-water interfacial tension, σ. Since both the crushing strength and the tensile strength for liquid bridge agglomerates are also found to be linearly proportional to σ (Newitt and Conway-Jones, 1958; Pietsch, 1990), we conclude the average agglomerate diameter is directly proportional to particle strength. To develop a relation between B, the absolute breakup rate constant and the particle strength, σ, we combine Eqs. 7.6, 7.7, 7.12, and 7.13 to find

$$B = k_3 \frac{1}{\sigma^v}. \tag{7.14}$$

Since v and p are found to be constant for the agglomeration systems studied here, the population balance model indicates that changes in ρ are the only way to influence the steady-state particle size distribution. Furthermore, we have seen that the aggregation rate alone controls the rate at which agglomeration proceeds to its steady-state configuration. Therefore, all of our experimental variables can be shown to affect either the aggregation rate, α (cationic starch), or the breakup rate, β (oil composition, temperature, agitation rate). Time does not affect either of these directly, of course, but the time needed for full agglomeration depends on α.

7.5 Conclusions

This chapter's results demonstrate how and why process conditions and ingredients control the success of oil-assisted agglomeration, using the collection of dispersed toner particles as our model system. By combining experimental investigations with a population balance model, a series of simple equations express the dependence of the particle size

distribution on time, temperature, agitation rate, oil composition and cationic starch presence. The experimental data follow a universal curve where a single parameter, here taken as the average particle size, predicts the particle size distribution.

The population balance model is simple but still captures the important physics of the process. It contains only three parameters but produces agreement with experimental size distributions. The ratio of breakup to aggregation contains the essential information on which successful agglomeration depends. Cationic starch affects this by reducing the aggregation rate through lowering the collision efficiency, and so both slowing the rate of agglomeration and its ultimate size. The factors temperature, agitation rate and oil composition interact by controlling the breakup rate, and through this influencing the agglomerate size distribution. The simple relation between particle size and aggregation and breakup rates are quantitatively expressed.

In a practical sense, this study stresses the need to reduce agitation rate as much as feasible during agglomeration, the need to allow long times when high levels of cationic starch are present, and the need to develop oil formulations that yield the strongest agglomerates. From a phenomenological consideration, we have demonstrated how oil-assisted agglomeration operates and how it can be effectively modeled, observing relatively simple relations between the important quantities to provide a clear conception of the underlying physics of the process.

7.6 Nomenclature

7.6.1 Latin Letters

A_{ijk} = aggregation rate third-order tensor, fixed for a given set of model parameters, dimensionless

B = rate constant for particle breakup, [=] s^{-1}

B_{ij} = breakup rate second-order tensor, fixed for a given set of model parameters, dimensionless

$\bar{d}$ = diameter of particle of number average volume (see Eqs. 7.1-7.2), [=] μm

G = the average rate of shear, $\left(\frac{\varepsilon}{\nu}\right)^{1/2}$ [=] s^{-1}

i,j,k = indices for bins

k, k_1, k_2, etc. = constants obtained from data fitting, dimensions as given in the text

n = number of bins in model simulation

t = time, [=] s

v_i = characteristic particle volume for bin i

V = volume fraction of aggregating particles in fluid

x_i = volume fraction of all dispersed particles in bin i

7.6.2 Greek Letters

α = collision efficiency (ratio of aggregate-forming particle-particle collisions to all such collisions).

β = dimensionless rate constant for breakup, = B/G

ε = energy input by stirring per unit mass of fluid, [=] W/kg

ν = exponent expressing dependence of breakup rate on particle diameter; also kinematic viscosity of fluid, [=] m^2/s

ρ = dimensionless ratio of breakup rate to aggregation rate constants, = $\beta/\alpha V$

σ = the standard deviation of a particle size distribution, [=] μm

τ = dimensionless time, = $t\alpha VG$

CHAPTER EIGHT

CONCLUSIONS AND RECOMMENDATIONS

8.1 Conclusions

The following are the major, novel conclusions of the work presented in the body of the dissertation, Chapters 4-7.

1. Toners used in toner-printed paper are susceptible to collection by a water-immiscible liquid that preferentially wets the toner particles, leaving the more hydrophilic fibers unaffected.

2. Toner-particle agglomeration proceeds by the steps of (1) dispersion of the immiscible liquid drops, (2) coalescence of the drops with toner particles, and (3) collection of the wet toner particles into growing clumps through enhanced adhesion engendered by the oil drops. Either the strength of liquid bridges or softening and fusing of the toner particles brings about the adhesion enhancement.

3. Toner particles in water with or without the presence of cellulose fibers (up to 5 wt% fibers tested) can be easily collected by liquid bridge agglomeration at room temperature into agglomerates with a diameter of order 1 mm with a simple aliphatic oil.

4. The cationic polymers used primarily as retention aids, sizing agent emulsifiers and dry surface sizing agents in fine printing and writing papers, including those used for toner printing, are partly released from the sheets during repulping and redissolve in the repulper. The cationic polymers, of which cationic starch is most prevalent, adsorb to all negatively-charged interfaces, including oil droplets and toner particles, providing an electrosterically-active adlayer on these surfaces. This has several important consequences for the surface chemistry in a de-inking process:

A. The toner particles go from negatively charged to weakly positively charged.

B. The toner particles exhibit a mixture of hydrophobic and hydrophilic properties, including a zero receding contact angle with water, due to the hydrophilization engendered by the cationic starch.

C. The coalesceability of oil drops and toner particles is severely reduced by the presence of this stabilizing adlayer.

5. Direct measurements of particle-drop interactions have been performed with the aid of an atomic force microscope, and a clear difference in the rate at which toner particles and drops of a simple aliphatic oil achieve coalescence was observed as cationic starch was added. The film drainage time in pure water was 52 milliseconds; with 1000 ppm cationic starch, it exceeded 191 milliseconds.

6. An oil consisting of a blend of oil-soluble surfactant with an aliphatic oil produces agglomeration with two interesting consequences: first, the oil blend engulfs the cationic starch adlayer through favorable solubility and has some ability to engulf the adlayer on the toner particles, too; second, it fuses the toner particles together at temperatures above 35 °C by dissolving the thermoplastic toner resin when the drops collide on the surface at high temperature. However, at room temperature, the lower interfacial tension of the blend compared to a pure oil produces weaker agglomerates, and therefore, smaller agglomerates. No cationic starch must be present, of course, for the pure oil to work at room temperature.

7. The oil composition, cationic starch concentration, degree of agitation, time and temperature of agitation all produce major effects on agglomeration performance, and the results presented in Chapter 7 clarify these, deducing quantitative relationships where possible (Eqs. 7.12-7.14). All factors relevant to agglomeration are shown to affect the competition between aggregation and breakup rates. The ratio of these rates determines the

steady-state agglomerate size distribution, while the absolute magnitude of the aggregation rate determines the kinetics of aggregation. The individual roles of the key variables are easily summarized:

A. Oil composition affects the aggregate strength, and hence, the breakup rate, by its interfacial tension and its ability to fuse the toner together; it affects the aggregation rate by its ability to increase collision efficiency when cationic starch is present.

B. Cationic starch does not affect the strength of agglomerates, but only reduces the aggregation rate, and so slows the process and reduces the ultimate particle size achieved.

C. Agitation rate fosters agglomeration by bringing particles together, but this effect is outweighed by its increase in the breakup rate. Thus, increasing the agitation rate (over the range examined) reduces the particle size produced. Increasing agitation also increases the rate at which steady-state is attained.

D. Temperature operates to increase the effectiveness of agglomeration by reducing particle breakup, a result engendered by fusing toner particles together when the oil composition contains some slightly polar, oil-soluble surfactant.

E. Time is needed when the absolute magnitude of the aggregation rate is low, which occurs when cationic starch is present. It also occurs when low concentrations of toner are present in the agglomeration vessel.

8.2 Recommendations

The following results follow from the conclusions.

1. Anything that can be done to enhance aggregate strength will help agglomeration. In particular, finding a suitable oil that serves to fuse the toner particles at low temperature would allow more effective agglomeration at low temperature; changing the oil composition, perhaps by the addition of viscoelastic compounds that render the liquid bridges tacky and breakup-resistant, could also improve performance.

2. A reduction in cationic polymer use in paper manufacture would benefit agglomeration. Alternatively, development of oil compositions that easily coalesce with toner particles in cationic starch solutions, a criterion that can be tested with the novel use of the atomic force microscope described in Chapter 6, would allow rapid and thorough agglomeration to occur in the current repulper environment.

3. The minimum necessary intensity of agitation should be used during agglomeration.

4. Similarly, toner concentrations should be kept as high as possible to foster rapid kinetics, which is particularly important when large amounts of cationic starch are present. High toner concentrations also foster larger steady-state particle sizes. This means practitioners should add exclusively toner-printed paper to a single agglomeration batch, and not include significant amounts of other types of printed stock, which would reduce the number of toner particles available for collision and agglomeration.

Future research efforts should focus on manipulations of the oil composition, particularly in trying to find a viscoelastic formulation that makes the toners tacky at room temperature and able to form strong adhesive bonds. Similarly, on a more phenomenological level, investigation of particle-drop interactions with the atomic force microscope as described in Chapter 6 would prove both interesting and valuable–

interesting because of the basic science accessible with the experiment and valuable because it can serve to uncover how changes in cationic polymers, oil components and other dissolved additives combine to influence the fundamental step of agglomeration, coalescence of oil-water and toner-water interfaces.

LIST OF REFERENCES

Adamson, A.W. (1990). *Physical Chemistry of Surfaces*, 5th ed., John Wiley & Sons, Inc., New York , pp. 21-2.

Akhadov, Y. Y. (1980). *Dielectric Properties of Binary Mixtures.* Oxford, Pergamon Press.

Amand, F. J. S. and B. Perrin (1991). "The Effect on Particle Size on Ink and Speck Removal Efficiency of the Deinking Steps", *Preprints from the First Research Forum on Recycling*, 39-47. Technical Section of the Canadian Pulp and Paper Association, Montreal.

Andreu-Villegas, R. and R.D. Letterman (1976). "Optimizing Flocculation Power Input". *J. Environ. Eng. Div. Proc. Amer. Soc. Civ. Eng.* 102, EE2, 251.

Aspler, J. *et al.* (1989). "Recycling and the Canadian Pulp and Paper Industry", Report. Pulp and Paper Research Institute of Canada (PAPRICAN), Sep. 5, 1989.

Ayazi Shamlou, P. and N. Titchener-Hooker (1993). "Turbulent Aggregation and Breakup of Particles in Stirred Vessels," *Processing of Solid-Liquid Suspensions*, P. Ayazi Shamlou, ed.; Butterworth-Heinemann, Oxford, pp. 1-25.

Basta, N. (1991). "Recycling Everything: Part 3, Paper Recycling's New Look", *Chem. Engng.* 1991, March, 45.

Bagster, D.F. (1993). "Aggregate Behavior in Stirred Vessels", In *Processing of Solid-Liquid Dispersions*, P. Ayazi Shamlou, ed.; Butterworth-Heinemann, Oxford, pp. 26-58.

Bemer, G.G. (1979). "Agglomeration in Suspension: A Study of Mechanisms and Kinetics," Ph.D. Dissertation, Delft University of Technology, Delft, Netherlands.

Bemer, G. G. and F. J. Zuiderweg (1980). "Growth Regimes in the Spherical Agglomeration Process" In *Fine Particles Processing*, Somasundaran, P., ed. pp. 1524-46. Am. Inst. of Mining, Metallurgical, and Petroleum Engng., New York.

Berg, J. C. (1986). "The Use and Limitation of Wetting Measurements in the Prediction of Adhesive Performance" In *C.omposite Systems from Natural and Synthetic Polymers*, Salmén, L., *et al.*, eds. p. 23. Elsevier, Amsterdam.

Biggs, S. and P. Mulvaney (1994). "Measurement of the Forces Between Gold Surfaces in Water by Atomic Force Microscopy", *J. Chem. Phys.* 100, 8501-5.

Binnig, G. and C. F. Quate (1986). "Atomic Force Microscope", *Phys. Rev. Lett.* 56, 930-3.

Blain, T., J. Grant and D. Oldroyd (1993). "Short Sequence Recycling: The Mechanism," *Preprints from 2nd Research Forum on Recycling* (Ste-Adèle, Quebec, October, 1993). pp.101-10, Technical Section of the Canadian Pulp and Paper Association, Montreal.

De Boer, G. B. J., G.F.M. Hoedemakers and D. Thoenes (1989). "Coagulation in Turbulent Flow" (in 2 parts), *Chem. Eng. Res. Dev.*, 67, 301-315.

Borchardt, J. K. (1993). "Office Wastepaper Deinking Process Using Fatty Alcohols". US Patent 5,258,099. Assigned to Shell Oil Company.

Butt, H.-J. (1991). "Measuring Electrostatic, van der Waals, and Hydration forces in Electrolyte Solutions with an Atomic Force Microscope.", *Biophys. J.* 60, 1438-44.

Butt, H.-J. (1994). "A Technique for Measuring the Force Between a Colloidal Particle in Water and a Bubble", *J. Colloid Interface Sci.* 166, 109-17.

Camp, T.R.and P.C. Stein (1943). "Velocity Gradients and Internal Work in Fluid Motion," *J. Boston Soc. Civ. Engng.*, 30, 219.

Capes, C. E. and K. Darcovich (1984). "A Survey of Oil Agglomeration in Wet Fine Coal Processing", *Powder Technol.* 40, 43-52.

Carr, W. F. (1991). "New Trends in Deinking Technology - Removing Difficult Inks from Wastepaper", *Tappi J.* 74, 2, 127-32.

Cathie, K. and H. Crow (1991). "Difficult to Deink Wastepaper Grades- The Way Forward", *TAPPI 1991 Pulping Conference*, 85-9. TAPPI Press, Atlanta.

Chen, W. (1991). "Protein Precipitation by Polyeletrolytes," Ph.D. Dissertation. Department of Chemical Engineering, University of Washington, Seattle, WA.

Christenson, H. K. and P. M. Claesson (1988). "Cavitation and the Interaction between Macroscopic Hydrophobic Surfaces," *Science* 239, 390-2.

Christenson, H. K. P.M. Claesson, J. Berg and P.C. Herder (1989). "Forces between Fluorocarbon Surfactant Monolayers: Salt Effects on the Hydrophobic Interaction", *J. Phys. Chem.* 93, 1472-8.

Christenson, H. K. J. Fang, B.W. Ninham and J.L. Parker (1990). "Effect of Divalent Electrolyte on the Hydrophobic Interaction", *J. Phys. Chem.* 94, 8004-6.

Christenson, H. K., P. M. Claesson and J. L. Parker (1992). "Hydrophobic Attraction: A Reexamination of Electrolyte Effects," *J. Phys. Chem.* 96, 6725-8.

Claesson, P. M. and H. K. Christenson (1988). "Very Long-Range Attractive Forces Between Uncharged Hydrocarbon and Fluorocarbon Surfaces in Water," *J. Phys. Chem.* 92, 1650-5.

Claesson, P. M., C.E. Blom, P.C. Herder and B.W. Ninham (1986). "Interactions between Water-Stable Hydrophobic Langmuir-Blodgett Monolayers on Mica," *J. Colloid Interface Sci.* 114, 234-42.

Cleveland, J. P. S. Manne, D. Bocek and P.K. Hansma (1993). "A Nondestructive Method for Determining Spring Constant of Cantilevers for Scanning Force Microscopy," *Rev. Sci. Instrum.* 64, 403-5.

Darlington, W. B. (1988). "A New Process for Deinking Electrostatic-Printed Secondary Fiber", *TAPPI 1988 Pulping Conference*, 95-100. TAPPI Press, Atlanta.

Darlington, W. B. (1989). "A New Process for Deinking Electrostatically-Printed Secondary Fiber", *Tappi J.* 72, 1, 35-8.

Darlington, W. B. (1992). "Method for Deinking Wastepaper Using Alkoxy Capped Polyethylene Oxide and a Polymeric Material." US Patent 5,102,500. Assigned to PPG Industries, Inc., Pittsburgh, PA.

Dubois, M., K.A. Gilles, J.K. Hamilton, P.A. Rebers and F. Smith (1956). "Colorimetric Method for Determination of Sugars and Related Substances", *Analy. Chem.* 28, 3, 350-6.

Ducker, W. A., T. J. Senden and R. M. Pashley (1991). "Direct Mesurement of Colloidal Forces Using an Atomic Force Microscope", *Nature* 353, 239-41.

Ducker, W. A., Z. Xu and J. N. Israelachvili (1994). "Measurements of Hydrophobic and DLVO Forces in Bubble-Surface Interactions in Aqueous Solutions", *Langmuir* 10, 9, 3279-89.

Dunstan, D., L. R. White and T. W. Healy (1986). "Kinetic Model of the Oil Agglomeration Process", *Trans. Inst. Mining Metallurgy. C.* 95, C127-32.

Epple, M. and J. C. Berg (1994). "The Effect of Adsorbed Surfactants on the Electrostatic Properties and Wettability of a Xerographic Toner", *Prog. Paper Recycling* 3, 3, 52-7.

Epple, M., D. Schmidt and J. C. Berg (1994). "The Effect of Froth Stability and Wettability on the Flotation of a Xerographic Toner", *Colloid & Polym. Sci.* 272, 10, 1264.

Eriksson, J.C.and S. Ljunggren (1995). "Comments on the Alleged Formation of Bridging Cavities/Bubbles between Planar Hydrophobic Surfaces,"*Langmuir, 11*, 2225-8.

Evans, D. F. and H. Wennerström (1994). *The Colloidal Domain.* VCH, New York.

Farnand, J. R., H. M. Smith and I. E. Puddington (1961). "Spherical Agglomeration of Solids in Liquid Suspension", *Canadian J. Chem. Engng.* 1961, April, 94-7.

Ferguson, K. H. (1992a). "Prime Fiber Recycles Laser-Inked Waste with Chemical/Mechanical Technologies", *Pulp Paper* 66, 13, 57-64.

Ferguson, L. D. (1992b). "Deinking Chemistry: part 1", *Tappi J.* 75, 7, 75-83.

Fielden, M.L., R.A. Hayes and J. Ralston (1996). "Surface and Capillary Forces Affecting Air Bubble-Particle Interactions in Aqueous Electrolyte", *Langmuir 12*, 3721-7. These authors also cite a relevant paper on particle interactions with a liquid-liquid interface for work done by Mulvaney and coworkers and submitted to *J. Colloid Interface Sci.*

Fisher, L.R., E.E. Mitchell, D. Hewitt, J. Ralston and T. Wolfe (1991). "The Drainage of a Thin Aqueous Film between a Solid Surface and an Approaching Gas Bubble",*Colloids & Surfaces, 52*, 163-74.

Fuerstenau, D. W., J. Diao and M. C. Williams (1991). "Characterization of the Wettability of Solid Particles by Film Flotation. 1. Experimental Investigations", *Colloids Surfaces* 60, 127.

Geake, E. (1994). "Photocopies: Now You See Them, Now You Don't," *New Scientist* 141, Jan. 15, 20.

Grabenbauer, G.C. and C.E. Glatz (1981). "Protein Precipitation– Analysis of Particle Size Distributions and Kinetics,"*Chem. Engng. Commun.* 12, 203.

Green, C. J. (1972). "Deinking of Waste Xerographic Copy Paper". US Patent 3,635,789 Assigned to Xerox Corp., Webster, NY.

Hadziioannou, G., S. Patel, S. Granick and M. Tirrell (1986). "Forces between Surfaces of Block Copolymers Adsorbed on Mica,' *J. Am. Chem. Soc.,108*, 2869-2876.

Hesselink, F. T. (1983). "Adsorption of Polyelectrolytes from Dilute Solution" In *Adsorption from Solution at the Solid/Liquid Interface*, Parfitt, G. D., Rochester, C. H., eds. pp. 377-412. Academic Press, London.

Hewitt, D., D. Fornasiero and J. Ralston (1995). "Bubble-Particle Attachment," *J. Chem. Soc. Faraday Trans., 91*, 1997-2001.

Higashitani, K., R. Ogawa and G. Hosokawa (1982). "Kinetic Theory of Shear Flocculation for Particles in a Viscous Fluid", *J. Chem. Engng. Japan* 15, 299-304.

Higashitani, K., K. Yamanchi, Y. Matsuno and G. Hosokawa (1983). "Turbulent Coagulation of Particles Dispersed in a Viscous Fluid", *J. Chem. Engng. Japan* 16, 299-304.

Hounslow, M.J., R. L. Ryall and V.R. Marshall (1988). "A Discretized Population Balance for Nucleation, Growth, and Aggregation," *AIChE J.*, 34, 1821.

House, C. I. and C. J. Veal (1992). "Spherical Agglomeration in Mineral Processing" In *Colloid and Surface Engineering: Applications in the Process Industries*, Williams, R. A., ed. pp. 188-212. Butterworth-Heinemann, Oxford.

Huang, P.Y. and J. D. Hellums (1993). "Aggregation and Disaggregation Kinetics of Human Blood Platelets" (in 3 parts), *Biophysical J.*, 65, 334-61.

Hulburt, H.M. and S.L. Katz (1964). "Some Problems in Particle Technology. A Statistical Mechanical Formulation," *Chem. Eng. Sci.*, 19, 555-574.

Hunter, R. J. (1987). *Foundations of Colloid Science.* 2 vols., Oxford, Clarendon Press.

Israelachvili, J. N. (1989). "Techniques for Direct Measurements of Forces between Surfaces in Liquids at the Atomic Scale", *Chemtracts-Analy. Phys. Chem.* 1, 1-12.

Israelachvili, J. N. (1992). *Intermolecular and Surface Forces.* London, Academic Press.

Israelachvili, J. N. and R. M. Pashley (1984). "Measurement of the Hydrophobic Interaction between Two Hydrophobic Surfaces in Aqueous Electrolyte Solutions," *J. Colloid Interface Sci.* 98, 500-14.

Jacob, P. N. and J. C. Berg (1993). "Contact Angle Titrations of Pulp Furnishes," *Tappi J.* 76(5), 133-8.

Jeffries, T. W. J.H. Klungness, M.S. Sykes and K.R. Rutledge-Cropsey (1994). "Comparison of Enzyme-Enhanced with Conventional Deinking of Xerographic and Laser-Printed Paper", *Tappi J.* 77(4), 173-9.

Johnson, R. E., Jr. and R. H. Dettre (1969). "Wettability and Contact Angles" In *Surface and Colloid Science*, E. Matijevic, ed. p. 85. Wiley-Interscience, New York.

Jones, W. S. (1992). "Laser Ink Dispersion: Another Approach", *Prog. Paper Recycling* 1(4), 51-56.

Kawashima, Y. and C.E. Capes (1974). "An Experimental Study of the Kinetics of Spherical Agglomeration in a Stirred Vessel," *Powder Technology*, 10, 85-92.

Kawashima, Y. and C.E. Capes (1976). "Further Studies of the Kinetics of Spherical Agglomeration in a Stirred Vessel," *Powder Technology*, 13, 279-288.

Klein, J. (1988). In *Molecular Conformation and Dynamics of Macromolecules in Condensed Systems* (Series: *Studies in Polymer Science*, vol. 2), Nagasawa, M, Ed.; Elsevier: Amsterdam, pp. 333-52.

Koopal, L. K., V. Hlady and J. Lyklema (1988). "Electrophoretic Study of Polymer Adsorption: Dextran, Polyethylene Oxide and Polyvinyl Alcohol on Silver Iodide", *J. Colloid Interface Sci.* 121, 1, 49-62.

Kruyt, J. R. and F. G. van Selms (1943). "The Influence of a Third Phase on the Rheology of Suspensions", *Rev. Trav. Chim.*, 62, 415-26.

Kurihara, K., S. Kato and T. Kunitake (1990). "Very Strong Long-Range Attractive Forces between Stable Hydrophobic Monolayers of a Polymerized Surfactant,"*Chem. Lett.* 9, 1555-8.

Labuschagne, B. C. J. (1986). "Die Invloed van Skiedingsvlakke op die Olie-Agglomerasie van Steenkool". D. Sc. Thesis, Potchefstroom Unversity for CHE, South Africa.

Lapointe, M., L. Marchildon and B. Bonnelly (1988). "The Deinking of Xerographic Paper by Flotation", *TAPPI 1988 Pulping Conference*, 81-94. TAPPI Press, Atlanta.

Larson, I. C.J. Drummond, D.Y.C. Chan and F. Grieser (1993). "Direct Force Measurements betwen Titania Surfaces", *J. Am. Chem. Soc.* 155, 11885-90.

Larsson, A. (1987). "Surface Chemistry in Flotation Deinking", *PTI* 1987, February, 388-390.

Larsson, A., P. Stenius and L. Ödberg (1984a). "Surface Chemistry in Flotation Deinking Part 1. The Floatability of Model Ink Particles", *Svensk Papperstidning* 1984, 18, R158-64.

Larsson, A., P. Stenius and L. Ödberg (1984b). "Surface Chemistry in Flotation Deinking Part 2. The Importance of Ink Particle Size", *Svensk Papperstidning* 1984, 18, R165-9.

Lea, A.S., J.D. Andrade and V. Hlady (1993). "Measurement of Steric Exclusion Forces with the Atomic Force Microscope", In*Colloid-Polymer Interactions: Particulate, Amphiphilic, Biological Surfaces* Dubin, P, Tong, P., Eds.; Amercian Chemical Society: Washington, DC, pp. 266-79.

Li, Y.Q., N.J. Tao, J. Pan, A.A. Garcia and S.M. Lindsay (1993). "Direct Measurement of Interaction Forces between Colloidal Particles using the Scanning Force Microscope", *Langmuir* 9, 637-41.

Lu, C.F. and L.A. Spielman (1985). "Kinetics of Floc Breakage and Aggregation in Agitated Liquid Suspensions," *J. Colloid Interface Sci.* 103, 95-105.

Luttrell, G.H. and R.-H. Yoon (1988). "Determination of the Probability of Bubble-Particle Adhesion using Induction Time Measurements," In *Production and Processing of Fine Particles*; Plumpton, A.J., Ed.; Pergamon Press: New York, pp. 159-65.

Marchildon, L., M. Lapointe and B. Chabot (1989). "The Influence of Particulate Size in Flotation Deinking of Newsprint", *Pulp Paper Canada* 90, 90-95.

Marton, J. and T. Marton (1976). "Wet-End Starch: Adsorption of Starch on Cellulosic Surfaces,"*Tappi J.* 59, 121.

McCool, M. A. and L. Silveri (1987). "Removal of Specks and Non-dispersed Ink from a Deinking Furnish", *TAPPI 1987 Pulping Conference*, 33-40. TAPPI Press, Atlanta.

Meagher, L. (1992). "Direct Measurement of Forces between Silica Surfaces in Aqueous $CaCl_2$ Solutions Using an Atomic Force Microscope", *J. Colloid Interface Sci.* 152, 293-5.

Mehrota, V. P. and K. V. S. Sastry (1985). "A Novel Method for the Calculation of Pendular Bond Characteristics between Unequal Size Particles", *Powder Technol.* 41, 259-63.

Meloy, T.P. (1962). In *Froth Flotation, 50th Anniversary Volume*; Fuerstenau, D.W., Ed.; American Institute of Mining, Metallurgical and Petroleum Engineers Inc.: New York, ch. 9.

Mestetsky, T. S. and B. G. Webster (1974). "Deinking of Wastepaper with an Aqueous Solution Containing an n-Alkyllactam Solvent". US Patent 3,846,227. Assigned to GAF Corp.

Muralidhar, R. and D. Ramkrishna (1986). "Analysis of Droplet Coalescence in Turbulent Liquid-Liquid Dispersions", *Ind. Engng. Chem. Fundam.* 25, 554-60.

Naimpally, A. V. (1981). "Note on the Use of Ultrasonics for Deinking Paper," *Appita* 35, 3, 242.

Newitt, D. M. and J. M. Conway-Jones (1958). "A Contribution to the Theory and Practice of Granulation", *Trans. Inst. Chem. Engng.* 36, 422-442.

Niwa, J. (1977). "The Effects of Mass Transfer and Surfactant Adsorption on the Instability of Capillary Jets in Liquid-Liquid Systems,".M. S. Thesis, University of Washington, Seattle, WA.

Norman, J. C., N. J. Sell and M. Danelski (1994). "Deinking Laser-Print Paper Using Ultrasound", *Tappi J.* 77, 3, 151-8.

O'Brien, R. W. and L. R. White (1978). "Electrophoretic Mobility of a Spherical Colloid Particle," *J. Chem. Soc. Faraday Trans. 2* 74, 1607.

Okada, E. and H. Urushibata (1991). "Deinking of Toner Printed Paper", *TAPPI 1991 Pulping Conference*, 857-63. TAPPI Press, Atlanta.

Olson, C. R. S.K. Richmann, F.J. Sutman and M.B. Letscher (1993b). "Deinking of Laser-Printed Dtock Using Chemical Densification and Forward Cleaning", *Tappi J.* 76(1), 136-44.

Olson, C. R., J. D. Hall and I. J. Philippe (1993a). "Laser Print Deinking Using Chemically-Enhanced Densification and Forward Cleaning", *Prog. Paper Recycling* 3, 2, 24-34.

Ortner, H. E. (1981). "Flotation Deinking", In series: *Recycling of Papermaking Fibers*, H. E. Corwin, ed. TAPPI Press, Atlanta.

Pandya, J.D. and L.A. Spielman (1982). "Floc Breakage in Agitated Suspensions: Theory and Data Processing Strategy," *J. Colloid Interface Sci.* 90, 517-31.

Parker, D.S., W.J. Kaufman and D. Jenkins (1972). "Floc Breakup in Turbulent Flocculation Processes", *J. San. Eng. Div. Proc. Amer. Soc. Civ. Eng.* 98, SA1, 79.

Parker, J. L., D. L. Cho and P. M. Claesson (1989). "Plasma Modification of Mica: Forces bgetween Fluorocarbon Surfaces in Water and a Nonpolar Liquid," *J. Phys. Chem.* 93, 6121-5.

Parker, J.L., P.M. Claesson and P. Attard (1994). "Bubbles, Cavities and Long-Ranged Attraction between Hydrophobic Surfaces," *J. Phys. Chem. 98*, 8468-72.

Pashley, R.M., P.M. McGuiggan, B.W. Ninham and D.F. Evans (1985). "Attractive Forces between Uncharged Hydrphobic Surfaces: Direct Measurements in Aqueous Solution", *Science* 229, 1088-91.

Paulsen, F.G., R. Pan, D.W. Bousfield and E.V. Thompson (1996). "The Dynamics of Bubble/Particle Attachment and the Application of Two Disjoining Film Rupture Models to Flotation. 1. Nondraining Model," *J. Colloid Interface Sci., 178*, 400-10.

Perry, R. H., D. W. Green and J. O. Maloney, eds. (1984). *Perry's Chemical Engineers' Handbook.* McGraw-Hill, New York.

Pfalzer, L. (1979). "Deinking of Xerographic and Carbonless Copy Paper", *Tappi J.* 62, 7, 27-30.

Pietsch, W. (1990). *Size Enlargement by Agglomeration.* Chichester, Wiley.

Puddington, I. E. and B. D. Sparks (1975). "Spherical Agglomeration Processes", *Minerals Sci. Engng.* 7, 282-8.

Pugh, R.J. and E. Manev (1992). "The Study of Thin Aqueous Films as Models For Froths and Flotation," In *Innovations in Flotation Technology*; Mavros, P., Matis, K.A., Eds.; Kluwer Academic, Dordrecht, pp. 1-24.

Quick, T. H. (1981). "Deinking Waste Electrophotography Copy Paper". US Patent 4,276,118. Assigned to Weyerhaeuser Company, Tacoma, WA.

Quick, T. H. and K. T. Hodgson (1986). "Xerography Deinking - a Fundamental Approach", *Tappi J.* 69, 102-8.

Rabinovich, Y. I. and B. V. Derjaguin (1988). "Interaction of Hydrophobic Filaments in Aqueous Electrolyte Solutions", *Colloids Surfaces* 30, 243-51.

Ralston, J. (1983). "Thins Films and Froth Flotation," *Adv. Colloid Interface Sci., 19*, 1-25.

Ramkrishna, D. (1978). "Drop Breakage in Agitated Liquid-Liquid Dispersions", *Chem. Eng. Sci.* 29, 987.

Ramkrishna, D. (1985). "The Status of Population Balances," *Rev. Chem. Engng.* 3, 49.

Rhodes, T. and L. Ferguson (1993). "Deinking Non-Impct Printed Office Waste: A Mill's Perspective", *TAPPI 1993 Recycling Symposium*, 123-9. TAPPI Press, Atlanta.

Richmann, S. K. and M. B. Letscher (1992). "Process and Composition for Deinking Dry Toner Electrostatic Printed Wastepaper." US Patent 5,141,598. Assigned to Betz Paperchem, Inc.

Richmann, S. K. and M. B. Letscher (1993a). "Use of Surfactants Having an HLB Less than 10 in the Deinking of Dry Toner Electrostatic Printed Wastepaper." US Patent 5,200,034. Assigned to Betz Paperchem, Inc.

Richmann, S. K. and M. B. Letscher (1993b). "Use of Surfactants Having an HLB Less than 10 in the Deinking of Dry Toner Electrostatic Printed Wastepaper." US Patent 5,248,388. Assigned to Betz Paperchem, Inc.

Richmann, S. K. and M. B. Letscher (1994). "Process and Composition for Deinking Dry Toner Electrostatic Printed Wastepaper." US Patent 5,302,242. Assigned to Betz Paperchem, Inc.

Safferman, P. G. and J. S. Turner (1956). "On the Collision of Drops in Turbulent Clouds," *J. Fluid. Mech.* 1, 16.

Schmidt, D. C. and J. C. Berg (1995). "The Effect of Particle Shape on the Flotation of Toner Particles", *Prog. Paper Recycling*, 5, 2, 67.

Schmidt, D.C. and J.C. Berg (1996). "A Preliminary Hydrodynamic Analysis of the Flotation of Disk-Shaped Toner Particles", submitted to *Prog. in Paper Recycling*, Sep. 1996.

Schwartzberg, H.G. and R.E. Treybal (1968). "Fluid and Particle Motion in Turbulent Stirred Tanks," *Industrial Engng. Chem. Fundam.* 7, 6-12.

Schulze, H. J. (1984). *Physico-chemical Elementary Processes in Flotation*. Amsterdam, Elsevier.

Schulze, H. J. (1991). "The Fundamentals of Flotation Deinking in Comparison to Mineral Flotation", *Preprints from the First Research Forum on Recycling*, 161-7. Technical Section of the Canadian Pulp and Paper Association.

Schulze, H.J. *Physico-chemical Elementary Processes in Flotation*; Elsevier: Amsterdam, 1984; p. 121.

Seldin, I. (1985). "Xerographic Copy Recycling", *1985 TAPPI Pulping Conference*, Tappi Press, Atlanta.

Senden, T. J. and W. A. Ducker (1994). "Experimental Determinations of Spring Constants in Atomic Force Microscopy," *Langmuir* 10, 1003.

Smoluchowski, M. (1917). "Mathematical Theory of the Kinetics of Coagulation of Colloidal Systems," *Z. Phys.Chem.*, 92, 129-168 (in German).

Snow, R. H., B.H. Kaye, C.E.Capes and G. C. Sresty (1984). "Size reduction and size enlargement" In *Perry's Chemical Engineers Handbook*, R. H. Perry, D. W. Green and J. O. Maloney, eds. p. 8-81. McGraw-Hill, New York.

Snyder, B. A. and J. C. Berg (1994a). "Effect of Particle Size and Density in Flotation Deinking Electrostatic Papers", *Tappi J.* 77, 7, 157-9.

Snyder, B. A. and J. C. Berg (1994b). "Liquid Bridge Agglomeration: A Fundamental Approach to Toner Deinking", *Tappi J.* 77, 5, 79-85.

Snyder, B. A., D. C. Schmidt and J. C. Berg (1993). "Characterization and Flotation Studies of Electrostatic Inks", *Prog. Paper Recycling* 3, 1, 17-27.

Snyder, B.A. and J.C. Berg (1996a). "Deinking Toner-Printed Paper by Selective Agglomeration," *Pulp Paper Can.* 97, 38.

Snyder, B.A., D.E. Aston and J.C. Berg (1996b). "Particle-Drop Interactions Examined with an Atomic Force Microscope," Submitted to *Langmuir* Sep. 1996.

Snyder, B.A. and J.C. Berg (1996c). "Oil-Assisted Agglomeration for Toner De-Inking: Population Balance Model and Experiments," Submitted to *AIChE J.* Sep. 1996.

Spielman, L. A. (1971). "Viscous Interactions in Brownian Coagulation," *J. Colloid Interface Sci.* 33, 562.

Spoelstra, J. (1989). "The Modeling of Oil Agglomeration of Coal Fines", *J. Computational Appl. Math.* 28, 359-66.

Stock, D. I. (1952). "Micro-Spherical Aggregation of Barium Sulphate", *Nature, London* 170, 423.

Sutherland, J. P. (1962). "Agglomeration of Aqueous Suspensions of Graphite", *Canadian J. Chem. Engng.* 1962, December, 268-72.

Swinkels, J. J. M. (1985). "Sources of Starch, its Chemistry and Physics" In *Starch Conversion Technology*, van Beynum, G. M. A. and Roels, J. A., eds. pp. 15-46. Marcel Dekker, New York.

TAPPI (1992). *TAPPI Test Methods.* TAPPI Press, Atlanta.

Tomi, D. and D.F. Bagster (1975). "A Model of Floc Strength Under Hydrodynamic Forces", *Chem. Eng. Sci.i,* 30, 269-78.

Tsao, Y. H., D. F. Evans and H. K. Wennerström (1993). "Long-Range Attraction between Hydrophobic Surface and a Polar Surface is Stronger than that between Two Hydrophobic Surfaces," *Langmuir* 9, 779.

Tsao, Y.-H. S.X. Yang, D.F. Evans and H. Wennerström (1991). "Interactions between Hydrophobic Surfaces. Dependence on Temperature and Alkyl Chain Length", *Langmuir* 7, 3154-9.

Turai, L. L. and C.-H. Teng (1978). "Ultrasonic Deinking of Wastepaper," *Tappi J.* 61, 2, 31.

Valentas, K.J., O. Bilous, and N.R. Amundson (1966). "Analysis of Breakage in Dispersed Phase Systems", *Ind. Eng. Chem. Fundam.* 5, 271-9.

van de Steeg, H. G. M. (1992). "Cationic Starches on Cellulose Surfaces". Ph.D. Thesis, Wageningen Agricultural University. Netherlands.

Vidotti, R. M., D. A. Johnson and E. V. Thompson (1993). "Repulping and Flotation Studies of Photocopied and Laser-Printed Office Wastepaper. Part 1: Repulping and Image Analysis", *Prog. Paper Recycling* 2, 4, 30-9.

Vidotti, R. M., D. A. Johnson and E. V. Thompson (1994). "Repulping and Flotation Studies of Photocopied and Laser-Printed Office Paper. Part 2: Flotation," *Prog. Paper Recycling* 3(3), 39.

Virden, J. W. (1991). "The Aggregation Stability of Vesicle Dispersions". Ph.D. Thesis, University of Washington, USA.

Wang, T. K. and R. Audebert (1988). "Adsorption of Cationic Copolymers of Acrylamide at the Silica-Water Interface: hydrodynamic layer thickness measurements", *J. Colloid Interface Sci.* 121, 1, 32-41.

Weisenhorn, A. L. *et al.* (1989). "Forces in Atomic Force Microscopy in Air and Water", *Appl. Phys. Lett.* 54, 2651-3.

Wood, D. L. and D. C. Wood (1985). "Xerographics Deinking." US Patent 4,561,933. Assigned to Shell Oil Company.

Woodward, T. (1992). "Deinking: What's Right for You?", *PIMA Magazine* 1992, January, 34-38.

Yoon, R.-H. and J.L. Yordan (1991). "Induction Time Measurements for the Quartz-Amine Flotation System," *J. Colloid Interface Sci. 141*, 374-83.

APPENDIX A

MATLAB PROGRAM FOR POPULATION BALANCE MODEL SIMULATIONS

This appendix provides a listing with commentary of the Matlab executable code that simulates the population balance for competition between aggreagation and breakup. Program executable lines are written in lowercase; comments and explanatory descriptions are written in upper case. The main program is called 'setup.m', and the subsidiary routines and functions are stored in separate files, called 'aggmatrix.m', 'breakmatrix.m', 'avgvols.m', 'findbin.m', 'diff.m', 'fun.m', and 'makeplot.m'. For execution, all these files must be stored in the same folder, 'setup.m' opened from Matlab, and executed. There is no input or output file; the input parameters are entered in lines of 'setup.m', while the resulting variables are accessible from the Matlab workspace after a simulation. Matlab can easily be programmed to save or read data files, if this is desired.

```
THIS PROGRAM IS WRITTEN FOR MATLAB VERSION 4.2.1**********

THE PROGRAM SIMULATES A STIRRED VESSEL CONTAINING PARTICLES OF
DIFFERENT SIZES INTERACTING THROUGH AGGREGATION, TENDING TO
PRODUCE A FEW VERY LARGE AGGREGATES, AND BREAKUP, TENDING TO
PRODUCE NUMEROUS SMALL PARTICLES. BOTH THE ULTIMATE PARTICLE
SIZE DISTRIBUTION AND THE EVOLUTION TOWARDS THAT DISTRIBUTION
GIVEN AN INITIAL CONFIGURATION CAN BE SOLVED FOR IN THE PROGRAM.

THE BASIC APPROACH IS TO DISCRETIZE THE RANGE OF PARTICLE SIZES TO
A REASONABLE NUMBER, AND THEN SOLVE SIMULTANEOUSLY EQUATIONS
THAT DESCRIBE THE RATE OF CHANGE OF DENSITY OF PARTICLES IN EACH
SIZE BIN. THE KEY PHYSICS IS CONTAINED IN THE RATE EXPRESSIONS
THAT DESCRIBE THE RATE AT WHICH PARTICLES OF DIFFERENT SIZES
COLLIDE AND AGGREGATE AND BREAKUP.
```

MAIN PROGRAM**********

THE PROGRAM CONSIDERS THE SIZE OF PARTICLES TO BE DISCRETIZED INTO A FINITE NUMBER OF BINS. THE VOLUME FRACTION OF PARTICLES IN EACH BIN IS TRACKED, INCLUDING CHANGES IN TIME THAT OCCUR FROM AGGREGATION AND BREAKUP.

TO RUN THE PROGRAM, THE MINIMUM PARTICLE SIZE, THE RANGE OF SIZES CONTAINED IN THE FIRST BIN, THE BIN SPACING, AND THE NUMBER OF BINS MUST BE GIVEN. HERE'S HOW THIS WORKS:

SIZE OF THE SMALLEST ALLOWABLE PARTICLE = vmin. THIS IS THE SMALLEST VOLUME PARTICLE ALLOWED IN THE SMALLEST BIN, THAT IS, IT'S THE MINIMUM SIZE PARTICLE IN THE FIRST BIN.
THE SIZE OF THE LARGEST ALLOWABLE PARTICLE IN THE FIRST BIN IS vmin+ vunit. VUNIT THUS CONTAINS THE WIDTH OF THE FIRST BIN, AGAIN IN VOLUME UNITS.

EXAMPLE: vmin = 1000 CUBIC MICRONS, vunit = 7000 CUBIC MICRONS.
NOW THE FIRST BIN CONTAINS PARTICLES FROM 1000 TO 8000 CUBIC MICRONS, WHICH IS FROM [(6/PI)^(1/3)]*10 TO [(6/PI)^(1/3)]*20 MICRONS IN DIAMETER

NEXT, THE PARAMETER a DETERMINES THE SIZE OF LARGER BINS. THE MODEL REQUIRES THE BINS TO INCREASE IN SIZE GEOMETRICALLY; THUS THE SIZE OF EACH BIN IS A CONSTANT *MULTIPLE* OF THE PRECEDING, AND THIS MULTIPLE IS a. THUS IF a = 2, THEN EACH BIN IS TWICE AS LARGE AS THE PREVIOUS.

EXAMPLE: a = 2 AND vmin = 10 CUBIC MICRONS. BIN 1 GOES FROM 10 TO 20 CUBIC MICRONS. THEN BIN 2 GOES FROM 20 TO 40 CUBIC MICRONS, BIN 3 FROM 40 TO 80 CUBIC MICRONS AND SO FORTH. IF a = 1.5 AND vmin = 10 CUBIC MICRONS, THEN BIN 1 GOES FROM 10 TO 20 CUBIC MICRONS, BIN 2 GOES FROM 20 TO 35 CUBIC MICRONS, BIN 3 FROM 35 TO 57.5 CUBIC MICRONS, ETC.

LASTLY, THE NUMBER OF SUCH BINS MUST BE DETERMINED. THIS IS THE PARAMETER n. IF n = 30, THEN THERE ARE 30 SIZE BINS TRACKED IN THE MODEL SIMULATION.

EXAMPLE: IF a = 2 AND n = 30, THEN BIN VOLUMES WILL COVER A RANGE (APPROXIMATELY–IT DEPENDS ON vmin; AND IS STRICTLY TRUE ONLY WHEN vmin = 0) OF 2^30 IN VOLUME, OR APPROXIMATELY 2^10 IN DIAMETER, WHICH IS A 1024-FOLD RANGE OF DIAMETERS.

FOR THE SIMULATIONS I USED IN THE DISSERTATION, THE FOLLOWING VALUES WERE USED TO DETERMINE THE BIN SIZES:
vmin = 500 CUBIC MICRONS
vunit = 3000 CUBIC MICRONS
a = 2

n = 30
THEREFORE, BIN 1 CONTAINS PARTICLES FROM 500 TO 3500 CUBIC MICRONS. BIN 2 CONTAINS PARTICLES FROM 500 + (3000 TO 9000)= FROM 3500 TO 9500 CUBIC MICRONS. BIN 3 CONTAINS PARTICLES FROM 500+(9000 TO 18000)= FROM 9500 TO 27500 CUBIC MICRONS AND SO FORTH.

THIS IS HOW THE BINS ARE SET UP. NOW WE CONSIDER HOW THE AGGREGATION AND BREAKUP RATE EXPRESSIONS ARISE.

FIRST, WE CONSIDER THAT AGGREGATION OCCURS IN ACCORD WITH SMOLUCHOWSKI'S 1917 THEORY FOR ORTHOKINETIC AGGREGATION. HE GIVES THE RATE OF PRIMARY PARTICLE LOSS AS (4/3)*G*(R1+R2)^3*N1*N2. G = SHEAR RATE, R1 AND R2 ARE THE RADIUS OF THE TWO PARTICLES COLLIDING, N1 AND N2 ARE THE NUMBER DENSITIES OF SUCH PARTICLES PER VOLUME.

SECOND, WE ADD A COLLISION EFFICIENCY FACTOR, α, TO THIS, CONVERT FROM NUMBER FRACTION FORMULATION TO VOLUME FRACTION FORMULATION, AND MAKE THE PROBLEM NON-DIMENSIONAL. FOR MORE INFORMATION, SEE EQUATIONS 7.5-7.8 IN THE DISSERTATION.

THIRD, WE CONSIDER PARTICLES FROM BIN i AND BIN j TO INTERACT AS IF THEY WERE OF AVERAGE VOLUME IN THEIR RESPECTIVE BINS. THUS, ALL PARTICLES IN A GIVEN BIN ARE ASSUMED TO ACT IDENTICALLY. THIS IS THE ENTIRE POINT OF DISCRETIZING THE SIZE RANGE OF PARTICLES IN THE FIRST PLACE.

THE FINAL EQUATION THAT RESULTS FOR AGGREGATION IS EQUATION 7.8, TO WIT, $dx_{i+j}/d\tau = (4/3)*(1/v_i + 1/v_j)*(i^{(1/3)} + v_i^{(1/3)})^3 * x_i * x_j$, WHERE x IS VOLUME FRACTION, i AND j AND BIN INDICES AND v IS THE VOLUME OF A PARTICLE IN A GIVEN BIN. THE DERIVATION OF THIS EQUATION ARISES FROM TAKING SMOLUCHOWSKI'S EQUATION ABOVE, AND SUBSTITUTING VOLUME FRACTION FROM NUMBER DENSITY AS THE INDEPENDENT VARIABLE, AND DEFINING A DIMENSIONLESS TIME, $\tau = \alpha GVt$.

NOW LET'S CONSIDER BREAKUP. WE USE A SEMI-EMPIRICAL EQUATION, USED BY MANY OTHER INVESTIGATORS, THAT ENDS UP, AFTER MAKING IT NON-DIMENSIONAL, AS EQUATION 7.9, WHICH IS: $dx_i/d\tau = -\rho * (d_i/d_1 - 1)^{\nu} * x_i$. HERE, ρ IS THE RATIO OF THE BREAKUP RATE TO THE AGGREGATION RATE (NON-DIMENSIONAL); $d_i/d_1 - 1$ IS THE RATIO OF PARTICLE DIAMETER TO THE SMALLEST PARTICLE DIAMETER, ADJUSTED SO THAT THIS TERM IS ZERO FOR $i = 1$, THE SMALLEST PARTICLE BIN. ν EXPRESSES THE DEPENDENCE OF THE BREAKUP RATE OF PARTICLE DIAMETER. IT ANSWERS, HOW DOES PARTICLE BREAKUP RATE INCREASE WITH PARTICLE DIAMETER? IF $\nu = 1$, THEN BREAKUP RATE IS PROPORTIONAL TO PARTICLE DIAMETER; IF $\nu = 2$, THEN BREAKUP RATE IS PROPOTIONAL TO PARTICLE DIAMETER SQUARED. NOTE THE COMPLICATED TERM $d_i/d_1 - 1$ IS USED

BECAUSE THIS GUARANTEES THAT NO BREAKUP OCCURS FOR PARTICLES IN THE SMALLEST SIZE BIN. AN IMPORTANT NOTE: THIS DERIVATION DESCRIBES HOW PARTICLE BREAKUP IS ACCOUNTED FOR, AND ACCORDS WITH THE DESCRIPTION IN CHAPTER 7. HOWEVER, IN THE CODE BELOW, THERE ARE SEVERAL MODIFICATIONS. FIRST, IN THE MODEL, INSTEAD OF d_i/d_1 - 1, THE TERM v_i/v_1 - 1 IS USED, SINCE THIS IS HOW THE MODEL DEVELOPED. THUS, THE MODEL USES A v THAT IS 1/3 THE v DISCUSSED ABOVE. SECOND, IN THE MODEL, INSTEAD OF ρ, β IS THE RATE CONSTANT IN THE BREAKUP RATE, AND THE AGGREGATION RATE HAS THE ADDITION OF αV IN FRONT OF IT AS THE AGGREGATION RATE CONSTANT. ρ IS OF COURSE JUST THE RATIO $\beta/\alpha V$.

THE FINAL ASPECT OF THE MODEL IS TO FIX *HOW* BREAKUP OCCURS. WE HAVE SPECIFIED THE RATE AT WHICH PARTICLES BREAKUP TO SMALLER ONES, BUT NOW NEED TO DESCRIBE QUANTITATIVELY WHAT SMALLER PARTICLES ARE FORMED AND IN WHAT PROPORTIONS. FOR INSTANCE, PARTICLES COULD ALWAYS BE CONSTRAINED TO BREAK INTO 2 HALVES, OR 3 THIRDS, OR INTO A GIVEN DISTRIBUTION OF SMALLER PARTICLES. NOW WE SHOULD NOTE THAT IN THE MODEL, ONLY THE BIN OF THE PARTICLES FORMED MATTERS. THUS, WHETHER A BREAKUP PARTICLE IS 3000 OR 3500 CUBIC MICRONS DOESN'T MATTER IN THE MODEL IF BOTH OF THESE VOLUMES FALL IN THE SAME BIN. CONSERVATION OF MASS IS GUARANTEED IN THE EQAUTIONS. CLEARLY, THERE IS AN OPPORTUNITY HERE TO PRODUCE ELABORATE, MANY-PARAMETER MODELS OF BREAKUP, ALLOWING DIFFERENT TYPES OF BREAKUP TO OCCUR, DEPENDING ON THE PARAMETER SETTINGS. ALSO, THE WAY PARTICLES BREAKUP (WHICH MEANS: THE TYPE OF DAUGHTER PARTICLES FORMED FROM A GIVEN BREAKUP EVENT) COULD EASILY BE MADE TO DEPEND ON THE SIZE OF THE BREAKING PARTICLE. FOR INSTANCE, LARGE PARTICLES MIGHT BE EXPECTED TO LOSE SMALL PARTICLES FROM THEIR SURFACE, WHILE SMALL PARTICLES MIGHT BREAKUP BY SPLITTING INTO HALVES. ALL THESE COMPLICATIONS ARE ESCHEWED IN FAVOR OF A SIMPLE, ONE-PARAMETER BREAKUP MODEL.

THE BREAKUP MODEL REQUIRES A VALUE OF THE PARAMETER p, WHICH DETERMINES THE VOLUME FRACTION OF A DAUGHTER PARTICLE TO THE PARENT PARTICLE. IF p = 0.5, BREAKUP OCCURS INTO 2 HALVES. IF p = 0.25, BREAKUP OCCURS INTO ONE PARTICLE WITH 1/4 THE MASS AND ONE WITH 3/4 THE MASS OF THE PARENT PARTICLE. AS p APPROACHES ZERO, THE BREAKUP OCCURS MOSTLY AS SMALL PARTICLE EROSION FROM LARGE PARTICLES; AS p APPROACHES 0.5, BREAKUP OCCURS MOSTLY BY SPLITTING INTO EQUAL HALVES. NOTE $0<p<1$, AND THAT p IS SYMMETRIC ABOUT 0.5. THUS, p = 0.25 AND p = 0.75 YIELD IDENTICAL MODELS; AS DO p = 0.1 AND p = 0.9.

THE MODEL THEREFORE REQUIRES THE INPUT OF 5 PARAMETERS, ONLY 3 OF WHICH ARE INDEPENDENT. THESE ARE α, β, V, p, AND v. THE EXPRESSION $\alpha V/\beta = \rho$, AND THE STEADY-STATE SOLUTION DEPENDS ONLY

ON RHO. THE DYNAMIC SOLUTION, IN TERMS OF τ, THE DIMENSIONLESS TIME, DEPENDS ONLY ON ρ, TOO; BUT WHEN THIS IS CONVERTED TO TRUE TIME, THE VALUES OF α AND V ARE NEEDED. V, BY THE WAY, IS THE VOLUME FRACTION OF TONER DISPERSED IN THE VESSEL. TYPICALLY, THIS IS LESS THAN 0.01, AND IN FACT, IN ALL OUR EXPERIMENTS IT IS 0.0005. THE THREE INDEPENDENT PARAMETERS ARE ρ, v AND p.

THE MODEL OUTPUT CONSISTS OF EITHER THE STEADY-STATE SIZE DISTRIBUTION, IN TERMS OF VOLUME FRACTION OF PARTICLES IN EACH BIN, OR WHEN RUN IN DYNAMIC MODE, THE SIZE DISTRIBUTION IN TERMS OF VOLUME FRACTION OF PARTICLES IN EACH SIZE BIN AT A RANGE OF TIMES FROM ZERO TO FINAL TIME. THE NUMBER OF TIME STEPS AT WHICH THE SIZE DISTRIBUTION IS REPORTED IS DETERMINED BY MATLAB. TYPICALLY, IT IS FOR SEVERAL HUNDRED TIME STEPS. THE OUTPUT IS CONTAINED IN THE VARIABLES x AND τ..

%%

METHOD OF SOLUTION. AN AGGREGATION MATRIX, A, AND A BREAKUP MATRIX, B, ARE FORMED. SEE EQUATIONS 7.10a,b AND 7.11. THESE CONTAIN ALL THE NECESSARY INFORMATION FOR SOLVING THE EQUATIONS.

FOR DYNAMIC SOLUTION, A SYSTEM OF n ORDINARY DIFFERENTIAL EQUATIONS IS SOLVED, WHERE n IS THE NUMBER OF BINS. THE EQUATIONS ARE NONLINEAR SINCE TERMS SUCH AS x_i*x_j OCCUR. HOWEVER, ALL COEFFICIENTS TO THESE TERMS ARE SIMPLE NUMBERS, AND TIME DOES NOT APPEAR IN THE EQUATIONS OUTSIDE OF THE DIFFERENTIAL. THE EQUATIONS MUST BE SOLVED SIMULTANEOUSLY SINCE THE CHANGE IN EACH BIN DEPENDS ON THE CONTENTS OF ALL THE OTHER BINS. THE EQUATIONS ARE SOLVED WITH MATLAB'S BUILT-IN RUNGE-KUTTA 4-5TH ORDER SOLUTION ROUTINE, WHICH NATURALLY HANDLES MATRICES.

FOR STEADY-STATE SOLUTION, THE SAME SYSTEM OF EQUATIONS IS SOLVED, BUT INSTEAD OF SOLVING THEM IN TIME, THE NON-LINEAR ALGEBRAIC SYSTEM OF EQUATIONS IS SOLVED. THAT IS, ALL THE DIFFERENTIALS ARE SET TO ZERO. MATLAB HAS A BUILT-IN NONLINEAR EQUATION SOLVER, WHICH SOLVES FOR THE STEADY-STATE CONFIGURATION.

ADDITIONAL NOTES%%

THE PROGRAM USES THE MATHEMATICAL IDENTITY FOR THE SUM OF A GEOMETRIC SERIES FREQUENTLY IN DEVELOPING ITS FORMULAS AND EXPRESSIONS. THIS IDENTITY IS

$$\sum_{k=1}^{n} a r^{k-1} = \frac{a\left(r^n - 1\right)}{r-1}, \qquad \text{(A.1)}$$

PROVIDED THAT 'r' DOES NOT EQUAL 1. THIS EXPRESSION GENERATES THE MANY FORMULAS USED, FOR INSTANCE, WHERE WE KNOW A VOLUME AND NEED TO FIGURE OUT WHICH BIN NUMBER THIS VOLUME FALLS INTO. THUS, FOR THE MINIMUM VOLUME OF SEGMENT *i*, WE FIND

$$v_{min} + \left(\frac{\alpha^{i-1} - 1}{\alpha - 1}\right) v_{unit}, \qquad \text{(A.2)}$$

AND FOR THE MAXIMUM VOLUME IN SEGMENT *i*,

$$v_{min} + \left(\frac{\alpha^{i} - 1}{\alpha - 1}\right) v_{unit} \qquad \text{(A.3)}$$

IN MATLAB, THE EXPRESSION NEEDED TO FIND THE BIN NUMBER OF A GIVEN PARTICLE OF VOLUME *y* IS THUS

$$\frac{\ln\left\{\frac{(y - v_{min})(\alpha - 1)}{v_{unit}} + 1\right\}}{\ln(\alpha)}. \qquad \text{(A.3)}$$

```
%%%%%%%%%%%%%%%%%%%%%%%%%%%%%%%%%%%%%%%%%%%%%%%%%%%%%%%%%%%%%%%%
MAIN PROGRAM: 'SETUP.M'%%%%%%%%%%%%%%%%%%%%%%%%%%%%%%%%%%%%%%%%%%
%%%%%%%%%%%%%%%%%%%%%%%%%%%%%%%%%%%%%%%%%%%%%%%%%%%%%%%%%%%%%%%%

clear
        %CLEARS ALL VARIABLES IN MEMORY

global A B n v vmin vunit a alpha V p
        %THESE VARIABLES MAY BE USED NOW IN ALL SUBROUTINES

diffeq = 1;
        %IF DIFFEQ =1 THEN THE TIME EVOLUTION PROBLEM IS SOLVED,
        %IF DIFFEQ =0 THEN THE STEADY-STATE PROBLEM IN SOLVED

a = 2;
        %THE MULTIPLE BY WHICH THE BIN WIDTH INCREASES FROM BIN I
        %TO BIN I+1.
n =30;
        %THE NUMBER OF PARTICLE SIZE BINS IN THE SIMULATION, WHICH
        %MEANS THE NUMBER OF EQUATIONS TO SOLVE. LARGE NUMBERS
        %TAKE MUCH LONGER TO SOLVE.
```

```
vmin = 500;
        %THE MINIMUM PARTICLE VOLUME CONSIDERED IN THE
        %SIMULATION, IN CUBIC MICRONS.  COULD BE USED IN ANY UNITS,
        %HOWEVER.
vunit = 3000;
        %THE WIDTH OF THE FIRST BIN IN CUBIC MICRONS.
alpha = 0.16;
        %THE COLLISION EFFICIENCY OF AGGREGATION, WHICH IS THE
        %FRACTION OF COLLISIONS RESULTING IN AGGREGATE FORMATION.
V = 0.0005;
        %THE VOLUME FRACTION OF PARTICLES DISPERSED.  THIS IS
        %MULTIPLIED BY ALPHA TO DETERMINE THE EFFECTIVE
        %AGGREGATION RATE.
p = 0.5;
        %THE VOLUME FRACTION OF THE DAUGHTER PARTICLE
        %TO THE PARENT PARTICLE ON BREAKUP.
nu = 0.2947;
        %THE POWER DEPENDENCE OF THE BREAKUP RATE ON PARTICLE
        %VOLUME.  THUS, 1/3 THE DEPENDENCE ON THE PARTICLE DIAM.
beta =32e-6;
        %THE BREAKUP RATE CONSTANT, DIMENSIONLESS.
start = clock;
        %STARTS A TIMER TO REPORT THE LENGTH OF TIME IN SECONDS
        %OF THE COMPUTER SIMULATION.
%%%%END OF VARIABLE AND PARAMETER SPECIFICATION

v = avgvols (a, vmin, vunit, n);
        %CALCULATES THE AVERAGE VOLUME OF A PARTICLE IN EACH BIN.
        %COMPLETE CODE IS PRESENTED BELOW.
d = (6*v'/3.142).^(1/3);
        %CALCULATES THE DIAMETERS OF THE AVERAGE VOLUME
        %PARTICLE FOR EACH BIN.
A = aggmatrix (a, vmin, vunit, n, v, alpha, V);
        %THIS CALCULATES THE AGGREGATION MATRIX, BASED ON INPUT
        %PARAMETERS.  PROGRAM GIVEN BELOW.
B = breakmatrix (a, vmin, vunit, n, v, p, nu, beta);
        %CALCULATES THE BREAKUP MATRIX, BASED ON INPUT
        %PARAMETERS.  PROGRAM GIVEN BELOW.


if diffeq == 1
        %DYNAMIC SOLUTION

        x0 = [1; zeros(n-1,1)];
                %STARTS THE SIMULATION WITH ALL THE PARTICLES IN THE
                %SMALLEST BIN
        tf = 5e4;
                %THIS IS THE TIME AT WHICH MATLAB STOPS
                %THE SIMULATION
        [t,x] = ode45 ('diff',0,tf,x0);
                %CALLS THE SOLUTION, WITH THE FUNCTION 'DIFF'
```

```
            %CONTAINING THE DEFINITION OF THE SYSTEM OF EQNS.

        y = makeplot(t,x,n,tf);
            %THIS SELECTS 5 EQUALLY SPACED TIME INTERVALS AND
            %AND COLLECTS THE PARTICLE SIZE DISTRIBUTIONS AT
            %THESE INTERVALS INTO THE VARIABLE Y FOR
            %PLOTTING.
        plot (y')
            %THIS PLOTS THE SIZE DISTRIBUTIONS AT FIVE TIMES,
            % T = 0.2, 0.4, 0.6, 0.8 AND 1.0 OF THE TOTAL SIMULATION
            %TIME.

        ndist = x*(1./v)';
            %THIS EXTRACTS THE NUMBER DISTRIBUTION FROM THE
            %VOLUME FRACTION DISTRIBUTION. THUS IT CALCULATES
            %THE ACTUAL DENSITY OF PARTICE COUNTS IN EACH BIN.
            %THERE IS AN ARBITRARY CONSTANT MULTIPLYING THESE
            %NUMBERS.
        davg = (6*(1./ndist)/pi).^(1/3);
            %CALCULATES THE AVERAGE PARTICLE DIAMETER BASED ON
            %THE NUMBER DISTRIBUTION. THE AVERAGE IS THE
            %NUMBER-WEIGHTED AVERAGE VOLUME, CONVERTED BACK
            %TO THE DIAMETER OF THE PARTICLE OF AVERAGE VOLUME.
            %SEE CHAPTER 7 IN THE DISSERTATION FOR MORE
            %INFORMATION ON HOW STATISTICS ARE CALCULATED.

        plot(davg)
            %THIS PLOTS THE AVERAGE DIAMETER VERSUS TIME

elseif diffeq == 0
        %SOLVES FOR THE STEADY-STATE CONFIGURATION.

        x0 = (1/n)*ones(n,1);
            %THIS IS THE STARTING GUESS FOR THE PARTICLE SIZE
            %DISTRIBUTION WHICH IS THAT THE PARTICLES ARE FOUND
            %EQUALLY IN ALL SIZE BINS. FROM TRIAL AND ERROR,
            %THIS IS THE BEST INITIAL GUESS WHEN NOTHING IS KNOWN
            %FOR SURE ABOUT THE SOLUTION.
        x = fsolve('fun',x0);
            %CALLS THE NONLINEAR EQUATION SOLVER WITH THE
            %FUNCTION 'FUN' CONTAINING THE DEFINITION OF THE
            %PROBLEM.

        plot(d,x);
            %PLOTS THE STEADY-STATE PARTICLE SIZE DISTRIBUTION

        ndist = x./v';
            %CALCULATES THE NUMBER DISTRIBUTION FROM THE
            %VOLUME FRACTION DISTRIBUTION
        vavg = 1/sum(ndist);
            %CALCULATES THE PARTICLE OF AVERAGE VOLUME FROM
```

```
        %THE NUMBER DISTRIBUTION
    vvar = vavg*sum(ndist.*((v'-vavg).^2));
        %CALCULATES THE VARIANCE IN VOLUME TERMS
    vstd = sqrt(vvar);
        %CONVERTS FROM VARIANCE TO STANDARD DEVIATION
    vcube = vavg*sum(ndist.*(v'-vavg).^3);
        %CALCULATES THE SKEWNESS

    davg = (6*vavg/pi)^(1/3);
    dstd = (6*vstd/pi)^(1/3);
    dskew = vcube/vstd^3;
        %THESE CONVERT FROM THE VOLUME STATISTICS
        %CALCULATED ABOVE TO DIAMETER EQUIVALENTS
        %SEE CHAPTER 7 OF THE DISSERTATION FOR MORE INFO.

    davg, dstd, reldev=dstd/davg, dskew
        %DISPLAYS THE CALCULATED STATISTICS

end


etime(clock,start)
    %DISPLAYS THE TIME TAKEN FOR THE PROBLEM SOLUTION IN
    %REAL SECONDS.

%%%%%%%%%%%%%%%%%%%%%%%%%%%%%%%%%%%%%%%%%%%%%%%%%%%%%%%%
SUBROUTINE: 'AGGMATRIX.M'%%%%%%%%%%%%%%%%%%%%%%%%%%%%%%
%%%%%%%%%%%%%%%%%%%%%%%%%%%%%%%%%%%%%%%%%%%%%%%%%%%%%%%%
```

THIS NEXT PART IS THE FUNCATION AGGMATRIX, THAT CALCULATES THE AGGREGATION MATRIX.

AS CAN BE SEEN, IT DEPENDS ON A, VMIN, VUNIT, N, AND 'v' AS PARAMETERS FIXING THE SIZE OF THE BINS, AND ALSO ON ALPHA AND V, WHICH ARE EFFECTIVELY AGGREGATION RATE CONSTANTS.

MATLAB DOES NOT HAVE THE ABILITY TO WORK WITH 3RD-ORDER TENSORS, SO A, THE AGGMATRIX, IS 'TILED', WHERE EACH N BY N BLOCK IS STACKED IN A 2-DIMENSIONAL FORM. THUS, THE ELEMENTS OF THE MATRIX ARE ARRANGED AS FOLLOWS:

111 121 131
211 221 231
311 321 331
112 122 132
212 222 232
312 322 332
113 123 133
213 223 233
313 323 333

```
function A = aggmatrix (a, vmin, vunit, n, v, alpha, V)

A=zeros(n^2,n);
        %WE START WITH ALL ZEROS IN A

for ni = 1:n
        for nj=1:n
                %WE STEP THROUGH EVERY ELEMENT

                imin = findbin (a, vmin, vunit, ni-1, nj-1);
                imax = findbin (a, vmin, vunit, ni, nj);
                        %FIND IMIN AND IMAX, THE MAXIMUM AND MINIMUM
                        %BIN NUMBERS

                        %ACCOUNT FOR GAINS:
                if imax>n
                        imax=n;
                end
                if imin>n
                        imin=n;
                end
                if imin==imax
                        A(ni+(imin-1)*n,nj)=1;
                else
                        A(ni+(imin-1)*n,nj)=(v(ni)+v(nj)-v(imax))/(v(imin)-v(imax));
                        A(ni+(imax-1)*n,nj)=(1-A(ni+(imin-1)*n,nj));
                end


                        %ACCOUNT FOR LOSSES:
                A(ni+(ni-1)*n,nj)=A(ni+(ni-1)*n,nj)-v(ni)/(v(ni)+v(nj));
                A(ni+(nj-1)*n,nj)=A(ni+(nj-1)*n,nj)-v(nj)/(v(ni)+v(nj));

        end
end


%ACCOUNT FOR RELATIVE RATES OF AGGREGATION, DEPENDING ON THE
%PARTICLE SIZE

for ni=1:n
        for nj=1:n
                r=((v(ni)+v(nj))*(v(ni)^(1/3)+v(nj)^(1/3))^3)/(v(ni)*v(nj));

                for nk=1:n
                        A(ni+(nk-1)*n,nj)=r*A(ni+(nk-1)*n,nj);
                end
        end
end

A=(4/3)*alpha*V*A;
```

```
%FINALLY, SCALE A TO THE ABSOLUTE RATE OF AGGLOMERATION

%%%%%%%%%%%%%%%%%%%%%%%%%%%%%%%%%%%%%%%%%%%%%%%%%%%%%%%%%%%%
SUBROUTINE: 'BREAKMATRIX.M'%%%%%%%%%%%%%%%%%%%%%%%%%%%%%%%%%
%%%%%%%%%%%%%%%%%%%%%%%%%%%%%%%%%%%%%%%%%%%%%%%%%%%%%%%%%%%%

THE FUNCTION BREAKMATRIX CALCULATES THE BREAKUP MATRIX
WHICH PROVIDES THE COEFFICIENTS NEEDED FOR SOLUTION OF THE
POPULATION BALANCE MODEL.

INPUT IS THE PARAMETERS DESCRIBING THE SIZE OF THE BINS–A, VMIN,
VUNIT, N, 'v'–AND THE PARAMETERS DESCRIBING THE BREAKUP RATE, P,
NU AND BETA.

THE DESCRIPTION BELOW PROVIDES A MORE DETAILED DESCRIPTION OF
HOW THE BREAKUP MATRIX IS CONSTRUCTED:

RATE OF BREAKUP, DX(I)/DTAU = (BETA*((V(I)/V(1) - 1)^NU)*X(I)
BETA IS THE SHEAR INDUCED CONTRIBUTION TO BREAKUP, GAMMA IS
THE SIZE DEPENDENCE
B CONTAINS THE MAP FROM BREAKUP OF I TO RESULTS ON J.
E.G. B(3,4) HAS THE RESULTS OF BREAKUP OF BIN 3 ON BIN 4.
LET'S ALLOW P = THE PARTICLE FRACTION OF BREAKUP
IN THIS SIMULATION, LET'S ASSUME ALL PARTICLES GO INTO THE
PROPER BIN
WHICH BIN GETS THE PARTICLES?
SIZE OF BIN = P*V(I).
WHICH BIN NUMBER IS THIS?
VMIN + VUNIT*(A^I-1)/(A-1)=V(I)-MAX
P*V(I) = VMIN + VUNIT*(A^J-1)/(A-1)
P*V(I)-VMIN*(A-1)/VUNIT = A^J-1
(P*V(I)-VMIN)*(A-1)/VUNIT)+1 = A^J
LOG((P*V(I)-VMIN)*(A-1)/VUNIT)+1)=J*LOG(A)
LOG((P*V(I)-VMIN)*(A-1)/VUNIT)+1)/LOG(A) = J


function B = breakmatrix (a, vmin, vunit, n, v, p, nu, beta)

B=-eye(n);
B(1,1)=0;
        % FIRST COMPUTE LOSSES

for ni=2:n
        %NOW ADD GAINS

        nj = ceil(log(((p*v(ni)-vmin)*(a-1)/vunit)+1)/log(a));
        nk = ceil(log((((1-p)*v(ni)-vmin)*(a-1)/vunit)+1)/log(a));

        if nj < 1, nj=1; end
        if nk < 1, nk=1; end
```

```
        B(ni,nj) = B(ni,nj) + p;
        B(ni,nk) = B(ni,nk)+1-p;

        B(ni,:)=beta*((v(ni)/v(1) -1)^nu)*B(ni,:);
end
```

%%%
FUNCTION: 'AVGVOLS.M'%%%%%%%%%%%%%%%%%%%%%%%%%%%%
%%%

FUNCTION 'AVGVOLS' SIMPLY COMPUTES THE AVERAGE VOLUME CHARACTERISTIC OF EACH SIZE BIN. THIS IS JUST THE MEDIAN VOLUME OF THE RANGE COVERED BY THE SIZE BIN.

```
function v = avgvols (alpha, vmin, vunit, n)

for ni=1:n
        v(ni) = vmin + (1/2)*vunit*(alpha^(ni)+alpha^(ni-1)-2)/(alpha-1);
end
```

%%%
FUNCTION: 'FINDBIN.M'%%%%%%%%%%%%%%%%%%%%%%%%%%%%
%%%

THIS FUNCTION DETERMINES WHICH BIN THE AGGREGATE OF TWO PARTICLES, ONE FROM BIN NI AND ONE FROM BIN NJ, WILL FALL INTO. THUS, IT REQUIRES AS PARAMETERS A, VMIN, VUNIT, NI, AND NJ AND RETURNS THE NUMBER OF THE BIN INTO THE WHICH THE AGGREGATES WILL FALL.

```
function bini = findbin (a, vmin, vunit, ni, nj)

bini = ceil(log((vmin+(a^(ni)+a^(nj)-2)*vunit/(a-1))*(a-1)/vunit+1)/log(a));
```

%%%
FUNCTION: 'DIFF.M'%%%%%%%%%%%%%%%%%%%%%%%%%%%%%%
%%%

THIS FUNCTION DESCRIBES THE TIME EVOLUTION OF THE PARTICLE SIZE DISTRIBUTION. IT IS A SYSTEM OF NONLINEAR DIFFERENTIAL EQUATIONS THAT ARE EASILY WRITTEN IN MATRIX MULTIPLICATION FORM, AND SO THE EQUATIONS ARE SURPRISINGLY SIMPLE ONCE A AND B, THE AGGREGATION AND BREAKUP COEFFICIENT MATRICES ARE KNOWN.

IT RETURNS A LISTING OF PARTICLE SIZES AT EVERY TIME STEPS, ALONG WITH THE TIME AT EACH TIME STEP. MATLAB USES ADAPTIVE TIME STEP-SIZE, SO IT IS NOT KNOWN IN ADVANCE WHAT THE REPORTED TIMES WILL BE.

```
function xdot = diff (t,x)

global A B n

for ni=1:n
        A_i = [];
        A_i = A(((ni-1)*n+1):(ni*n),:);
                xdot(ni) = (x'*A_i+B(:,ni)')*x;
        end
end

%%%%%%%%%%%%%%%%%%%%%%%%%%%%%%%%%%%%%%%%%%%%%%%%%%%%%%%%%%%%%%
FUNCTION:  'FUN.M'%%%%%%%%%%%%%%%%%%%%%%%%%%%%%%%%%%%%%%%%%%%%%
%%%%%%%%%%%%%%%%%%%%%%%%%%%%%%%%%%%%%%%%%%%%%%%%%%%%%%%%%%%%%%

THIS FUNCTION POSES THE STEADY-STATE POPULATION BALANCE
PROBLEM FOR SOLUTION BY 'FSOLVE' IN THE MAIN PROGRAM. ONLY THE
NUMBER OF BINS, N, AND THE AGGREGATION AND BREAKUP MATRICES, A
AND B, ARE REQUIRED TO POSE THE PROBLEM.


function f = fun(x)

global A B n

for ni=1:n
        A_i = [];
        A_i = A(((ni-1)*n+1):(ni*n),:);
                f(ni) = (x'*A_i+B(:,ni)')*x;
        end
end

f(n+1)=sum(x)-1;

%%%%%%%%%%%%%%%%%%%%%%%%%%%%%%%%%%%%%%%%%%%%%%%%%%%%%%%%%%%%%%
FUNCTION:  'MAKEPLOT.M'%%%%%%%%%%%%%%%%%%%%%%%%%%%%%%%%%%%%%%%%
%%%%%%%%%%%%%%%%%%%%%%%%%%%%%%%%%%%%%%%%%%%%%%%%%%%%%%%%%%%%%%

THIS FUNCTION SELECTS FROM THE PARTICLE SIZE DISTRIBUTIONS AT
EACH TIME STEP, THE SIZE DISTRIBUTIONS AT 20%, 40%, 60%, 80% AND
100% OF THE TOTAL TIME CONSIDERED IN THE SIMULATION AND REPORTS
THE SIZE DISTRIBUTIONS AT THESE TIMES. THESE ARE GATHERED IN THE
MATRIX Y.

THE PURPOSE OF THIS IS TO SIFT THROUGH THE TREMENDOUS DATA
GENERATED BY DYNAMIC SIMULATION TO GET SEVERAL REPRESENTATIVE
DISTRIBUTIONS TO PLOT.


function y = makeplot(t,x,n,tf)
```

```
N = 5;

nj=1;

for ni=1:N
        a = tf*ni/N;
                while a>t(nj)
                        nj=nj+1;
                end
                y(ni,:)=x(nj,:);
end
```

VITA

Bret Alan Snyder was born on November 23, 1969 in Wilmington, Delaware. He attended public school in Newark, Delaware and Elkton, Maryland through 10th grade, after which he transferred to Wilmington Friends School for 11th and 12th grade. He graduated from Wilmington Friends School in June, 1987, and subsequently entered Brown University. After four years at Brown, he obtained a Sc.B. in Chemical Engineering in May, 1991. The following September, he entered the Department of Chemical Engineering at the University of Washington to pursue doctoral studies. He expects to receive his Ph.D. on October 28, 1996, a result of his research under Professor John Berg and presented in this dissertation. After graduation, he will begin work as an entrepreneur with his brother, Sean.

The research resulted in the submission of six manuscripts to peer-reviewed journals, the first four of which are in print, the latter two awaiting reviewers' comments. They are listed chronologically below:

Snyder, B. A., D. C. Schmidt and J. C. Berg (1993). "Characterization and Flotation Studies of Electrostatic Inks", *Prog. Paper Recycling* 3, 1, 17-27.

Snyder, B. A. and J. C. Berg (1994). "Liquid Bridge Agglomeration: A Fundamental Approach to Toner Deinking", *Tappi J.* 77, 5, 79-85.

Snyder, B. A. and J. C. Berg (1994). "Effect of Particle Size and Density in Flotation Deinking Electrostatic Papers", *Tappi J.* 77, 7, 157-9.

Snyder, B.A. and J.C. Berg (1996). "Deinking Toner-Printed Paper by Selective Agglomeration," *Pulp Paper Can.* 97, 38-41.

Snyder, B.A., D.E. Aston and J.C. Berg (1996). "Particle-Drop Interactions Examined with an Atomic Force Microscope," Submitted to *Langmuir* Sep. 1996.

Snyder, B.A. and J.C. Berg (1996). "Oil-Assisted Agglomeration for Toner De-Inking: Population Balance Model and Experiments," Submitted to *AIChE J.* Sep. 1996.